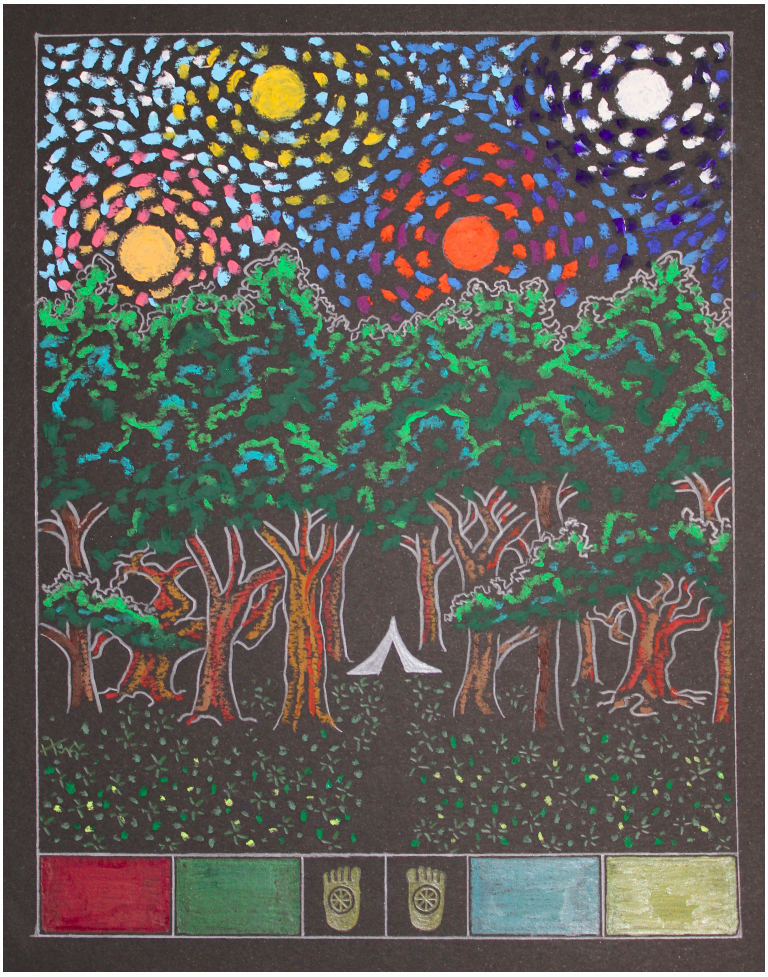
Mathematical Ecology in a More-Than-Human World

Siddharth Unnithan Kumar



Pembroke College, University of Oxford

Thesis for the degree of Doctor of Philosophy

Supervised by Dr. Samuel A. Cushman and Prof. Philip K. Maini

00:00 5th February 2023 (The Snow Moon in Port Meadow)

Out beyond ideas of rightdoing and wrongdoing,
there is a field. I'll meet you there.
When the soul lies down in that grass,
the world is too full to talk about.
Ideas, words, even the phrase *each other*
doesn't make any sense.

–Jalaluddin Rumi, translated by Coleman Barks

Title page artwork by Hugo Shakeshaft, reproduced here with permission of artist.
Final page artwork by Allegra Wint, reproduced here with permission of artist.

Abstract

This thesis is centered around the fundamental inquiry of ecology, which is to understand the relationships between organisms and their environment. Two core themes run and intertwine throughout the following work, beginning in parallel and then moving steadily towards synthesis in the concluding chapter. The first is concerned with developing and testing novel mathematical and computational methods which provide richer understanding of these species-environmental relationships. The second draws on emerging research from branches of the environmental social sciences and humanities, using the mathematical and scientific analyses in the earlier chapters as the entry into a more holistic engagement with ecology than is possible from any one disciplinary perspective alone.

We begin in Chapter 2 with the realm of community ecology and species distribution modelling, where we introduce the *smoothing function* and the *environmental manifold*. These two concepts provide new techniques for mapping the Hutchinsonian niche and working with the nonlinear and multivariate patterns emerging within and strongly influencing the quantitative relationships between species and environment. The following three chapters then shift focus to animal movement and landscape connectivity, each working from a different angle to provide more depth and breadth in addressing salient questions from this increasingly influential field of ecology. Chapter 3 introduces *Pathwalker*, a new individual-based computational method for modelling animal movement and connectivity, which is then used in Chapter 4 to provide the simulated data required for a comparative evaluation of major models in landscape connectivity.

Chapter 5 then keeps one foot in ecological science and places the other amongst areas of environmental geography, in order to analyse and overcome epistemological and methodological limitations in scientific studies of animal movement and landscape connectivity. This sufficiently motivates and widens the aperture of the thesis for disciplinary boundaries to dissolve in the heartfelt investigation of the final chapter, where we conclude by painting the possibility of an *ecological mathematics*.

Contents

1 Introduction: Mathematical ecology and the more-than-human world 6

1.1 Preface . . . 7

1.2 Thesis overview . . . 10

1.2.1 Community ecology and the Hutchinsonian niche . . . 11

1.2.2 Animal movement and landscape connectivity . . . 12

1.2.3 Ecological mathematics . . . 16

2 Smoothing and the environmental manifold 19

2.1 Introduction . . . 20

2.1.1 Chapter overview . . . 21

2.2 Smoothing and the environmental manifold . . . 22

2.2.1 The smoothing function . . . 22

2.2.2 The environmental manifold . . . 26

2.3 Comparative simulation analysis: methods . . . 31

2.4 Comparative simulation analysis: results . . . 36

2.5 Discussion . . . 39

2.6 Appendix A: Details on smoothing in environmental space . . . 44

2.6.1 Nonlinear correlations from linear responses . . . 44

2.6.2 Sample code for the smoothing function . . . 45

2.7 Appendix B: Mathematical aspects of the environmental manifold . . . 47

2.7.1 Defining the environmental manifold . . . 47

2.7.2 Ecological explorations with the environmental manifold . . . 48

2.7.3 The geometry of intersections . . . 49

3 Pathwalker **53**

3.1 Introduction: Animal movement and landscape connectivity 54

3.1.1 Chapter overview 57

3.2 The Pathwalker model 59

3.2.1 Input layers 59

3.2.2 Model parameters 60

3.2.3 Output layers 66

3.2.4 Summary of Pathwalker setup 66

3.3 Case study 67

3.3.1 Analysis methodology 67

3.3.2 Results 69

3.4 Discussion 70

3.5 Appendix A: Effects of autocorrelation on movement density 75

3.6 Appendix B: Pathwalker technical details 78

4 Evaluating landscape connectivity models **86**

4.1 Introduction 87

4.1.1 Chapter overview 87

4.1.2 An introduction to simulation experiments 88

4.2 Methods 90

4.2.1 Creating the connectivity model predictions 90

4.2.2 Creating the simulated connectivity maps 90

4.2.3 Measuring the accuracy of the connectivity model predictions 92

4.2.4 Summary of analysis methodology 93

4.3 Results 94

4.3.1 Connectivity model performance without destination bias 94

4.3.2 Connectivity model performance with destination bias 95

4.4 Discussion 97

4.5 Supplementary figures and tables 100

5 Moving beyond landscape resistance **106**

5.1 Introduction 107

5.1.1 Chapter overview . . . 107
5.2 Landscape connectivity and resistance surfaces: a brief history . . . 108
5.2.1 The emergence of landscape resistance . . . 108
5.2.2 Estimating landscape resistance . . . 108
5.2.3 Resistance-based connectivity modelling . . . 109
5.2.4 Combining individual- and resistance-based approaches to connectivity 111
5.3 The trouble with resistance surfaces: or, getting back to the wrong landscape 112
5.3.1 Spatiotemporal effects . . . 113
5.3.2 Context dependence . . . 116
5.4 Moving beyond landscape resistance . . . 122
5.4.1 Hypothesis testing, validation and simulation experiments . . . 123
5.4.2 Interdisciplinary collaboration: models, methodologies, practice . . . 124
5.4.3 Conclusion . . . 125

6 Conclusion: Ecological mathematics 127
6.1 Crossing the threshold . . . 127
6.1.1 The path we have walked . . . 127
6.1.2 The landscape before us . . . 129
6.2 Mathematical histories and the ethnosphere . . . 129
6.2.1 Ethnomathematics . . . 131
6.2.2 Abstraction and direct experience . . . 134
6.3 Ecologising mathematics . . . 137
6.3.1 Spacetime in the oral universe . . . 138
6.3.2 Embodying topology . . . 141
6.3.3 To be continued . . . 142
6.4 Love, truth, and the mystery . . . 143
6.5 Epilogue: Ecology and the Dhamma . . . 145

Acknowledgements 149

Bibliography 157

Chapter 1

Introduction: Mathematical ecology and the more-than-human world



Figure 1.1: Approaching the yew tree by the church at the end of Binsey Lane. Photograph by Andrew Fowler, 12th November 2022.

Three summers ago I walked through Port Meadow to the church at the end of Binsey Lane, and sat down to play the song Space Oddity on the little reed organ in the church. As the last chord faded, I was astonished to hear the sound of someone clapping, and I turned around to see a lady who came to introduce herself as Helen Jeans. At that time, I don't think I was consciously aware of the natural world beyond the viewpoint presented by modern science, but some ancient powers greater than me guided the conversation between us to arrive at her recommending me a certain book. Helen gave me a copy of David Abram's *The Spell of the Sensuous: Perception and Language in a More-Than-Human World*, which I read through the seasons of the following year. No single book has opened my heart and mind to the aliveness and wonders of our animate earth as much as this one, no writer as lyrically compelling in weaving my attention back into this world which we all call home and returning me to an intimate engagement with the cosmos which I had perhaps once known but long forgotten. And whether golden in the blazing sunset, breathing its ethereal mist, or framed by the star-studded sphere of the midwinter night sky, no single place has given me so much beauty, friendship and love as the landscapes of Port Meadow. Thus, I begin this thesis, whose fabric is suffused with the goodness of so many people and places, with a bow of gratitude to Helen Jeans, David Abram, and Port Meadow.

1.1 Preface

This work is a journey of ecology through academic disciplines and beyond, centered around exploring some of the relationships which constitute how animals live in and move through their environment. I understand ecology as the study of the relationships, patterns and processes which substantiate this living and breathing world. No phenomenon of this earthly cosmos need lie outside its reach, and the angles through which to engage with ecological questions are diverse and have no single privileged viewpoint, all arising from the ground of our direct experience with the more-than-human world. This is a very different sense of ecology from the conventional scientific perspective with which I began this research. Scientific approaches to ecology now increasingly abound with mathematics. The field of mathematical ecology brings analytical tools from mathematics to try and distil the complex and mysterious relationships involved in how a snow leopard navigates the local topography of a Himalayan valley, how the distribution of marbled cats in Sabah is influenced by the

geometries of tropical forest cover, or how the spatiotemporal flux of elephant movement relates to seasonal variation in weather patterns throughout southern Africa.

Having studied abstract mathematics for many years, I entered into ecological science looking excitedly for underlying mathematical structures in empirical wildlife data, seeing the movements and sightings of animals as the conduits through which my favourite mathematics could come alive in the vibrance of nonhuman life. I began by investigating possible geometric and topological patterns which could emerge from complex and nonlinear empirical wildlife data, bringing this novel perspective to look at camera trap observations of a range of different species in Borneo, gathered from a long-term field study of the Sunda clouded leopard conducted by ecologists in the Wildlife Conservation Research Unit (WildCRU). After spending some time in this realm of species distribution models and community ecology, I later shifted focus to studying the movement paths of the African lion in southern-central Africa, collected from decades of fieldwork by members of WildCRU. This led to analysing the mathematical underpinnings of concepts and techniques in modern ecological science which are concerned with mapping animal movement, such as 'landscape connectivity' and 'landscape resistance'. In turn, this motivated developing a new individual-based model for mapping animal movement, which we then used to perform a comparative evaluation of the major methods used in landscape connectivity studies.

Around this time - and thoroughly precipitated by reading *The Spell of the Sensuous* - my engagement with ecology blew open beyond the confines of mathematical modelling, bringing me to encounter vast swathes of ecological work in geography, anthropology, and other environmental social sciences. This expansion in awareness arose from a growing appreciation for how much of the more-than-human world, at this moment in scientific history, ostensibly lies beyond the realm of the quantifiable – that the mathematical tools currently used in ecology are limited by a constellation of assumptions and narratives which are largely unexamined and unobserved within the world of mainstream ecological science itself. Fundamentally, what became apparent – particularly through conversations with friends, and attending to my own direct experience of the world – is that how we understand 'nature', and the human place within it, will deeply determine how relevant and beneficial these mathematical models will be for our fellow humans and nonhuman friends. Do we see the landscapes and their inhabitants as separate from us, a suite of resources to abstractly map and govern with the

'perfect' scientific models? Or do we see, and express in our work, that we exist embedded within the rich and boundless web of ecological relationships which we study, and that much of the environmental challenge facing us in the present day is a manifestation of how we relate to each other, to the land beneath our feet, and to the more-than-human world in which we live?

Important questions, many answers to which can be found in a great diversity of human cultures and academic disciplines. The evolving trajectory of this thesis is guided by a sense that our own personal and collective answers to these questions, whether overtly asked or left implicit, have great influence on mathematical and scientific approaches to the environment, and the ripple effects they create. With the hope of cultivating a deeper and embodied engagement with the vast mysteries of ecological phenomena, I slept in a tent during my third year of research, an endeavour which was made possible by the love and generosity of my friends, and by the magic of the glade which kept my tent safe during raging storms and bellowing winds. And as the owls hooted above me, as the badgers snuffled around my tent, and as the seasons danced their cyclical tune through my body and the enfolding landscape, it became clear that the second of the two understandings of nature suggested above was more true to my emerging sense of ecological reality. This constellation of experiences guided me to an interdisciplinary collaboration of mathematics, ecological science and geography, involving my doctoral supervisor Sam, and three geographers – Jonny, Oscar and Tim. We synthesised many perspectives in looking at the limitations of landscape resistance and connectivity modelling (mentioned above) as a framework for mapping movement patterns, and sought to creatively explore approaches to develop models which attend more fully to the lively details of animal movement.

And when the stars are shining brightly above me, and I am surfing a wave in my heart and mind borne of a connection to both mathematical beauty and environmental healing, I wonder if there is a way to reorient the core of mathematics itself, to bring it into greater intimacy and reciprocity with the fullness of ecological reality – for our embodied and direct experience of the world, in its everchanging and interdependent wholeness, to provide the ground for a different interplay of mathematics and ecology. It is with a brief exploration of such thoughts that this thesis concludes. I cannot say for sure what sensibilities will guide the prose which begin my writing in the next chapter of livelihood, but I know in my heart that

I would like to work at the intersection of the biosphere and the ethnosphere – integrating ecology and nonhuman wellbeing with cultural, social and spiritual dimensions of human life – for it now seems to me that truly timely, resilient and healing ecological work must attend to these intertwining realms in balance, and above all, to do so with love.

1.2 Thesis overview

The following work gathers around two threads which run through all of the forthcoming chapters. The first is concerned with developing and testing novel mathematical and computational methods for studying the relationships between animals and their environment, and comprises the major analytical portion of this thesis. The second, beginning quietly and then growing to increasingly shape the direction of the later chapters, is a synthesis of recent ecological research from various branches of the environmental social sciences and humanities, ranging through geography, philosophy, anthropology and history. The mathematical and scientific analyses of ecological relationships in the earlier chapters provide the frame through which the material of later chapters is woven, with the intention being to arrive at a more holistic understanding of ecology than is possible from any one disciplinary perspective alone. The writing style and analytical emphases of the main four chapters are influenced by the fact that they have been closely adapted from articles written for a mainstream ecological science audience; this is not to say that they are devoid of content from other branches of ecology, but rather that the phrasing and presentation of viewpoints potentially unfamiliar to the intended readership have been chosen with care, in an attempt to tread the middle ground between not alarming the conventional scientist whilst also developing an appreciation of interdisciplinary perspectives on ecology.

This introductory chapter is more conversational than technical, inviting the reader to first dip their toes into the waters of each chapter, before diving in bodily and coming up for air amongst a mass of literature and citations. The first main chapter of this thesis, and the three which follow, then respectively address two central areas of ecological science: community ecology and species distribution models, and animal movement and landscape connectivity. These two topics are introduced, studied, and wrapped up in a self-contained manner within the space of their respective chapters. This structure then allows the thesis conclusion to open and develop the deeper themes of this research in a novel direction, and

this final chapter can thus be read independently of the earlier chapters.

The general audience (and, especially, the curious friend) may wish to leap over the following four chapters, alighting solely for the concluding chapter on *ecological mathematics*. A social scientist may wish to instead dance across the following pages and touch down one chapter prior, for the discussion on landscape connectivity and resistance surfaces. Those from the realms of ecological science may find themselves more at home in the first three chapters to follow, but are highly encouraged to additionally give their attention to the discussion and conclusion chapters. A mathematician may wish to peruse only the first of the following four chapters, pausing to drop anchor in the sidewaters of its appendices, before subsequently setting a direct course for the concluding chapter. And the interdisciplinary ecologist, or committed family member, will likely find work of interest in each chapter to come.

1.2.1 Community ecology and the Hutchinsonian niche

We begin in the realm of community ecology, which is concerned with understanding the composition of a coexisting assemblage of different species, and how their distribution in space and time is shaped by their environment. A central idea in community ecology is the 'Hutchinsonian niche' of a species, which, roughly speaking, seeks to map the theoretical range of environmental conditions in which that species could live. The niche concept has been of fundamental importance in ecological science, giving rise to an enormous body of work developed over many decades. Yet the attempts to describe its shape and properties, often requiring the use of a number of spatial dimensions beyond what we can visualise, have used fairly rudimentary mathematics. This made the Hutchinsonian niche a suitable setting in which to explore possible new insights granted by mathematical techniques from the fields of topology and geometry; although they have provided exceptional tools for the physical sciences to describe nonlinear phenomena, only slivers of these two mathematical disciplines have seen application to complex quantitative questions in ecology and conservation science.

Hence, this chapter is premised upon understanding more deeply the spatial patterns of species distributions, many details of which are lost in the linear statistical analyses that are commonplace in ecological science. It is the only part of this thesis with an overtly mathematical presence, which even then is largely translated into the language of ecology.

The material of this chapter is concerned with mapping the spatially varying presence of multiple species in the setting of temporally static camera trap data. The two main techniques introduced here are the *smoothing function* and the *environmental manifold*, which are both mathematical tools for describing the nonlinearities in how environmental factors affect species abundance. The smoothing function is a conceptually simple statistical method for transforming noisy empirical occurrence data into spatial patterns which are amenable to inference and mathematical analysis. The primary analytical material of this chapter is concerned with assessing the predictive abilities of the smoothing function as a species distribution model, in comparison with two popular such methods – the generalised linear model, and the random forest machine learning algorithm.

The environmental manifold is the shape of the data cloud which results from mapping the geospatial data of environmental conditions from two-dimensional geographical space into multi-dimensional 'environmental space', in which the Cartesian axes are given not by latitude and longitude, but by the environmental variables (such as elevation, human footprint, or forest cover) themselves. While being of both theoretical and empirical relevance to ecology, a deeper investigation into the ideas regarding the environmental manifold is left unexplored here due to the thematic shift in my research to animal movement, which provides the setting for the next part of the thesis. Nonetheless, this chapter aims to show that, as a lens through which to describe and analyse multiple nonlinear environmental effects on species distribution simultaneously, with potentially substantial implications for developing the niche concepts lying at the heart of ecological science, the environmental manifold provides fertile ground for further exploration into the utility of novel mathematical techniques for working with the spatiotemporal complexities of how environmental conditions shape the patterns of species abundance.

1.2.2 Animal movement and landscape connectivity

For the next three chapters, we continue to look at the relationship between environmental conditions and spatial patterns of animal presence. However, whereas the previous chapter explores the spatial distribution of a species without temporal variation, the focus now changes to understanding the actual pathways and environmental drivers of animal movement. Namely, we study how the landscape and its inhabitants shape the movement be-

haviours and travel routes of animals, and we do so mostly through the lens of 'landscape connectivity'. In its broadest definition, landscape connectivity is often understood as the extent to which a landscape facilitates the flow of an ecological process. Over the last two decades, it has grown to comprise a vast body of work in ecological science, and the models and methodologies of landscape connectivity have become commonplace in analyses of animal movement. This is largely because the conceptual and practical toolkit from developments in landscape connectivity provide a widely applicable framework to study animal movement patterns, which are usually very complex and difficult to map with precision. Connectivity models typically seek to predict the emergent routes through a landscape which are the most important (according to a variety of possible metrics) for a given group of animals.

Most connectivity models today use 'resistance surfaces' to provide their spatial input data. These are pixelated maps of a specific region that give a measurement of how landscape features affect the movement of a particular individual or population. Each pixel on the resistance surface is assigned a value which represents the estimated 'cost of movement' through the part of the landscape mapped by that pixel. Modern connectivity models typically run a chosen mathematical algorithm on a resistance surface to provide a prediction of landscape connectivity.

Three of the major such connectivity models are Circuitscape, resistant kernels, and factorial least-cost paths. Detailed descriptions of these models are given later in this thesis; it suffices to say at this stage that, while sharing the same framework of landscape resistance as the basis for their connectivity predictions, they differ in their conceptualisation of how animals move, and in which factors are deemed important enough to include as parameters for estimating connectivity. It would be no understatement to say that these three models have had tremendous influence in conservation science, and have often been used to provide the quantitative evidence for guiding policy and management decisions.

Despite their widespread usage, however, these three models are rather simplistic in how they map connectivity, typically involving only a handful of mathematical parameters which exclude many key factors shaping movement patterns. Moreover, upon closer analysis, the landscape resistance framework itself appears ill-suited for attending to many of the fundamental drivers of animal movement. All scientific models necessitate a simplification of ecological dynamics in their formulation, but do the limitations of connectivity modelling at

present render its methods and predictions ineffective for use in environmental theory and policy?

These three chapters, each from their own angle, work to provide more depth and breadth to our understanding of animal movement and landscape connectivity, which are now a central focus in several ecological disciplines. The first two of these chapters lie in the realm of ecological modelling, whereas the third keeps one foot there and places the other amongst areas of the environmental social sciences – contemporary strands of geography in particular – in order to address some of the broader questions which arise from these scientific analyses of animal movement and require perspectives from beyond ecological science alone.

Pathwalker

Individual-based movement models – those which simulate individual movement pathways as a function of the 'mechanisms' which influence movement – were used to study animal movement at least two decades earlier than the modern connectivity models mentioned above. While these older models often incorporated greater behavioural detail into the parameters which generate these simulated individual pathways, their movement predictions were typically based on a landscape which was either spatially homogeneous or composed of simple binary-valued habitat patches. The lack of spatial complexity in these models rendered them ineffective for application to conservation practice, in which landscape heterogeneity is an unavoidable component in understanding movement patterns and subsequently making management decisions.

In light of this, Chapter 3 presents a new model for mapping movement and connectivity, called Pathwalker, which combines the spatially-explicit framework of landscape resistance used in more recent connectivity models with the greater flexibility and detail afforded to predicting movement patterns found in the earlier individual-based models. It introduces parameters for simulating drivers of movement which are well established in their importance in movement behaviour but are absent in major connectivity models like Circuitscape, resistant kernels and factorial least-cost paths. For example, Pathwalker includes parameters for degrees of autocorrelation in movement, mortality risk during travel, and behavioural response to the landscape at multiple spatial scales. Pathwalker provides a way to simulate individual movement paths in response to a spatially complex landscape, while also being

able to predict landscape connectivity with greater attention to the factors which shape how animals move.

Evaluating landscape connectivity models

A second major utility of Pathwalker – and indeed, an equal motivation for its development – is the framework it provides to evaluate a range of important hypotheses in the field of connectivity modelling. Chapter 4 is devoted to assessing the predictive abilities of Circuitscape, resistant kernels, and factorial least-cost paths, using movement data simulated by Pathwalker. Namely, we create a large collection of connectivity maps with Pathwalker, each produced from a suite of movement data generated by a different combination of movement parameters and spatial complexity, and use these simulated maps to test the accuracy of the above three models in a wide variety of possible and spatial and behavioural scenarios.

Simulation techniques are essential for a comparative analysis of model performance, which this chapter explains in detail. Briefly, although several studies have examined the predictive abilities of the above three connectivity models using empirical movement data, the unknown relationships and variables influencing observed movement patterns in any specific empirical study preclude the possibility of assessing the relative efficacy of these models to accurately predict the most important pathways of connectivity in general.

Working instead with suitably generated simulated data, as we do in Chapter 4, allows us to compare model predictions with a 'known truth' – namely, the connectivity map generated by simulated movement paths resulting from a controlled set of known parameters – and thus enables a more definitive evaluation of model performance. Given the widespread usage of Circuitscape, resistant kernels and factorial least-cost paths across an enormous range of connectivity analyses in recent years, a comprehensive evaluation of their predictive abilities using simulation techniques is crucial for guiding the appropriate and effective application of these models for environmental policy and practice.

Moving beyond landscape resistance

Synthesising individual-based modelling with complex spatial input data, and providing a comparative evaluation of major connectivity methods, are contributions which address two salient issues in the field of connectivity modelling. Nonetheless, emerging empirical research

in conservation science points towards key drivers of animal movement which remain unaccounted for by existing connectivity models, including Pathwalker. Primarily, these involve spatial and temporal variability, and other more contextual details, in the behaviours and relationships which shape movement patterns. While such factors can be given some attention using existing modelling techniques, fully understanding and moving beyond these limitations requires looking at the broader epistemologies and assumptions which provide the ground for scientific research in landscape connectivity.

Chapter 5 investigates how the framework of landscape resistance introduces a 'bottleneck' of reductionism to connectivity modelling, through which only a fraction of the information contained in empirical movement data is retained for subsequently making predictions of landscape connectivity. This is analysed by combining recent empirical studies of movement and connectivity in conservation science with adjacent methods and concepts in environmental geography, which together elucidate the many levels at which resistance-based connectivity modelling fails to capture some of the most important aspects of animal movement. As a result, we call into question the relevance and effectiveness of these major connectivity models for application to environmental work in practice. Drawing on the richness of interdisciplinary research in movement and connectivity, this chapter then moves beyond critique to explore a variety of ways for overcoming these present constraints and developing modelling techniques which speak more fully to the true complexities and liveliness of animal movement.

1.2.3 Ecological mathematics

The preceding discussion chapter widens the aperture of the thesis by integrating closely related environmental knowledges from different academic disciplines, for the sake of understanding more clearly the impasse between current scientific models and ecological reality, and to offer some immediate steps for remedying this divide. Motivated thus, the confines of disciplinary boundaries now dissolve in the heartfelt exploration of this concluding chapter, which interweaves mathematics, anthropology, natural sciences, history, geography, and the Buddha's teachings, in service to painting the possibility of a new and holistic interplay of mathematics and ecological science – an *ecological mathematics*.

The entry point into this conclusion is the understanding that, while mathematics is the prized tool for distilling and analysing relationships in natural world, it is also a system of

knowledge which has been developed over the centuries by humans, whose way of relating to the world is necessarily conditioned by the cultural, social, political and geographical contexts in which they have been embedded. As a result, the lens through which mathematics is brought into ecological science is firmly situated within Western Enlightenment worldviews of nature, which, implicitly and explicitly, are shaped and narrowed by those particular ideologies deemed appropriate for studying the natural world. Becoming cognizant of the limits to understanding environmental relationships introduced by such an approach to ecology leads us to look at the mathematical practices in cultures embodying a different engagement with nature and the human place within it, which we do indeed find to give rise to different expressions of mathematics and its interplay with other dimensions of existence.

To take Western science and mathematics as the truest lens through which to study ecological processes would be to don red-tinted glasses and insist that the world is red. Perspectives on ecology from other academic disciplines, and more broadly from the astonishing diversity of cultural relationships with nature throughout human history, reveal many foundational aspects of the natural world which lie beyond the reach of quantitative methods and models in their current form. Yet for ecological science to dismiss or avoid these fundamental realms of ecology – in particular, the insights that arise through embodied, direct experience with nature – would be a myopic failure of the scientific tradition to engage with the deep and holistic thinking that is needed to meet the environmental challenges of the present day. Can we find a way for mathematical ideas and techniques to be used in ecology in a manner which not only retains their greatly valued analytical power and beauty, but which also frees them from some of the cultural reductionisms and ossified ideological cloisters in which they are currently ensconced? I am convinced that this is not only possible, but is also an extraordinarily timely and promising endeavour upon which to embark. Although such an investigation would be the premise of a new thesis, rather than the concluding lines of this one, in this final chapter I attempt to sow these seeds of possibility by briefly looking at a case study illustrating how alternative cultural understandings of space and time in nature may provide fertile soil for new mathematical insights into the complexities of ecological processes.

Traveling deeply into ecology with an open mind and spirit necessarily brings us to intimacy with the boundless mysteries of this rich and beautiful existence. At the heart of the journey of this doctoral research is friendship and love, infused with the guidance I have

received from my teachers in working with experiences and questions which confound the available methodologies of established academic disciplines. Here, I have found the Buddha's teachings (the *dhamma*) as a robust and powerful compass with which to approach ecology in the vast space of human experience, and as a companion and refuge for which I am eternally grateful. And as I allow for ecology and the dhamma to converse and synthesise within my being, I begin to see the main themes from the Buddha's teachings appear in the recent shifts and developments many academic disciplines are taking to better meet the environmental challenges of the present day. Thus, this concluding chapter ends with an epilogue touching on the great value I find in the dhamma as the ground for engaging with the timeless questions of mathematics and ecology in this more-than-human world.

Chapter 2

Smoothing and the environmental manifold



Figure 2.1: This chapter is closely adapted from the *Ecological Informatics* article *Smoothing and the environmental manifold* (Unnithan Kumar, Maini, et al. 2021). Each day of writing this piece through the autumn and winter would begin with a swim in the river in Port Meadow. Photograph by Siddharth Unnithan Kumar, 13th October 2022.

2.1 Introduction

A central question of community ecology is to understand how a coexisting assemblage of species is spatially distributed, and the environmental factors (such as elevation, or forest cover) which influence these patterns of abundance. The foundational concept in this context is that of the ecological niche: it encompasses a variety of related ideas, such as the Grinnellian and Eltonian niches, which are used to describe and understand these species-environment relationships (Soberón 2007). The formulation of the niche concept which has perhaps most informed quantitative ecological analyses is the Hutchinsonian niche, proposed in the mid-20th century by G. Evelyn Hutchinson (Hutchinson 1957). The Hutchinsonian niche has two aspects: the *fundamental niche*, and the *realised niche*. The former is considered to be the region of abstract multi-dimensional environmental space (or 'niche space') which corresponds to the combination of conditions theoretically required for a species to survive and thrive; the latter is defined to be the subset of this region which the species is empirically observed to inhabit (Holt 2009). There has been a great deal of work in recent times focused on describing the shape and properties of these two aspects of the Hutchinsonian niche (Blonder et al. 2014; Broennimann et al. 2012), with deeper insights now made possible by substantial advances in high-quality GIS and occurrence data (Cushman and Huettmann 2010).

In light of this, a range of statistical tools has been developed to quantitatively study this species-environment relationship, and to describe the details of the fundamental and realised niches (Hegel et al. 2010). Two of the most popular tools for this endeavour are the generalised linear model (GLM) and the random forest machine learning algorithm (Cutler et al. 2007; Nelder et al. 1972). The GLM proceeds by assuming a linear relationship between species abundance and environmental variables, and subsequently estimating the linear combination of these environmental variables which best predicts the observed species distribution.[1] Random forest is a machine learning method, which uses a predictive technique called 'bootstrapping' in combination with a classification and regression algorithm.

[1] It is possible to incorporate nonlinearities into the GLM (such as square or exponential relationships), but these are required to be precisely specified when setting up the model, which is difficult *a priori* (Ash, D. W. Macdonald, et al. 2021; Whittingham et al. 2006). Indeed, by prescribing the functional shape prior to analysis, the GLM is limited in its ability to accurately account for the complex and unknown relationships constituting how animals respond to environmental conditions. Hence, in this chapter, we configure the GLM with linear predictors, as it is used in most ecological analyses (McGarigal, Wan, et al. 2016).

In contrast with the GLM, it is nonparametric, and has become a popular tool for working with the nonlinearities of ecological relationships (Mi et al. 2017).

2.1.1 Chapter overview

In this chapter, we investigate the behaviour and performance of the GLM and random forest in predicting simulated species-environment relationships, together with a new method which we introduce, called the 'smoothing function'. In essence, the smoothing function numerically smooths the noisy species occurrence data along environmental gradients in multiple dimensions. It can be used to describe and predict species-environment relationships nonparametrically, and to address questions of scale regarding these relationships in environmental space. While there has been much attention to scale dependence of species-environment relationships in geographical space (Wiens 1989), questions of scale in environmental space have been almost completely unexplored in the ecological literature. However, understanding scale dependence in environmental space is essential for accurately measuring niche structure and analysing how environmental variables limit species occurrence, as we discuss further in this chapter.

In addition to the smoothing function, we introduce a new concept called the 'environmental manifold', which we describe in detail in Section 2.2.2. Briefly, the environmental manifold is the shape of the data cloud of sampled environmental variables in multi-dimensional environmental space. It provides a lens for deeper understanding of the observed response between a species and their environment, as discussed in Sections 2.2.1 and 2.6.1, and its multivariate nature affords new insights into ecological data by providing a methodology to observe and analyse the nonlinear interactions of several environmental variables simultaneously. A fuller exploration of its properties, and its relation to other fields of ecological analysis, lies beyond the scope of this chapter, but we will touch on its key connection to the Hutchinsonian niche in Section 2.5. As will become clear from its construction in this chapter, the environmental manifold is precisely the *realisable niche*: the geographically realised subset of environmental space on which the realised niche is constrained to occur. This leads to novel and potentially profound implications for community ecology theory and methodology.

After describing the smoothing function and the environmental manifold, we turn to a comparative analysis which involves simulating patterns of species occurrence and sub-

sequently investigating the ability of the GLM, random forest and smoothing methods to recover these relationships. Although no computational simulation of ecological processes can fully capture their subtleties in reality, such techniques do have particular advantages for this kind of evaluative investigation. Namely, we stipulate, *a priori*, a known mathematical relationship between species occurrence and multiple environmental gradients, and this in turn enables us to have a 'known truth' to which we can compare the performance of the different methods, in terms of their ability to correctly identify the relevant variables and estimate their effects on species distributions (see Atzeni et al. 2020; Chiaverini et al. 2021). Using this simulation framework, we address the following question. Do all three methods recover the known relationship which describes the response between the species and their environment, and do they perform equally well when this relationship is more complex? To do this, we evaluate their performance along two gradients of increasing complexity: (1) from a linear response to a nonlinear response, and (2) from a simple isotropic environmental manifold, across a range of more interesting geometries, to the actual complexity of a three-dimensional environmental manifold from a case-study landscape in Borneo (Hearn et al. 2018). In this way, we establish the smoothing function and environmental manifold as relevant and powerful new methods for ecological science.

2.2 Smoothing and the environmental manifold

2.2.1 The smoothing function

The smoothing function, which we now describe in detail, is mathematically defined as a Gaussian kernel smoothing function (similar to the Gaussian kernel density function seen in Silverman 1986). We begin with an occurrence dataset distributed along an environmental gradient, which can either consist of binary presence-absence data or abundance data with multiple occurrences. The value $V(x)$ at each location[2] x is then replaced by a weighted average $S(x)$ of the values at the locations x' which are neighbours with proximity σ to x along this environmental gradient. The weighting function K_σ is, in this case, a Gaussian function. This can be expressed mathematically as

[2]Namely, a value of 0 for absence or 1 for presence if presence-absence data is being used, or a non-negative integer n representing n occurrences if abundance data is being used.

$$S(x) = \frac{\sum K_\sigma(x, x') \cdot V(x')}{\sum K_\sigma(x, x')}, \quad \text{where} \quad K_\sigma(x, x') = e^{-\frac{(x-x')^2}{2\sigma^2}}$$

where the sum is taken over all points x' in the dataset. Sample code for the smoothing function is provided in Section 2.6.2.

Like random forest, and in contrast with the linearity condition of the GLM, this approach is nonparametric because no underlying form of relationship is prescribed. The smoothing method can be used for predicting species distributions, by using the smoothed occurrence points to obtain an estimated probability distribution of species occurrence, and in this chapter we will compare its predictive ability with that of the GLM and random forest. One key difference between this and the other two methods is that it may be expressed as a genuine mathematical function on the occurrence data points themselves, and is thus more straightforward to work with from a mathematical point of view, as discussed in the appendices to this chapter. In comparison with the regression coefficients predicted by the GLM, and the bagging rules used by random forest, we have not yet developed the smoothing approach to produce parameter estimations which could allow for extrapolation to predict species occurrence patterns with a set of environmental conditions different to that in the given dataset – however, we note also that such parameter estimations, when extrapolated to a different suite of environmental variable values, need not give reliable predictions of species distributions.

Applying the smoothing function to empirical camera trap data from Borneo

In Figure 2.2, we illustrate the effect of this Gaussian smoothing on the response of the Sunda clouded leopard to elevation, using empirical data from the study in Hearn et al. 2018 in Sabah, Borneo. We see the effect of the smoothing function as we increase the bandwidth parameter σ, moving from left to right in the Figure and starting from the top-left graph in which $\sigma = 0$ (which means that no smoothing has been applied). An analogous multivariate smoothing happens when we work with multiple environmental variables simultaneously.

We see that a correlation emerges as we smooth the original graph, from an initial collection of binary values to a smoothly increasing graph. In the first two cases, noise obscures any clearly observable pattern, but in the last case we have potentially smoothed away all information aside from the most basic pattern of a positive correlation. The fourth and fifth

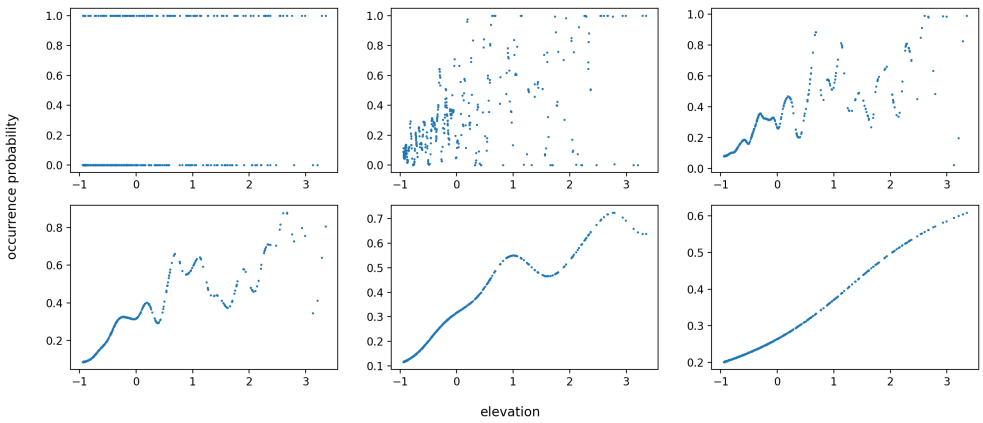


Figure 2.2: The effects of smoothing on binary presence-absence data. The top-left graph consists of the original occurrence data, with increasing smoothing as we move from left to right along the first and then second row ($\sigma = 0, 0.01, 0.05, 0.1, 0.3, 1$ respectively). The data are occurrences of the Sunda clouded leopard, plotted along a gradient of increasing elevation which has been normalised with standard scaling to have zero mean and unit variance.

graph contain information more coherent than the first, and more rich than the last, with the apparent emergence of two peaks as elevation increases. Figure 2.3 gives another example, using the same empirical occurrence data for the clouded leopard, but now along the gradient of a human footprint metric.

As one may expect, with the extensive smoothing resulting in the sixth graph, we see a negative correlation between occurrences of the Sunda clouded leopard and increasing human presence. But, beyond this basic inference, we can say little else. How do we explain the clear peak in the fifth graph, in which their presence increases synchronously with human footprint as this variable ranges between 0 and 1? Similarly, how shall we understand the double peak seen in the fifth elevation graph? Human-nonhuman relationships are multifaceted, and it may be naive to presume a simple monotonic relationship between species presence and an environmental variable such as anthropogenic presence. Yet there is another phenomenon at play here which is influencing the shape of these correlations.

Now comes the key point. What we are observing here is the correlation of species occurrence relative to *one particular environmental variable*, ranging across different sites in geographical space. But across these different sites, *other environmental variables will be*

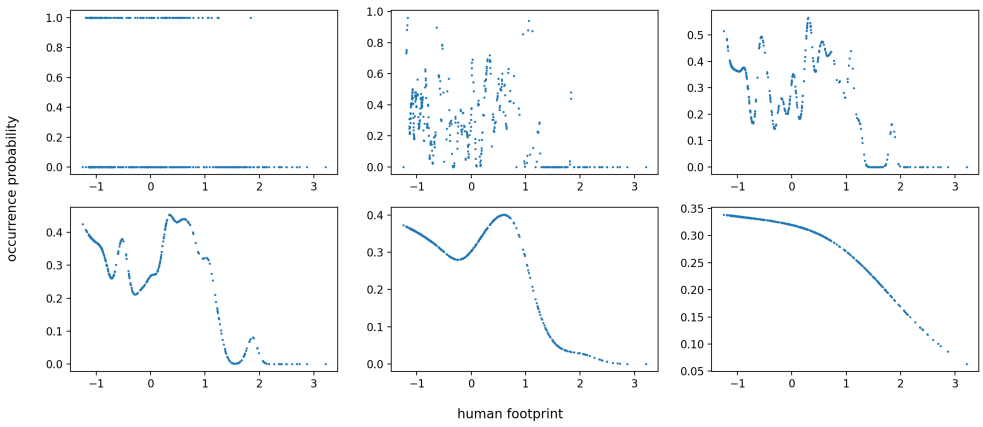


Figure 2.3: Another example of the effects of smoothing. The data are again occurrences of the Sunda clouded leopard, now along an increasing gradient of human footprint, normalised with standard scaling to have zero mean and unit variance. The smoothing function has been applied to these graphs with the same values of σ as in Figure 2.2 ($\sigma = 0, 0.01, 0.05, 0.1, 0.3, 1$ respectively).

changing too. This means that we are not observing their response to one given variable independently of the other environmental variables to which they may be simultaneously responding. For example, rather than the Sunda clouded leopards favouring intermediate levels of human footprint (as one may think Figure 2.3 suggests), it may indeed be the case that the *covariance* of the environmental variables – how they change together across different locations – is what has largely shaped this pattern. In other words, those regions of Borneo for which human footprint increases from low to intermediate may also see another environmental variable (such as elevation, or forest cover) changing simultaneously in such a way that the 'positive' response to this environmental variable outweighs their 'negative' response to increasing human footprint. Crucially, even in the mathematically ideal scenario whereby a linear relationship describes the response between a species and *every* environmental gradient, the observed correlations may exhibit the nonlinear and multimodal shapes seen in Figures 2.2 and 2.3, due to the complexity not of the species response but rather the nonlinear covariance of environmental variables, which we prove in Section 2.6.1. So, to better understand the multivariate relationships shaping these patterns between species and environment, we need to see how the environmental variables themselves vary together. This leads us to consider

the *environmental manifold*.

2.2.2 The environmental manifold

The environmental manifold, described in detail below, is the shape of the data cloud of sampled environmental variables when mapped into niche space, and it encodes precisely how this set of environmental variables co-vary. In practice, it is straightforwardly created from empirical GIS data. One motivation for the importance of the environmental manifold is given by the above discussion on observed abundance patterns relative to environmental gradients, the implications of which for ecological theory and practice are revisited in Sections 2.5 and 2.6.1. A second reason is its fundamental relevance to the Hutchinsonian niche, which was mentioned in Section 2.1 and will be revisited in Section 2.5. Finally, the environmental manifold is a concept which opens avenues for new mathematical insights into ecological data, affording a visual viewpoint into underlying spatial complexities hitherto unavailable in ecology, which will be discussed in Appendix 2.7. But first, let us see how the environmental manifold is created.

Constructing the environmental manifold

We begin with three GIS layers – elevation, forest cover and human footprint – sampled across the entire island of Borneo (Figure 2.4). Any combination of environmental variables could be chosen to build an environmental manifold; here, we choose a total of three for ease of visualisation, and these specific three variables because of their demonstrated importance as a predominant influence on biodiversity in this region (D. W. Macdonald et al. 2020). Elevation is derived from the SRTM dataset (Jarvis et al. 2008). Forest cover is a continuous variable ranging from 0 to 100 – corresponding to no tree cover and full canopy closure, respectively – and is taken from the NASA global tree cover dataset (Hansen et al. 2013). Human footprint is obtained from the global human footprint dataset (WCS et al. 2005).[3] We used the Python package `rasterio` (Gillies et al. 2013) to import these empirical GIS layers into Python as matrices.

[3]These variables were evaluated at 90m for elevation, 30m for forest cover and 1,000m for human footprint. All variables were then re-sampled in ArcGIS to a common resolution of 250m, following D. W. Macdonald et al. 2020.

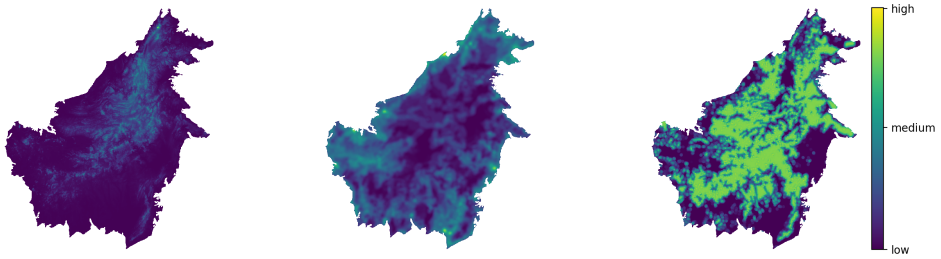


Figure 2.4: Three GIS layers of Borneo, from left to right: human footprint and forest cover, respectively. Yellow corresponds to higher values for these variables, and blue to lower values.

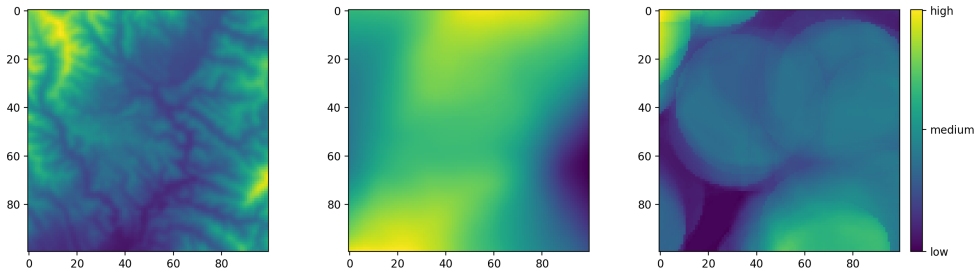


Figure 2.5: Zooming into the three geospatial layers of Borneo in Figure 2.4. These 100×100 pixel maps show the three environmental variable values over the same geographical region: as previously, they display the values for elevation, human footprint and forest cover, respectively.

Now we zoom in to a 100×100-pixel subset of the above three geospatial layers (Figure 2.5). Each of the three subset layers are demarcated by the same geospatial coordinates, and thus they present the values of these three variables for the same region of Borneo. Since we are viewing each environmental variable in a different plot, it is difficult to see here how they co-vary: namely, how do their values change simultaneously as we move across this landscape in Borneo? The exact nature of this covariance becomes apparent if we move from geographical space to environmental space (referred to by Hutchinson in Hutchinson 1957 as 'niche space', and similar to the 'gridded environmental space' in Broennimann et al. 2012). This is simply the space where the axes are given by the different environmental variables instead of latitude and longitude. We label this space as $\mathbb{E}$.

Moving from geographical space to environmental space means that each pixel in our GIS layer of Borneo is mapped into three-dimensional space (since in this example we are working with three environmental variables), to the point whose coordinates are given by the environmental variable values at that pixel. For example, if a pixel has elevation α_1, with human footprint value α_2 and forest cover value α_3, then this pixel of the Borneo layer gets sent to the point with coordinates $(\alpha_1, \alpha_2, \alpha_3)$ in our three-dimensional environmental space $\mathbb{E}$. Doing this for all pixels in this 100×100-pixel grid, we call the resulting shape the environmental manifold, labeling it as M. In Figure 2.6, we see how our 100×100-pixel subset of the Borneo geospatial layer twists and bends in a highly nonlinear manner, demonstrating the geometrically complex covariance of these environmental variables. In Figure 2.7, we see the graph of this same portion of Borneo projected onto two-dimensional environmental spaces, where in each case the two axes are given by two of the three environmental variables considered above.

Despite its seeming complexity, we are actually working with a shape which in some sense we understand well, since we know it is in fact sampled from a region of two-dimensional geographical space, which means that we know which points on the environmental manifold neighbour each other in geographical space. Thus, we can create a linear approximation to this surface from these points, and hence obtain a clearer representation of its shape. In Figure 2.8, we see this for three different 20×20-subsets of the environmental manifold displayed in Figure 2.6, where we have 'joined up the dots' by using the knowledge from geographical space of which points are contiguous with each other. In the analysis which follows in this chapter,

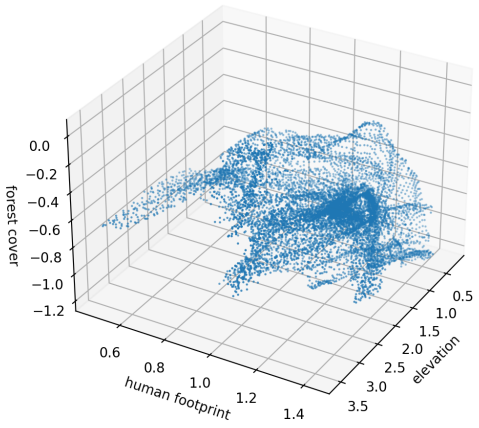


Figure 2.6: Visualising the environmental manifold. This is the result of mapping the pixels from the 100×100 pixel subset of the GIS layers into three-dimensional environmental space, with axes given by the three environmental variables (elevation, human footprint and forest cover). The three environmental variables have been normalised using standard scaling to have zero mean and unit variance. Intuitively, we can think of this mapping from geographical space into environmental space as folding and contorting a piece of paper, where the paper is the flat GIS layer of Borneo in geographical space (parameterised by latitude and longitude).

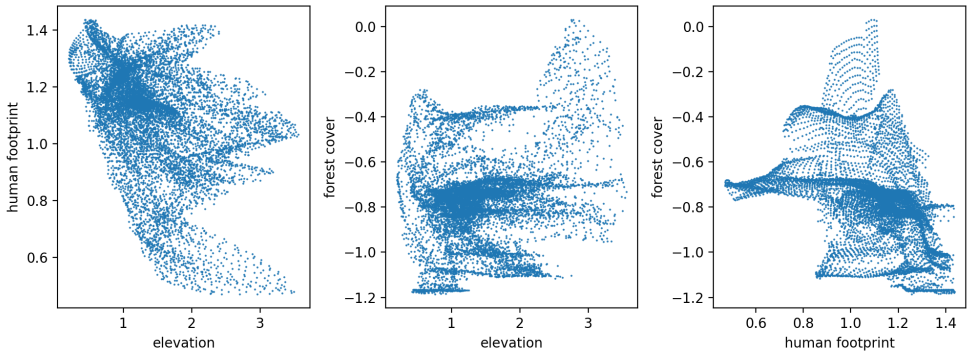


Figure 2.7: The same 10,000 points as in Figure 2.6 have now been plotted in two-dimensional environmental space, with axes given by the three different possible pairings of the three environmental variables above. Visually, this is equivalent to flattening the shape in Figure 2.6 onto the floor or the two walls of the axes seen in Figure 2.6.

we stick to using three environmental variables for the sake of visualisation. However, we may construct the environmental manifold using as many variables as desired in the same manner as presented here, which we discuss in Section 2.7.

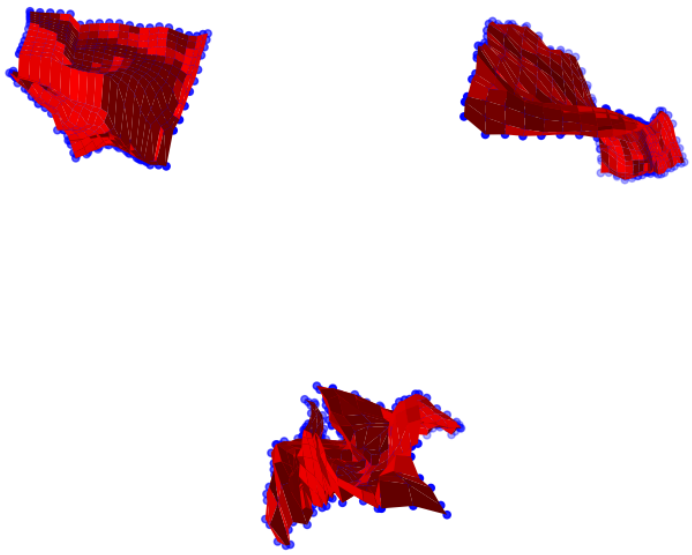


Figure 2.8: This figure illustrates three different examples of a 20×20-pixel subset of the environmental manifold seen in Figure 2.6. We have the knowledge of which points in Figure 2.6 are adjacent to each other in the geographical sense, because the points in this data cloud retain their contiguity from geographical space. Thus, by simply 'joining the dots', we obtain a linear approximation to any chosen portion of Borneo's surface when mapped into environmental space. The images in this figure demonstrate the geometrically interesting and varied structures that arise from the covariance of environmental variables.

A note on scale dependence in environmental space

Scale dependence in geographical space has become a key ingredient in ecological science for understanding the relationships which shape patterns of organism distribution and movement,

and is concerned with how a species responds to their habitat features at multiple spatial scales (Wiens 1989). Using kernel smoothing in geographical space plays a key role for discerning these scale-dependent effects (Chandler et al. 2016; Cushman and McGarigal 2002). Scale dependence and smoothing in environmental space, however, is an inherently different phenomenon, due to the different axes over which the scaling is considered: whereas the axes in geographical space are given by latitude and longitude (under a chosen mapping projection from the sphere to the plane), the axes in environmental space are given by the gradients of the environmental variables themselves. Thus, smoothing in environmental space is tied to how variation in niche dimensions influences habitat suitability, in which scale dependence relates to the sensitivity and degree to which changes in niche variables affect and limit species occurrence. Therefore, it is crucial to consider scale dependence in environmental space in order to assess the niche structure of a species and to assess how issues such as sampling bias affect its estimation.

The smoothing function introduced in this chapter addresses this second aspect of scale, as illustrated in Section 2.2.1. A similar smoothing method, for measuring niche overlap in environmental space, appeared in Broennimann et al. 2012, which highlighted the promising role such functions could have in ecological analyses, and in which it was said that 'the use of a kernel smoother makes the process of moving from geographical space to multivariate environmental space independent of both sampling effort and arbitrary choice of resolution in environmental space', a claim which we will revisit in Section 2.5.

2.3 Comparative simulation analysis: methods

Analysis methodology

With the smoothing function and environmental manifold now introduced, we will study the accuracy of the GLM, random forest and smoothing methods in recovering simulated species-environment relationships, as we vary both the relationship z and also the shape of the simulated environmental manifold M. These simulated environmental manifolds will consist of 10,000 points in environmental space, just like the empirical environmental manifold obtained from the GIS layers in Section 2.2.2. The metric of accuracy will be calculated from the difference between the true simulated values and the values predicted by each of the three

models. Specifically, accuracy will be measured by the Pearson correlation coefficient and mean squared error between the simulated and predicted values at each of the 10,000 points on M for the GLM and smoothing function; for random forest, at each of the 1,000 points on M obtained from a 9 to 1 split between train and test data.

We will consider the linear relationship $z_1 = X + Y - Z - 1$ and the nonlinear relationship $z_2 = (0.3X)^3 + YZ + (0.2Y)^4 - 1$ for our simulated species-environment relationships, where X, Y, Z are variables in our simulation which play the role of environmental variables, and which are scaled to have zero mean and unit variance.[4] For the shape of the environmental manifold, we consider four cases: a collection of random points (sampled from a uniform distribution), a plane, a sphere, and the empirical environmental manifold seen in Figure 2.6. These are illustrated in Figure 2.9.[5] In this comparative analysis, we use the term 'empirical environmental manifold' to denote the shape arising from the empirical GIS layers of geographical space in Section 2.2.2, in order to distinguish it from the three simulated shapes in our analysis. See the end of this section for a summary of this methodology.

After this first analysis with simulated environmental data, we again look at the accuracy of the GLM, random forest and smoothing methods with the same linear and nonlinear species response (given by z_1 and z_2 respectively), but now on two different subsets of points from the empirical environmental manifold. This corresponds more closely to the situation which arises in reality from unevenly sampled camera trap data. Our first subset is a sample of 5,000 points selected randomly across Borneo. In the second, we use the actual 484 locations where camera traps were placed in Sabah to collect species occurrence data (Hearn et al. 2018).

[4]We chose these two relationships since they gave a distribution of binary values on the environmental manifolds which did not lead to an extreme of either very few presences or absences, and we used a nonlinear relationship of this form so as to include a variety of possible nonlinearities (such as cross terms and different powers). Other than these two aspects, the particular coefficients of z_1 and z_2, and the form of z_2, could just as well have been chosen differently.

[5]We chose the uniformly random sample since it represents a null model for the environmental manifold, and the plane and sphere in order to have a variety of different possible geometries for our study, noting that approximations to all three shapes may be realised in empirical environmental data.

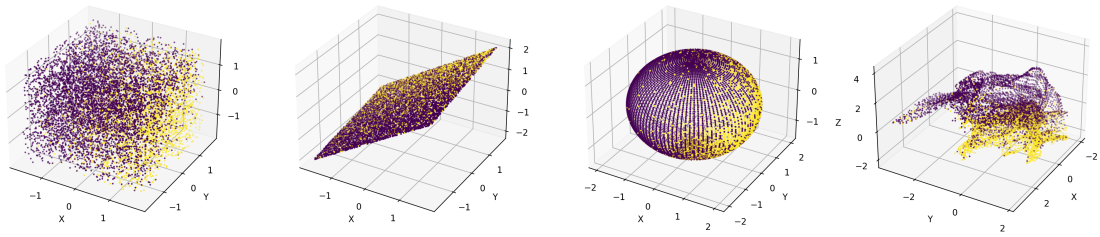


Figure 2.9: These are the four different shapes for the simulated environmental manifold in our analysis, constituted of 10,000 points: respectively, a uniform random selection, a plane, a sphere, and the empirical environmental manifold itself. They are plotted in three-dimensional environmental space, where the axes X, Y, Z represent environmental variables; for the first three shapes, these are simulated variables, and for the last (the empirical environmental manifold) they are the same empirical variables as in Figure 2.6. As in the previous figures of environmental space, the axes are normalised with standard scaling to have zero mean and unit variance. The colouration shows presence (yellow) and absence (blue), given by the linear simulated relationship z_1. For details on how these binary values are obtained, see the subsection below on creating a simulated data set.

Creating a simulated dataset

To create the simulated datasets for our analyses, we consider three environmental variables X, Y, Z. We first make our simulated environmental manifold M by sampling 10,000 points from the three-dimensional environmental space defined by X, Y, Z, to obtain one of the shapes mentioned above. Then, we choose our species-environment relationship z, which is given by a function of these three variables. For this analysis, z is a polynomial in X, Y and Z, being one of the two functions z_1 or z_2 above.

Now, to obtain a probability distribution on M from the mathematical function z, taking values between 0 and 1 (where values closer to 1 indicate a higher likelihood of our simulated species occurring, and values closer to 0 a lower likelihood), we use the logistic transform $\phi = e^z/(1 + e^z)$. This transformation produces a value $\phi(p)$ between 0 and 1 for each point p of the 10,000 points on our environmental manifold M. This value $\phi(p)$ corresponds to the probability of the simulated species occurring at each location, as a function of the

environmental variables at that location and the specified species-environment relationship z.

With this probability of species occurrence, we now generate a simulated presence-absence dataset which reflects those probabilities by, at each point p on M, sampling a random number $r(p)$ uniformly between 0 and 1, and calculating the difference $\phi(p) - r(p)$, giving a value between -1 and 1. If the resulting value is negative, then we relabel it as 0, and else relabel it as 1. This is a stochastic simulation of presences and absences that reflects the stipulated probability of occurrence at each location as a function of z. Our simulated dataset is the resulting collection of binary values, 0 and 1, at each point p on the environmental manifold. Figure 2.10 gives an illustration of this process on the environmental manifold, first coloured by the value of ϕ and then by the resulting binary value.

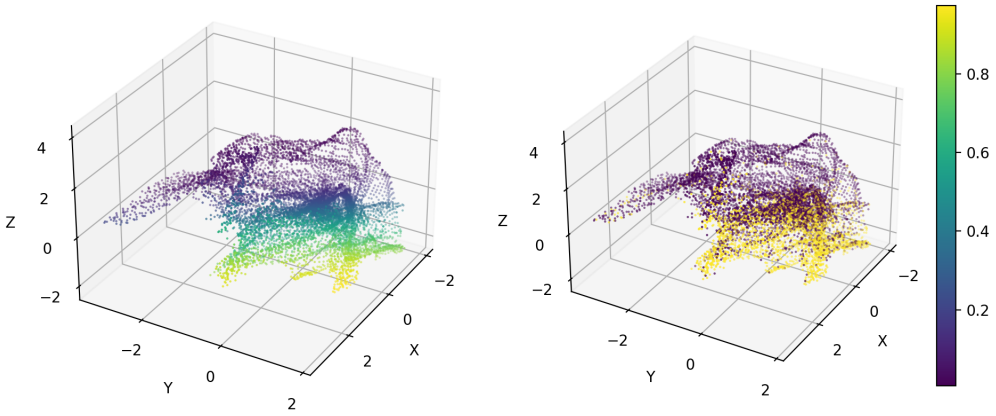


Figure 2.10: Colouration of the empirical environmental manifold: on the left, by the probability surface ϕ, and on the right, by the resulting stochastic presence-absence value. On the left, yellow and blue correspond to a higher chance of presence and absence, respectively; on the right, to the resulting binary presence and absence values. These values are obtained as described in this section.

Model setup

We use a logit link function for the GLM, due to the binary nature of the simulated data. As mentioned in the introduction, in configuring the GLM we are also required to choose a

priori the functional shape (e.g. linear, squared, exponential) for the species-environment relationship. We choose the linear predictor for our analysis due to its use being by far the most prevalent in ecological studies (McGarigal, Wan, et al. 2016). Since the GLM is a parametric model, whose parameters are the slope coefficients defining the predicted linear regression plane, we will also investigate its ability to recover these regression coefficients. The GLM and random forest are implemented in Python 3.7, the former with the `statsmodels` package and the latter with `sklearn`, versions 0.12.1 and 0.24.1 respectively (Seabold et al. 2010; Pedregosa et al. 2011).

For configuring the random forest and smoothing methods, there is the question of hyperparameters (also known as model parameters), which are the parameters chosen in the setup of a model and which determine how the model will run. For random forest, we use a 9 to 1 split between the training and test data, which is the default value in the `sklearn` package. In this study, we found that the only hyperparameter which increased the accuracy of random forest when changed from its default value was the maximum depth of a tree (which is the number of splits in each decision tree). For the smoothing function there is only one hyperparameter involved, namely the variance (or, bandwidth) σ of the Gaussian function K_σ defined in Section 2.2.1. Thus, for each of these two models, there was only one hyperparameter to tune: for random forest, a maximum depth of 7 and 8 was most accurate for z_1 and z_2, respectively; for smoothing, the optimal value for σ depended on both the relationship and the environmental manifold shape, and varied between 0.05 and 1.

All analyses were performed in Python 3.7 using Jupyter notebook. Since the simulated occurrence datasets have a random component, we run the simulation 100 times for each case of relationship, and environmental manifold or sample type, and take the mean average of the resulting correlation and error.

Summary of methodology

In summary, we first create our simulated environmental manifold M by sampling 10,000 points from environmental space, with axes X, Y, Z. We then define our species response z as a function of X, Y, Z, and apply the logistic transform $\phi = e^z/(1 + e^z)$ to obtain a probability of occurrence for each of the 10,000 points on M. From this we stochastically obtain the binary presence-absence data on M, as described in Section 2.3, which comprises our

simulated presence-absence species occurrence dataset. We apply the GLM, random forest and smoothing methods to these binary data, and determine their accuracy by calculating the resulting Pearson correlation coefficient and mean squared error from the difference between the true simulated values and predicted values at each point. We further evaluate the accuracy of all three methods on two smaller samples of environmental space. Lastly, we determine the predictive ability of the GLM to recover the slope coefficients of the regression plane defining the linear species relationship $z_1 = X + Y - Z - 1$.

2.4 Comparative simulation analysis: results

Simulation on the fully sampled environmental manifold

We present in Table 2.1 the results of our study on the fully sampled environmental manifold with 10,000 points. For each shape and method, we see the accuracy in recovering the simulated species occurrences, first for the linear and then for the nonlinear relationship. The first of the two numbers gives the Pearson correlation coefficient between the predicted values and the true simulated values, and the second gives the mean squared error between these values, both to four decimal places. A high correlation means that the predicted values are, on average, roughly proportional to the distribution of the true values; a low error means that there is little variance and bias between the individual predicted and true values. Thus, by these two metrics, the overall accuracy is higher when the first number is closer to 1, and when the second is closer to 0.

Simulation on sparser samples of environmental gradients

In empirical research, samples are taken at a subset of possible locations, rather than exhaustively (as was the case with the simulated datasets on the environmental manifold in Section 2.3). In this section, therefore, we present the results for the simulated relationships in the two sampling examples described above. This gives an illustration of the difference in inference and effectiveness of the three methods between 'ideal' sampling, consisting of a large random sample, and 'actual' sampling, which is typically smaller and nonrandom. These two smaller environmental manifolds are illustrated in Figure 2.11, and the results of this analysis are shown in Table 2.2.

Relationship	Manifold	GLM	Random forest	Smoothing
	Random	(0.9997,0.0001)	(0.9837,0.0031)	(0.9948,0.0014)
Linear	Plane	(0.9995,0.0001)	(0.9678,0.0014)	(0.9936,0.0006)
$z_1 = X + Y - Z - 1$	Sphere	(0.9998,0.0001)	(0.9877,0.0024)	(0.9958,0.0008)
	Empirical	(0.9997,0.0001)	(0.9774,0.0030)	(0.9881,0.0017)
	Random	(0.0399,0.0332)	(0.9557,0.0038)	(0.9899,0.0025)
Nonlinear	Plane	(0.0730,0.0099)	(0.9552,0.0009)	(0.9870,0.0005)
$z_2 = (0.3X)^3 + YZ + (0.2Y)^4 - 1$	Sphere	(0.0776,0.0184)	(0.9241,0.0042)	(0.9812,0.0020)
	Empirical	(0.1747,0.0124)	(0.8984,0.0026)	(0.9642,0.0011)

Table 2.1: Pearson correlation coefficient and mean squared error for each relationship, environmental manifold geometry and method, shown to four decimal places.

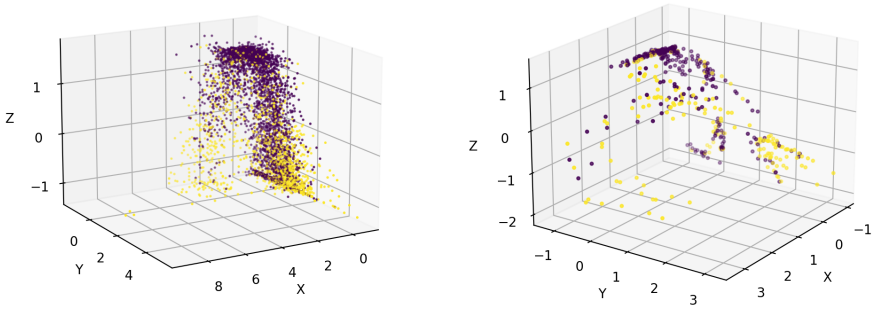


Figure 2.11: Two sets of locations, plotted separately in environmental space with axes X, Y, Z, defined by elevation, human footprint and forest cover, respectively. On the left, a 5,000-point random sample of locations from across Borneo; on the right, the actual 484 locations of the camera traps in Sabah, as detailed in Hearn et al. 2018. Blue represents species absence and yellow represents species presence, distributed according to the stochastic simulated dataset on these locations. As before, the axes have been normalised with standard scaling.

Relationship	Sample	GLM	Random forest	Smoothing
Linear	5,000	(0.9995,0.0001)	(0.9760,0.0037)	(0.9875,0.0020)
$z_1 = X + Y - Z - 1$	484	(0.9946,0.0015)	(0.9513,0.0097)	(0.9797,0.0081)
Nonlinear	5,000	(0.5292,0.0143)	(0.9174,0.0034)	(0.9610,0.0019)
$z_2 = (0.3X)^3 + YZ + (0.2Y)^4 - 1$	484	(0.5839,0.0112)	(0.7921,0.0067)	(0.8887,0.0040)

Table 2.2: Pearson correlation coefficient and mean squared error for each relationship, sample type and method, recorded to four decimal places.

Sensitivity of the GLM to environmental covariance

For the last part of our analysis, let us suppose that the GLM has accurately recovered the true simulated values on the environmental manifold, as was the case with the linear relationship $z_1 = X + Y - Z - 1$ above. Since it is a parametric model, we may further measure its accuracy in recovering the underlying parameters $(\beta_0, \beta_1, \beta_2, \beta_3)$ defining the species-environment relationship $z = \beta_1 X + \beta_2 Y + \beta_3 Z + \beta_0$. So, in our case, can the GLM recover the coefficients $(1, 1, -1, -1)$ of the terms in the relationship $z_1 = X + Y - Z - 1$? Surprisingly, the accuracy in recovering the simulated values of the linear relationship (seen in Table 2.1) need not reflect its accuracy in recovering these slope coefficients.

When the environmental manifold had a nonlinear shape (as was the case with the random points, sphere, and empirical environmental manifold), the GLM recovered the parameters β_i with an average error of approximately 0.02. However, when the environmental manifold had the shape of a plane (which, in this case, was given by $4X + Y - 2Z - 5 = 0$), the GLM predicted $(-0.063, 0.705, 0.113, -1.013)$ for the coefficients, which, for β_1, β_2 and β_3 is extremely inaccurate (Table 2.3). This error still occurred, sometimes to a greater magnitude, when varying the coefficients β_i of the linear relationship z_1, when rotating and translating the environmental manifold plane, and when adding small degrees of noise or nonlinearities orthogonal to the plane. In the language of statistical linear algebra, this problem arises because the design matrix (which is the matrix of values of the predictor variable X, Y, Z) does not have sufficient rank to provide a unique value for the slope coefficients of the regression plane. If you are mathematically inclined, then you may wish to see in Section 2.7.3 how this can be expressed by a visual geometric argument involving the environmental manifold.

Environmental manifold	Predicted coefficients
Random	(0.975,0.998,-1.005,-1.037)
Plane	(-0.063,0.705,0.113,-1.013)
Sphere	(0.994,1.040,-1.040,-1.040)
Empirical	(0.994,0.983,-0.965,-0.988)

Table 2.3: The GLM's prediction for the slope coefficients $(1, 1, -1, -1)$ of the linear relationship $z_1 = X + Y - Z - 1$, with each of the four shapes from Section 2.3.

2.5 Discussion

Describing the Hutchinsonian fundamental and realised niches, and understanding scale dependence in the response of a species to their environment, are two central questions in modern ecological science, both of which have received substantial attention in recent years (Blonder et al. 2014; Chandler et al. 2016; Holt 2020). In this chapter, we have illustrated how smoothing in environmental space, and the hitherto unexplored environmental manifold, are novel and capable tools for gaining greater insight into these two topics. As explained throughout this chapter, and treated with more detail in the two appendices below, the environmental manifold gives us a precise description of the *realisable niche*: the subset of niche space in which the Hutchinsonian realised niche is constrained to occur. Moreover its multivariate nature means that the environmental manifold is a concept which can lead to surprising findings in ecological data, since it allows us to consider and observe the nonlinear interactions of several environmental variables simultaneously. Furthermore, with its capacity for handling scale-dependence and nonlinearities in both the species response and the environmental manifold, we have demonstrated that smoothing in environmental space performs very well in comparison with mainstream models such as the GLM, and with modern machine learning tools in ecology such as random forest.

By stipulating known 'species-environment relationships', the techniques of simulation give us the ability to quantify and compare the performance of the different statistical methods which are widely used in modelling and predicting these relationships.[6] Recent work

[6]When discussing species-environment relationships in this chapter, it is in the context of how a species responds to changing gradients of environmental variables, both of which are studied through a quantitative viewpoint. The quotation marks appear here to remind the reader that simulation techniques and mathemat-

has used simulation experiments similar to this study, also for the purpose of evaluating the efficacy of various methods to infer predictors of species abundance (Atzeni et al. 2020; Chiaverini et al. 2021). This chapter develops the simulation framework further, by investigating both linear and nonlinear relationships, and also different interactions between environmental variables. In our analysis, we used these techniques to compare the predictive ability of the smoothing function with that of the GLM and random forest. We found that the random forest model outperformed GLM when there were nonlinear and interactive terms in the species-environment relationship, and also found, for the first time, that random forest machine learning is robust to the shape of the environmental manifold. Furthermore, we found the smoothing function to be more accurate than the random forest in every setting, particularly in situations with greater sampling bias. Finally, we saw that the GLM was unable to recover the slope coefficients of the linear species-environment relationship for certain shapes of the environmental manifold.

Effects of functional complexity

To our knowledge, this is the first investigation into how functional complexity (which is determined by, for example, the number of variables and nonlinearities in the predicted response) interacts with environmental covariance in affecting the performance of different models to infer species-environment relationships. We found that when the relationships were linear, all three methods performed well in correctly predicting species occurrence. Additionally, when the environmental manifold was of a highly nonlinear shape in our study, the GLM accurately recovered the slope coefficients β_i of the regression plane.

Nonlinearity of the response function strongly affected the performance of the GLM, greatly reducing its ability to predict species occurrence and estimate slope coefficients. This sensitivity of the GLM to complex responses stands in contrast with recent studies such as Ash, D. W. Macdonald, et al. 2021. On the other hand, random forest and smoothing performed very well with the nonlinear relationship – almost as well as they did on the linear relationship – suggesting these two methods to be highly capable of recovering complex nonlinear species responses. Moreover, the smoothing function proved more accurate than

ical formulae, while often very helpful and powerful, do not capture the fullness of ecological relationships in reality.

random forest in all cases, regardless of functional complexity.

Effects of geometric complexity

With the metrics of accuracy used for the comparative analysis in this chapter, the geometric complexity of the environmental manifold generally did not have a great influence on the performance of any of the three methods. The exception is the case of a planar environmental manifold affecting the ability of the GLM to recover the coefficients β_i. Upon further investigation, we found this error with the GLM to still occur in other similar instances, such as when degrees of noise or nonlinearities were added orthogonal to the planar environmental manifold. Although a perfect planar geometry is not to be expected in empirical environmental data, this finding means that if there are portions of approximate constancy among any linear combination of the environmental variables, the GLM may be unable to accurately recover the parameters defining even a linear species response; this may very well arise if any of the environmental gradients are not well-sampled. From this, we conclude that the random forest and smoothing function are highly robust to the geometric complexity of the environmental manifold, but the ability of the GLM to predict regression coefficients can be strongly affected by certain types of environmental covariance.

Effects of sampling bias

With a linear species-environment relationship, we found the GLM to be the most accurate method for determining the species response, for all types of sampling; however, the strong sensitivity of the GLM to functional complexity remains, regardless of sampling effort. As with the fully sampled environmental manifold, in the case of the sparser empirical data (which reflects the sampling bias arising in practice), we found the smoothing function to be more robust than random forest, particularly with the more complex species response. We also see that the larger 5,000-point random sample gives rise to greater model performance than with the smaller, opportunistic sample; all models, however, were most accurate with the full sampling represented by the 10,000-point environmental manifold. This shows that, while the smoothing function is not strongly affected by sampling bias, its accuracy cannot be considered to be independent of sampling effort, in contrast with the aforementioned claim in Broennimann et al. 2012 regarding kernel smoothing methods.

Further routes of development for the environmental manifold

As motivated in Section 2.2.1, having a precise understanding of the way in which environmental gradients vary together can give important and nuanced insight into species-environment relationships. Furthermore, as demonstrated in detail in Section 2.6.1 below, *observed nonlinearities in a species response may arise solely because of the nonlinear shape of the environmental manifold*, even when all components of the underlying relationship are linear. With the increasing availability of highly accurate and fine-scale GIS data, it is possible to actually visualise, quantify and work with the environmental manifold as a practical tool in ecological analyses, which gives us access to a deeper understanding of the species-environment relationships we may observe from empirical data. In this chapter we used only three environmental variables when working with the environmental manifold, for ease of visualisation and exposition, but the concept and insights of the environmental manifold are equally applicable for any number of environmental variables, suggesting the environmental manifold to be a uniquely valuable concept and technique for ecological analyses with large and complex datasets. Thus, the development of the environmental manifold as such a tool for ecological science could form the basis for promising future theoretical and empirical work, in line with the latest developments in computation ecology (Hoogen et al. 2019; Rey et al. 2020).

Another salient aspect of the environmental manifold is its relevance to the Hutchinsonian realised niche, the modelling of which is of fundamental importance in community ecology. With the methods developed in this chapter, we are now afforded a precise description of the subset of niche space which is geographically realised: the environmental manifold is the *realisable* Hutchinsonian niche. This means that even if the Hutchinsonian fundamental niche is simply described and presumed to be geometrically isotropic, traditional niche descriptions will fail if the realisable niche (in other words, the environmental manifold) is complex and nonlinear. As a result, without the information provided by the environmental manifold, we can only tell half the story of a species' niche structure. For example, we may find from empirical data that the occurrence probability of a certain species is close to zero in a region of three-dimensional niche space; this may reflect an intolerance of the species to this set of environmental conditions - but equally, it may represent a region of this niche space *which is not geographically realised*. The knowledge to discern between these two very different realities is provided by the environmental manifold, which has heretofore been absent in

attempts to quantify the ecological niche (such as Blonder et al. 2014; Broennimann et al. 2012; Holt 2009; Swanson et al. 2015). We have also shown in this chapter that random forest and smoothing are capable of handling these nonlinearities which arise in the realised niche, in contrast with the GLM which assumes the underlying predictor space to be isotropic.

Conclusion

Simulation frameworks can be very helpful for exploring the effectiveness of different modelling methods, and in studying the influences of factors such as sampling design, sample size, complexity of response and environmental covariance on the performance of such methods. The results of our comparative simulation analysis show that random forest and smoothing are robust to the complexity of both species response and environmental covariance, with the smoothing function proving more accurate in every case; in contrast, the GLM is strongly affected by the functional complexity of the species response. Furthermore, the GLM can also be highly impacted by certain shapes of the environmental manifold. This suggests that, given the expected nonlinear and interactive relationships in empirical ecological data, methods like random forest and smoothing which are equipped to handle complex and *a priori* unknown responses are likely to be preferable and more capable than parametric models like the GLM.

This chapter shows that applying a kernel smoothing function to species occurrence data in environmental space is a promising and powerful way to explore and observe the patterns of species-environment relationships and scale dependence in environmental space, the latter of which remains little understood despite its relevance in community ecology. The smoothing function provides a conceptually simple and mathematically tractable approach to recover complex and nonlinear species occurrence patterns, in a manner which inherently accounts for sampling bias. In addition to the smoothing function, we have introduced the environmental manifold, a novel concept for ecology with deep implications for understanding the Hutchinsonian niche. The possibility of delving into the mysteries of the environmental manifold and its connections with other ecological questions lies beyond the scope of this study. Nonetheless, this chapter aims to make apparent that the environmental manifold applies to contexts much wider than that studied in this chapter. Indeed, the combination of its underlying ubiquity in questions pertaining to species-environment relationships, together

with its mathematical richness and depth, makes it a tantalising realm of further study - both as an accomplice in future ecological explorations, and also as a matter in its own right.

2.6 Appendix A: Details on smoothing in environmental space

2.6.1 Nonlinear correlations from linear responses

We present here some visual examples of the phenomenon discussed in Section 2.2.1, in which we prove that nonlinearities in the environmental manifold explain why, even after accounting for sampling bias with the smoothing function, the observed correlations of species abundance along an environmental gradient may very much not reflect their response to that variable 'in general'.[7] In this manner, we may find highly nonlinear and multimodal correlations to arise even from very simple species-environment relationships, such as when the response to some or all environmental variables is linear.

To illustrate this, on the same 484 empirical camera trap locations mentioned in Section 2.3, we used the techniques of Section 2.3 to simulate four different species-environment relationships as a function of the three environmental variables (elevation, human footprint and forest cover) discussed in Section 2.2.2, which we label here as X, Y, Z respectively. These four functions are $z_1 = X$, $z_2 = X + 5Y$, $z_3 = X + 3Z$, and $z_4 = X + 2Y^2 - 3Z^2$, which are all linearly increasing with respect to the elevation variable X. Thus, as elevation increases, we may expect that the occurrence probability of our simulated species also increases. However, in Figure 2.12 we see that the correlations which emerge after accounting for sampling bias show this only to be roughly the case for $z_1 = X$, which is a function solely of elevation; when the species responds also to human footprint and forest cover, such as in z_2, z_3 and z_4, we observe correlations which do not at all reflect the linearity (or even monotonicity) of its response to elevation.

These nonlinearities arise from a linear response to elevation precisely because of the complexity with which the three environmental variables co-vary across these locations, as discussed in Sections 2.2.1 and 2.2.2. What if we instead sample our locations uniformly

[7] The quotation marks are used here to remind the reader of the impossibility to accurately isolate and subsequently generalise the relationship between a species and one environmental variable. This is because, for every empirical site of data collection, the response to one variable necessarily occurs simultaneously in response to other variables.

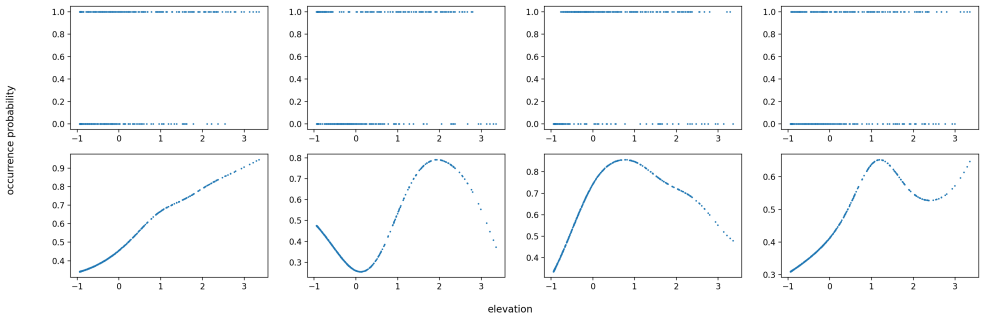


Figure 2.12: Nonlinear correlations arising spuriously from linear relationships, due to nonlinear environmental covariance. From left to right, we see the emergent correlations for the four species-environment relationships z_1, z_2, z_3 and z_4 respectively, with elevation on the horizontal axis. For each relationship, the upper graph displays the binary presence-absence data, and the lower graph shows the occurrence probability which emerges when applying the smoothing function to account for sampling bias ($\sigma = 0.5$). Though all relationships are linearly increasing with respect to elevation, the only observed correlation which approximately reflects this is that of z_1, which is a function of elevation only.

randomly across environmental space? Figure 2.13 shows that if the environmental covariance were isotropic, then all of the smoothed graphs in Figure 2.12 would have instead displayed a linearly increasing shape. We can thus conclude that the environmental manifold, which gives us the precise information of how our environmental variables co-vary in geographical space, plays a fundamental role in understanding the correlations which emerge from the response of a species to their environment.

2.6.2 Sample code for the smoothing function

First, let us recall the formula for the smoothing function, as defined in Section 2.2.1:

$$S(x) = \frac{\sum K_\sigma(x, x') \cdot V(x')}{\sum K_\sigma(x, x')}, \quad \text{where} \quad K_\sigma(x, x') = e^{-\frac{(x-x')^2}{2\sigma^2}}$$

As noted before, the sum is taken over all points x' in the dataset.[8] We now present the sample code for the smoothing function used in our simulation, implemented in Python 3.7:

[8] If the dataset is much larger than those used in this analysis, then the kernel can be truncated to improve run times.

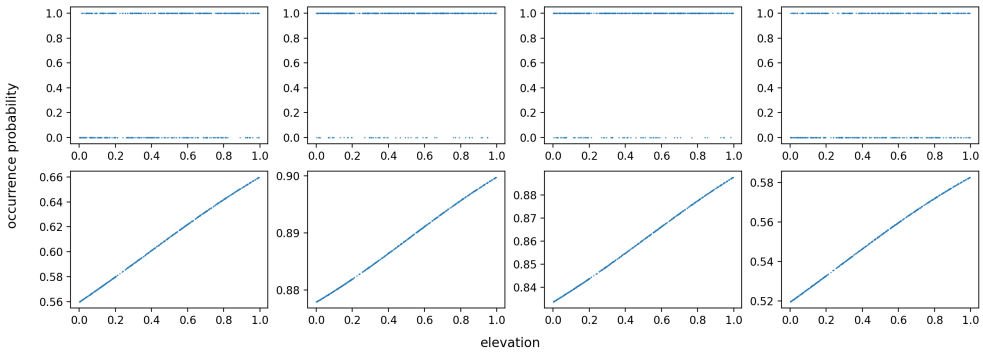


Figure 2.13: Emergent correlations for the same relationships z_1, z_2, z_3, z_4 as before, again with elevation on the horizontal axis, but now with the 484 data points instead sampled uniformly randomly from three-dimensional environmental space. These smoothed graphs show the true linear nature of the underlying response to elevation, which now becomes visible precisely because of the uniformity of the environmental manifold.

```
import numpy as np
from scipy.spatial import distance


def S(x, V, sigma):
    D = distance.cdist(x, x, 'sqeuclidean')
    K = np.exp(- D / (2 * sigma ** 2))
    return np.sum(K * V, axis = 1) / np.sum(K, axis = 1)
```

The input data consist of the following: `x`, an array consisting of the coordinates of the points in environmental space, with each row giving the coordinates of one point; `V`, a vector of binary presence-absence values at each point; `sigma`, the smoothing parameter for the Gaussian kernel K_σ defined in Section 2.2.1. The smoothing function, `S`, first computes the matrix of squared distances `D` for the occurrence points in environmental space (whose coordinates are given by `x`), then calculates the kernel `K`, and finally returns the vector of smoothed `V`-values. For example, in our simulation on the environmental manifold in three-dimensional space, `x` is a 10,000×3 numpy array and `V` is a vector of length 10,000.

2.7 Appendix B: Mathematical aspects of the environmental manifold

2.7.1 Defining the environmental manifold

In this section, we touch on some of the more mathematical aspects of the environmental manifold. We begin by noting that our environmental space $\mathbb{E}$ can be thought of as the m-dimensional space of real numbers $\mathbb{R}^m$, where m is the number of environmental variables used for the axes in $\mathbb{E}$. Consider the construction of the environmental manifold from Section 2.2.2, which involves the three environmental variables of elevation, human footprint and forest cover. We label them here as e_1, e_2, e_3 respectively. Mathematically speaking, in constructing the environmental manifold we think of the GIS polygon representing Borneo as a subset U of two-dimensional space $\mathbb{R}^2$ parameterised by latitude and longitude. We then look at the image $M = f(U)$ of the map $f : U \to \mathbb{R}^3$ defined by $f(x, y) = (e_1(x, y), e_2(x, y), e_3(x, y))$ for (x, y) in U. In practice, the function f is defined on discrete data, namely the pixels of the GIS polygon. However, f can be theoretically seen as continuous and piecewise-linear: it takes the flat GIS polygon of Borneo and maps it to a piecewise-linear surface, by 'joining up the dots' of the pixels of the GIS polygon in environmental space $\mathbb{E}$ (as seen in Figure 2.8).

In practice, the resulting position of these pixels in $\mathbb{E}$ is provided by the values of those pixels in the empirical GIS layers of the environmental variables. Namely, we define the mapping f by sending each element (x, y) of a meshgrid to the point in $\mathbb{R}^3$ given by $(e_1(x, y), e_2(x, y), e_3(x, y))$ as mentioned above, where the e_i are the matrices in Python obtained from the environmental GIS layers and $e_i(x, y)$ is the (x, y)-entry of that matrix.

More generally, we could use any number m of environmental variables, and consider the image $f(U)$ in $\mathbb{R}^m$. This map f would be equivalent (up to isometry of $\mathbb{R}^m$) to considering the metric $||.||_{\mathbb{E}}$ on U, where $d(p, q) \coloneqq ||p - q||_{\mathbb{E}}$ is the Euclidean distance between $f(p)$ and $f(q)$ in m-dimensional environmental space $\mathbb{E}$. Note that the environmental manifold may not be a 'manifold' strictly in the mathematical sense, and that $||.||_{\mathbb{E}}$ may not be positive definite, since the environmental manifold could cross over itself. This would happen precisely when two points in the region U of geographical space have the same value for each of the m environmental variables considered in $\mathbb{E}$. In light of this last point, we have not shortened the name 'environmental manifold' to 'manifold' at any instance in this thesis.

2.7.2 Ecological explorations with the environmental manifold

One exciting aspect of the environmental manifold is that it provides a fertile ground for mathematical insights in an ecological context, particularly those of a multi-dimensional differential, geometric or topological nature. The visual explanation below of the surprising inaccuracy of the GLM in certain settings gives a basic example of this, affording the insight that an important role is played by the shape of the environmental covariance in predicting species distributions.

There is much to explore with this new multivariate concept in ecology. One example which arises in this chapter is that the occurrence probability of a species over some geographical region U can be thought of as a map from U to the unit interval $[0, 1]$. In our case, we obtained this as the composition of the three maps $\phi \circ z \circ f : U \to f(U) \to \mathbb{R} \to [0, 1]$. Recall that the map ϕ was given by the logistic transform $\phi(z) = e^z/(1 + e^z)$ of a function $z : \mathbb{E} \to \mathbb{R}$. As a result, we can view the 'thickened' level sets $c_\epsilon = \{\mathbf{x} \in f(U) \mid |\phi(\mathbf{x}) - c| < \epsilon\}$ of ϕ restricted to the environmental manifold $f(U)$ as those regions of $f(U)$ with occurrence probability approximately c, which will typically look like 1-dimensional subspaces of $f(U)$. Framing species abundance thresholds in terms of these level sets, and using the smoothing function to help us recover these level sets from noisy occurrence data, could notions of gradient descent, Morse theory, and persistent homology (see Ghrist 2014) be valuable for describing the realised niche?

Furthermore, among methods which seek to recover the environmental drivers of species occurrence patterns, the smoothing function is unique in being a genuine mathematical function on the occurrence data points themselves, and so is open to mathematical analysis in a way in which models such as the GLM and random forest are not. For example, could we understand more deeply the shapes of the correlations seen in Figures 2.2 and 2.3 from the knowledge of: (1) the environmental manifold geometry, and (2) the smoothed species data on the environmental manifold? This would give us insight into not just a richer and more accurate description of the Hutchinsonian niche, but could also help practitioners in environmental management effect policy which better reflects how species abundance is shaped by environmental conditions.

2.7.3 The geometry of intersections

We now look at the error of the GLM when the environmental manifold is a plane P, in its ability to recover the slope coefficients $(\beta_0, \beta_1, \beta_2, \beta_3)$ in the linear relationship $z = \beta_1 X + \beta_2 Y + \beta_3 Z + \beta_0$. The answer has an intuitive geometric interpretation, and is due precisely to the shape of the environmental manifold. Let us denote the specific linear relationship $X+Y-Z-1$ and environmental manifold plane $4X+Y-2Z=5$ from our earlier analysis by z_1 and P_1 respectively, to distinguish it from a general linear relationship z and environmental manifold plane P, which we use in this section.

First, recall that the GLM tries to predict the coefficients β_i defining z. So, from the GLM we obtain a prediction $\overline{z} = \overline{\beta}_1 X + \overline{\beta}_2 Y + \overline{\beta}_3 Z + \overline{\beta}_0$, where the $\overline{\beta}_i$ are the predictions for the β_i. This equation for $\overline{z}$ defines a set of planes in three-dimensional space as the value of $\overline{z}$ varies, corresponding to different levels of occurrence probability. These planes of $\overline{z}$ move along the normal direction $\mathbf{n} = (\overline{\beta}_1, \overline{\beta}_2, \overline{\beta}_3)$, and thus intersect the environmental manifold plane P in a series of parallel straight lines.

The key point is that the accuracy of the GLM in recovering the simulated linear relationship z_1 (Table 2.1) must mean that these parallel lines of intersection between the predicted planes of $\overline{z_1}$ and P_1 are almost exactly the same as those of z_1 and P_1. However, given these parallel lines of intersection, there is still one degree of freedom in defining the planes given by $\overline{z_1}$. With this information, the GLM was only able to recover z_1 up to a rotation along the axis of these parallel lines, as we see in Figure 2.14. Indeed, the environmental manifold plane P_1, relationship plane z_1 and predicted plane $\overline{z_1}$ all differ by a rotation about the same axis of intersection with P_1, with the true relationship z_1 and the predicted relationship $\overline{z_1}$ differing by approximately 65 degrees along this axis.

To investigate this further, I explored rotating and translating the environmental manifold plane P (which, for this problem, would be equivalent to varying the coefficients β_i defining z), adding degrees of noise orthogonal to P, and adding nonlinearities orthogonal to P (such as a sinusoidal surface). I found that, when the environmental manifold was a plane, the accuracy of the predicted slope coefficients was determined by the angle between the environmental manifold plane P and the relationship planes defined by z, where accuracy of $\overline{z}$ increases with orthogonality between z and P. When nonlinearities were added, the accuracy of the predicted coefficients depended on the manner in which the relationship plane z intersected

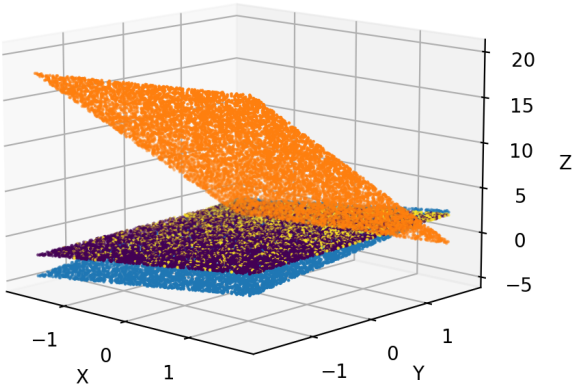


Figure 2.14: The environmental manifold plane P_1 used in our simulation analysis, defined by the equation $4X + Y - 2Z - 5 = 0$. It is coloured by yellow and dark blue, corresponding to locations of respective presence and absence of the simulated species. The plane given by the linear relationship z_1 is coloured light blue, and the plane predicted by the GLM is coloured orange. The predicted plane has coefficients $(-0.063, 0.705, 0.113, -1.013)$, in contrast with the true relationship plane $(1, 1, -1, -1)$, and they differ by an angle of approximately 65 degrees.

the environmental manifold. Some of these findings are displayed in Table 2.4.

Manifold	Predicted coefficients
P_1	(-0.063,0.705,0.113,-1.013)
Plane orthogonal to z_1	(0.996,1.013,-0.979,-0.958)
Plane approximately tangent to z_1	(0.010,0.014,0.017,0.007)
Plane defined by $Z = 0$	(1.013,1.010,0,-0.968)
P_1 with 0.1 orthogonal random noise	(2.148,1.263,-1.554,-2.334)
P_1 with 0.5 orthogonal random noise	(0.898,1.016,-0.951,-0.893)
Sinusoidal surface with amplitude 0.5	(0.778,0.763,-0.008,-0.999)
Sinusoidal surface with amplitude 5	(1.068,0.946,-0.991,-1.003)

Table 2.4: The GLM's prediction for the slope coefficients $(1, 1-1, -1)$ of the linear relationship $z_1 = X + Y - Z - 1$, with six different shapes for the environmental manifold. Some are linear, and some are nonlinear to differing degrees. P_1 is the environmental manifold plane used in our simulation analysis.

These examples demonstrate that when the environmental manifold plane P lies orthogonal to a linear relationship z, the GLM's predicted coefficients are most accurate. In contrast, when P and z are approximately tangent, the predictions are extremely inaccurate. In the case of the plane P defined by the equation $Z = 0$, we find the coefficients of X, Y and the intercept accurately recovered, but the coefficient of Z is predicted to be 0. This is an example of the phenomenon that, if the environmental sampling is approximately constant along some environmental gradient, then the GLM cannot predict the coefficient for this environmental variable. The latter four cases in the table relax the constraint of nonlinearity, and demonstrate that if the environmental manifold is not sufficiently nonlinear, then the same errors can arise.

So, the GLM can only 'see' the species-environment relationship z where it intersects the environmental manifold. Thus, when the environmental manifold is a plane - or more generally, approximately constant along some linear combination of axes in environmental space - the GLM does not have enough information to recover the coefficients β_i defining a linear relationship z. This also explains the accuracy of $\overline{z}$ in the other three choices of environmental manifold in our simulation analysis, in which the GLM sees enough of the

species response planes z via their intersections with the environmental manifold M to fix the remaining degree of freedom. For example, if the intersections are shaped like a circle (like the case in our simulation when M was a sphere), then M curves into enough dimensions of environmental space to fix the predicted planes $\overline{z}$.

Thus, in this simple example in three-dimensional space, if the environmental data are constant along certain axes (as is the case for a plane) – or, more generally, when the intersections of z with M are not sufficient to fix the coefficients $\overline{\beta}_i$ – the GLM may be highly inaccurate in predicting the parameters of a species-environment relationship, precisely because of the manner in which the environmental variables co-vary, as captured by the shape of the environmental manifold.

Chapter 3

Pathwalker



Figure 3.1: This chapter is closely adapted from the *International Journal of Geo-Information* article *Pathwalker: A New Individual-Based Movement Model for Conservation Science and Connectivity Modelling* (Unnithan Kumar, Kaszta, et al. 2022). Much of Pathwalker was written while staying with Sam in Arizona, where each day I would walk in the Coconino forest and greet the land with my animal senses. Photograph by Siddharth Unnithan Kumar, 12th July 2021.

3.1 Introduction: Animal movement and landscape connectivity

Movement is fundamental to all ecological processes of this more-than-human world. In conservation science, animal movement is usually studied in the context of gene flow, dispersal, population dynamics, and shifting habitats in response to changes in climate and human activity (Gibbs 1998; Moller et al. 2004; Tucker et al. 2018). Here, movement is often understood in response to a range of biotic and abiotic drivers, constituting a complex relationship between individuals and the landscape that varies at multiple scales in space and time (Wiens 1989). Understanding and predicting animal movement pathways forms a cornerstone of ecological science and its application to conservation practice, but they are usually very challenging to model accurately due to the countless factors which shape and affect movement patterns (Nathan et al. 2008).

'Landscape connectivity', commonly defined to be the extent to which a landscape facilitates the movement of individuals or populations, is a dynamic phenomenon based on the cumulative movement choices of individuals across space and time (Tischendorf et al. 2000). Conceptually, it provides a tractable and powerful methodology for analysing and mapping organism movement patterns, and its widespread utility has been established across an enormous body of ecological work (Hilty et al. 2006; Rudnick et al. 2012). As such, the theory, modelling and prediction of landscape connectivity has grown to become a central focus of applied ecology and conservation science (Cushman, McRae, et al. 2013). Modelling connectivity typically requires two components: (1) a 'landscape resistance surface', and (2) a mathematical algorithm which then uses this resistance surface to predict landscape connectivity.

Resistance surfaces

Several techniques for modelling landscape connectivity have been developed in recent years (Unnithan Kumar, Turnbull, et al. 2022b). The most prominent methods today use 'resistance surfaces', which are pixelated maps (in the form of geospatial image layers) that provide the spatially-explicit input data necessary for modern connectivity models (Zeller, McGarigal, and Whiteley 2012). Each pixel is assigned a numerical value which reflects the estimated

'cost of movement' through the region of the landscape corresponding to that pixel, giving a spatiotemporally static approximation to how landscape structure affects movement. Despite its widespread usage as the basis for modern connectivity models, the paradigm of landscape resistance does have its limitations as a framework for modelling animal movement, which we analyse in detail in Chapter 5.

Resistance surfaces can be estimated empirically using any of a wide variety of data types, including occurrence data, relocation data, genetic data, and GPS telemetry data. The latter two data types are thought to have the strongest performance in estimating resistance (Zeller, Jennings, et al. 2018), and fine-scale telemetry data are often preferred since they are more sensitive to temporal variation than genetic data (Zeller, McGarigal, and Whiteley 2012). Moreover, since dispersal is considered to be the primary process by which organisms move between populations, data types like telemetry that reflect dispersal events in a spatially explicit manner are particularly important for understanding landscape connectivity and its drivers (Elliot, Cushman, D. W. Macdonald, et al. 2014).

Modelling connectivity

Using these resistance surfaces, connectivity models typically then evaluate landscape connectivity with an algorithm based on either cost-distance measurements, or electrical circuit theory from classical physics (Cushman, McRae, et al. 2013). The simplest cost-distance algorithm is the 'least-cost path', which identifies a path (or corridor) between two geographical locations on the resistance surface that minimises the accumulated cost of movement between those locations (Adriaensen et al. 2003). This was later extended by synoptic approaches like the factorial least-cost paths algorithm, which computes the least-cost paths between any set of source points simultaneously (Cushman, McKelvey, et al. 2009).

However, there are substantial constraints to using these least-cost path approaches in practice. There is little reason to assume that an animal knows the route of the least-cost path, or even thinks in those terms. Moreover, the destination may not be known to the animal, and even if this were the case, obtaining the knowledge of their precise destination can be very difficult, especially with dispersing animals. To remedy this latter issue, the resistant kernels method was developed (Compton et al. 2007). It is a cost-distance algorithm that estimates connectivity as a function of source locations, landscape resistance and dispersal

thresholds, without requiring knowledge of target locations.

In contrast, based on electrical circuit theory, Circuitscape is a connectivity model which simulates electrical current flow across a resistance surface (McRae et al. 2008). Source locations of movement are treated as nodes of a circuit, resistance values as the strength of electrical resistors, and animals are modelled as electrons 'flowing through this circuit'. This algorithm produces a current density for each pixel on the resistance surface, with higher current values assumed to reflect higher degrees of connectivity. See Figure 3.2 for an illustration of the outputs of Circuitscape, factorial least-cost paths and resistant kernels, each using the same simulated resistance surface.

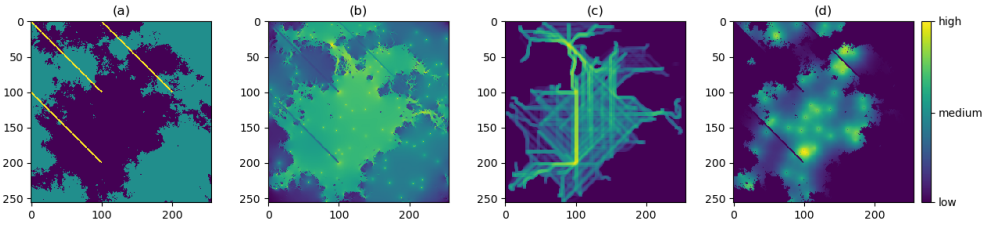


Figure 3.2: Illustrations of three connectivity models – Circuitscape (b), factorial least-cost paths (c), and resistant kernels (d) – applied to a resistance surface (a). For the resistance surface, the blue, green, and yellow background colours, respectively, represent low (1), medium (50), and high (100) resistance values. For the three connectivity maps, the blue, green, and yellow background colours, respectively, represent low, medium, and high connectivity. Axes are labelled by matrix coordinates.

Individual-based models

Despite their widespread usage and application in diverse ecological contexts, many fundamental drivers of animal movement are absent in the above models. For example, they do not account for varying mortality risk or patterns of autocorrelation occurring in movement (Cushman, Chase, et al. 2005; Dray et al. 2010). Nor do they attend to the multiple spatial scales at which movement choice occurs (Wiens 1989). These are among several other factors which play a major role in shaping movement patterns, including: spatiotemporal variability (Kaszta, Cushman, and Slotow 2021; Osipova et al. 2019), demography (Elliot, Cushman, D. W. Macdonald, et al. 2014), and interspecific interactions (Gorini et al. 2012). We return

to discuss this further in Chapter 5.

The algorithms mentioned above predict landscape connectivity primarily using a resistance surface and a collection of specified locations. In contrast, individual- (or agent-) based methods model the movement within a landscape by explicitly simulating the processes that may influence individual movement choice, and thus can provide a 'process-based' approach to predicting connectivity. They are often easier to adapt to include parameters that account for the aforementioned aspects of movement which are absent in algorithms such as Circuitscape, meaning that individual-based methods typically incorporate much more behavioural detail in modelling animal movement (DeAngelis et al. 2005).

Early agent-based models were limited in their use for conservation practice due to the lack of detail afforded to spatial complexity, in which they treated the landscape either as homogeneous or as a binary patch mosaic (see Hargrove et al. 2005; Kareiva and Shigesada 1983; Schumaker 1996). More sophisticated individual-based algorithms have since been developed, such as HexSim and RangeShifter (Bocedi et al. 2021; Schumaker and Brookes 2018), which now use resistance surfaces to provide the same degree of spatial data as used in circuit- or cost-based connectivity models. However, while there has been a proliferation of computational algorithms implementing circuit- and cost-based connectivity models, spatially-explicit individual-based models have not yet seen comparatively widespread application in connectivity modelling, likely because their configuration and usage are generally focused in the field of population dynamics (but see Schumaker, Brookes, et al. 2014).

3.1.1 Chapter overview

Motivated thus, in this chapter we introduce and describe a new spatially-explicit, individual- and process-based movement model called Pathwalker, designed to predict individual movement paths and map connectivity with relatively few parameters. Pathwalker also uses resistance surfaces for its spatial input data. This algorithm combines three basic movement mechanisms, based on: energetic cost of movement, resistance-biased movement choice, and mortality risk. There are two further parameters which incorporate two kinds of directional bias: differing degrees of autocorrelated movement, and movement towards a given destination. Additionally, Pathwalker accounts for a multi-scale response to the spatially heterogeneous resistance surface by allowing the movement mechanisms to be functions of landscape

resistance at different spatial extents around the focal point of movement. Pathwalker outputs individual paths starting from given source points on a resistance surface, together with useful statistics about each path. These paths can be aggregated to produce a movement density surface, which estimates the distribution of movement on the resistance surface and thus gives a process-based prediction of landscape connectivity. There is also the option to produce figures of the individual paths and the density surface (Figure 3.3).

Within the currently employed framework of landscape resistance and connectivity, the flexibility and detail made available by Pathwalker make it a valuable tool for modelling movement paths in complex landscapes, and for providing predictions of connectivity which may more accurately reflect the multitude of ways an organism moves through their environment. Unlike more elaborate software such as HexSim and RangeShifter, we have designed Pathwalker to have a similar straightforward interface and setup to the major connectivity models like Circuitscape and resistant kernels, for the sake of familiarity to the connectivity modelling community and to enable its immediate uptake as a software for mapping movement and connectivity. Furthermore, the process-based simulated movement data provided by Pathwalker can be used to test the performance and accuracy of different modelling methods and data sources used in movement and connectivity studies, which is the focus of the next chapter.

This chapter illustrates how Pathwalker works. We describe the model structure and parameters, and then perform some elementary computations to show how the different parameters interact and the extent to which they influence the resulting simulated movement. In addition, we provide an appendix which demonstrates a result of theoretical interest using Pathwalker: we derive a movement density function for different levels of autocorrelated movement, which gives insightful information for modelling the effects of dispersal thresholds on connectivity predictions. The Pathwalker software is written in Python 3 and can be obtained freely online at `https://github.com/siddharth-unnithankumar/pathwalker` (accessed on 29th May 2022), replete with documentation and a test example. To run, it requires Python 3, and the commonly used Python packages `numpy` and `matplotlib`. Relevant technical details are provided in a second appendix to this chapter.

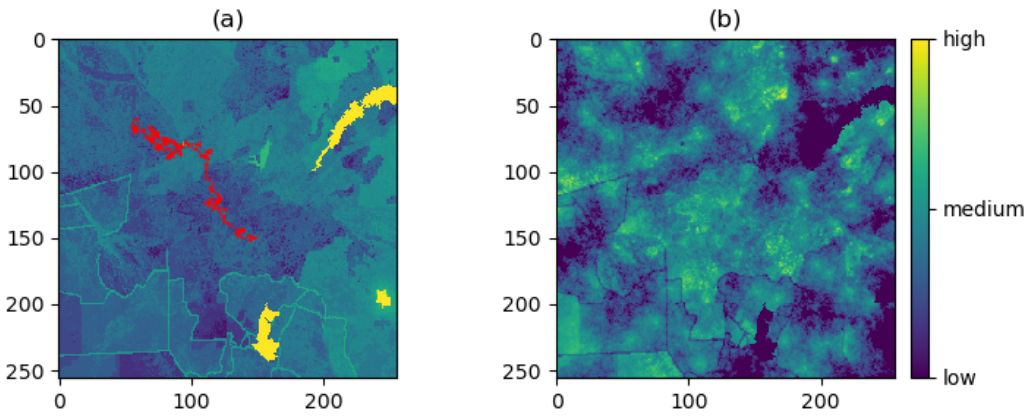


Figure 3.3: (a) An example of individual path (in red) simulated by Pathwalker, on the resistance surface used for the study in Elliot, Cushman, D. W. Macdonald, et al. 2014. Yellow, green and blue depict areas of high, medium and low resistance respectively. (b) An example of a connectivity map produced by Pathwalker, made by aggregating 100 paths from 100 different source locations on the resistance surface shown in (a). In the connectivity map, yellow, green and blue respectively depict areas of high, medium and low movement density.

3.2 The Pathwalker model

The movement simulated by Pathwalker is governed by a set of specified input layers and movement parameters. The model proceeds by tracing a path on a chosen resistance surface from a given set of source points, moving at each step to one of a choice of nine pixels – either staying in the current position or changing to one of the neighbouring eight pixels – according to certain specified probabilistic movement parameters. In this section, we describe the input layers, parameters, and output layers of the model. More technical details, and information on file formats, can be found in the second appendix to this chapter, and in the Pathwalker documentation at `https://github.com/siddharth-unnithankumar/pathwalker`. As of November 2021, the first version of Pathwalker is available to freely download at this link (file size 1 MB).

3.2.1 Input layers

To run Pathwalker, we require two essential input data: (1) a resistance surface, and (2) a list of source point coordinates. A third and optional input is (3) a list of destination coordinates,

which are required if the user wants to simulate movement towards destination points. A fourth and optional input is (4) a risk surface, for use with the risk mechanism (see below).

The resistance surface (and, if used, the risk surface) is to be in ascii format, with the six header rows included. The source coordinates – which typically represent the distribution and density of the studied or simulated population – are to be provided in a `.txt` file, using the same geospatial projection as the resistance surface layer; this same format applies to the destination coordinates, if used.

3.2.2 Model parameters

Movement mechanisms

The core model parameter is the choice of movement mechanism (Figure 3.4): energy, attraction, risk, or any combination of these three basic mechanisms, giving a total of seven options. Along with the chosen movement mechanism, the user specifies a second parameter: the maximum total number of steps for the movement path.

1. Energy. We first specify a value for the 'total energy' parameter, which represents the maximum allowed cumulative energetic cost of movement. The pathwalker then follows an unbiased random walk on the resistance surface, and thus at each step chooses any one of the nine pixels with equal probability. For the pixels traversed in the walk, a cumulative sum of the resistance values is computed. The walk ends once this sum reaches or exceeds the chosen total energy value, or once the maximum number of steps has been reached.

2. Attraction. The pathwalker now follows a resistance-biased random walk. The probability of choosing any one of the nine pixels is given by the inverse of that pixel's resistance value. Here, the inverse resistance values are scaled so that the nine inverse values sum to 1 (so that they give a probability distribution). Thus, the pathwalker will be more likely to move to pixels of lower resistance value and vice versa. The four diagonally adjacent pixels are given a weighting of $1/\sqrt{2}$ to account for the increased distance when moving diagonally. This mechanism does not require any additional parameters to be specified, and the walk ends once the maximum number of steps has been reached.

3. Risk. We first specify a chosen risk surface. This may be proportional to our resistance surface (the default setting); or, a different surface may be chosen, but must be scaled so that the values of the risk surface lie between 0 and 1. The pathwalker then follows an unbiased random walk on the risk surface. At each step, the probability that the walk ends is given by the value of that pixel in the risk surface. Thus, a pixel value of 0 corresponds to no risk, and a pixel with risk value 1 will end the walk. The maximum length of the walk is capped at the chosen maximum number of steps.

Spatial scale of movement choice

In addition to the choice of one of the seven movement mechanisms described above, we can choose the spatial scale at which these mechanisms work. This involves two parameters: the scale of the response (the 'window size'), and the functional form of the response (the 'scaling function').

1. The window size determines the spatial scale at which the movement responds to resistance values. For example, if the chosen window size is 7×7, then the movement will be affected by resistance values in a 7×7 pixel neighbourhood of each of the nine pixels. The default scale, a 1×1 window, is equivalent to not incorporating spatial scaling.

2. The scaling function determines the way in which the pathwalker responds to landscape resistance at a chosen spatial scale n. There are three choices for the scaling function: focal mean, focal maximum, and focal minimum. With the focal mean, the resistance value of a pixel is replaced by the mean average of the resistance values of all pixels in an $n \times n$ neighbourhood of that pixel. With the focal maximum, the value of a pixel is replaced by the maximum pixel value in that neighbourhood; with the focal minimum, it is replaced by the minimum value. The window size and scaling function also act in this way on the risk surface (if used).

Let us look at an example of this, to see in more detail how this scaling interacts with the movement mechanisms. Suppose we choose a 5×5 window with the focal mean scaling function. Define the 'scaled value' of a pixel to be the mean average of the resistance values in a 5×5 neighbourhood of this pixel. Then, in the case of energy, the cumulative sum is

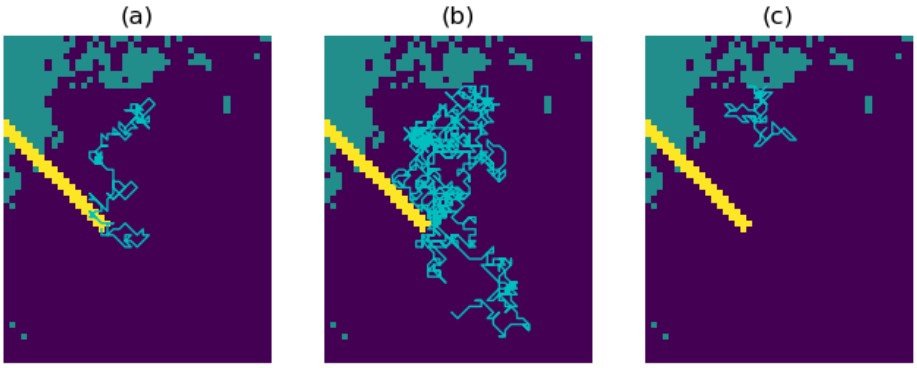


Figure 3.4: Three example paths, shown by the thin line of cyan colour, produced by Pathwalker. They are simulated on the resistance surface from Figure 3.2, and are capped at a maximum length of 1,000 steps. The blue, green, and yellow background colours, respectively, represent low (1), medium (50), and high (100) resistance values. (a) is parameterised by the energy mechanism with a total energy of 1,000; (b) by the attraction mechanism; (c) by the risk mechanism, with risk surface proportional to the resistance surface. All other parameters are set to their default values. See Figure 3.17 for an example of how this is configured in Pathwalker.

These three images demonstrate how the different movement mechanisms alter the nature of the paths simulated by Pathwalker. Since the energy mechanism, shown in (a), is an unbiased random walk, the pathwalker does not avoid the barrier of high resistance (in yellow, resistance value 100); thus, the walk ends soon after the pathwalker enters the yellow region, because the high resistance values mean that the total allowed energy of 1,000 is quickly reached. The attraction mechanism is biased towards pixels of lower resistance value, hence the path in (b) avoids the yellow and green areas and stays in the blue region, which has the lowest resistance; moreover, this path is longer than the paths in (a) and (c), since a path parameterised by the attraction mechanism without energy or risk will only conclude once the maximum number of steps has been reached. The risk mechanism, modelled in (c), has a probability of ending at each step proportional to the values of the risk surface (which, in this case, is given by the resistance surface, scaled to have values between 0 and 1); thus, as expected, the walk ends while the pathwalker is moving on a region of higher resistance – the green region has a resistance value (and thus a probability of ending the walk) 50 times that of the blue region.

computed from the *scaled* values of the pixels traversed; for attraction, the probability of choosing one of the nine possible pixels is given by the inverse of the *scaled* resistance values; with risk, the probability of the walk ending at each pixel traversed is given by the pixel's *scaled* value on the risk surface (Figure 3.5).

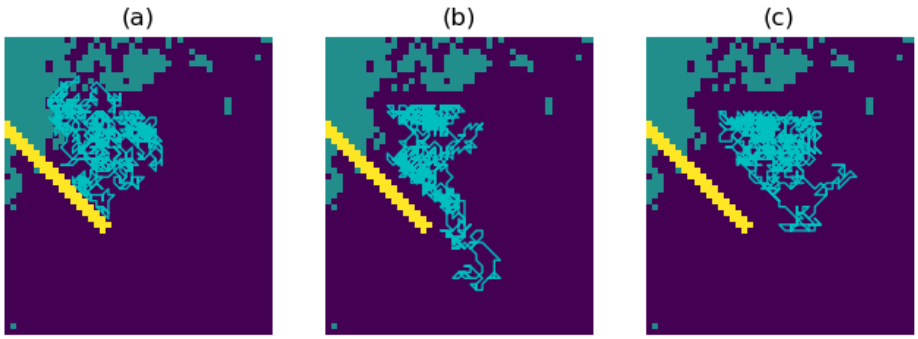


Figure 3.5: Three example paths which demonstrate the effects of spatial scaling, using the same colour scheme and resistance surface as in Figure 3.4. Each is configured with the attraction mechanism, set to run for 1,000 steps. They are parameterised with a spatial scale window size of (a) 1×1, (b) 5×5, and (c) 9×9. All three use the focal mean scaling function, and all other parameters are set to their default values.

In the absence of spatial scaling, as seen in (a), the path remains on the blue region (which has the lowest resistance value), but moves along pixels adjacent to areas of higher resistance (green and yellow). As the window size parameter value increases – with a buffer of 2 pixels in (b) and 4 pixels in (c) – the pathwalker avoids the areas of higher resistance at a greater spatial scale, as seen by the increasing distance between the path and the green and yellow regions.

Directional parameters: autocorrelation and destination bias

Pathwalker provides two parameters for determining the directional bias of the movement: the autocorrelation C parameter, and the degree of bias D towards a particular destination. They work synchronously with the movement and scaling mechanisms (Figure 3.6). C and D may both be chosen to be nonzero simultaneously, but neither can take negative values,

and the sum $C + D$ is required to equal at most 1.[1]

1. Autocorrelation. This parameter C takes values between 0 and 1, and determines the degree to which the pathwalker is inclined to continue in the present direction of travel. The default value of C is 0, an uncorrelated random walk. If we increase the value of C, then our walk becomes more correlated, with the extreme case $C = 1$ resulting in a straight line (in other words, a path in which the pathwalker continues in the same direction with probability 1). For example, if we choose $C = 0.3$, then the nine movement probabilities are scaled to sum to $1 - 0.3 = 0.7$ instead of summing to 1, and there will now be an added probability of 0.3 for continuing in the same direction as the previous step.

2. Destination bias. This parameter D takes values between 0 and 1, and determines the degree to which the walk will be biased towards a destination point X on the resistance surface. It works by giving additional preference to moving to the pixel closest to the direction of where X lies. The default value is 0, in which there is no bias towards the destination. As we increase the value of D, the walk becomes more biased towards X, with the extreme case $D = 1$ resulting in a path which heads directly towards X. For example, if $D = 0.2$, then the nine movement probabilities are scaled to sum to $1 - 0.2 = 0.8$ instead of summing to 1, and there will now be an added probability of 0.2 for moving to the pixel closest to the direction of X.

Additional parameters

Finally, the user specifies four parameters that determine the output of the model: (1) the manner in which the source and destination locations are paired; (2) how many times the model is to run for each source–destination pair; (3) which outputs (individual paths, path statistics, and density surface) are desired; and (4) which figures are desired.

[1]The quantity $C + D$ is required to lie between 0 and 1 because it defines the proportion of the movement governed by directional bias, and thus values outside of this range produce an error in calculating the movement probability distribution.

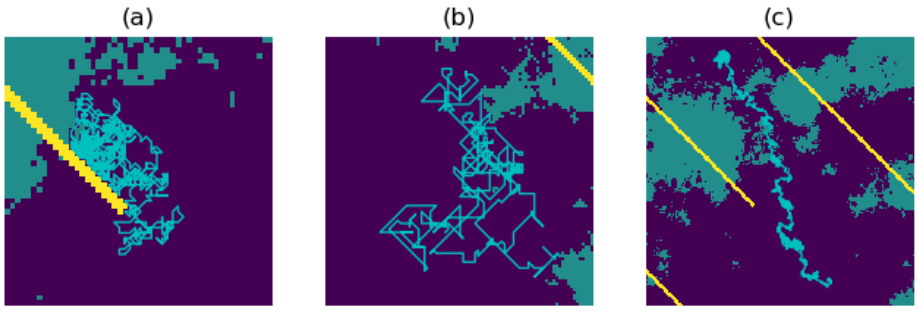


Figure 3.6: With the same resistance surface and colour scheme as previously, these three images demonstrate the effects of the two directional parameters (autocorrelation C and destination bias D) on the movement paths simulated by Pathwalker. They are configured with the attraction mechanism and a total of 1,000 steps, and all other parameters are set to their default values. In (a), no directionality is used, so C and D both equal 0; in (b), we have autocorrelation $C = 0.7$ and destination bias $D = 0$; in (c), we have autocorrelation $C = 0$ and destination bias $D = 0.2$.

(a) illustrates that, with both directional parameters set to their default values of zero, the path does not cover a large area and frequently changes direction – indeed, in this case, the software is configured identically to when it produced the paths shown in Figures 3.4(b) and 3.5(a), and the path in this image thus has the same characteristics. In (b), with the autocorrelation parameter now nonzero, the pathwalker has continued in the same direction of travel for many sections of its path, and as a result has covered a much larger area than in (a). In (c), with the destination bias parameter now nonzero, we see that – although there is still stochastic variation in travel direction throughout the path – the overall direction of the path leads from the source point (near bottom of image) to the specified destination point (near top of image). All three paths in this figure are configured with the attraction mechanism; however, the greater inclination to continue in the previous direction of travel (b), or in the direction of a specific destination (c), means that the pathwalker is more likely to move across areas of higher resistance than in (a), in which both directional parameters are zero and the movement is governed only by the attraction mechanism.

3.2.3 Output layers

By default, the algorithm will output one movement path for each source point – in other words, the model will return the list of coordinates for the path from each source point. We can also choose for the model to output three statistics for each path: (a) the total number of steps taken, (b) the cumulative energetic cost reached (if energy is involved), and (c) the total accumulated risk (if risk is involved).

In addition to the individual movement paths and their statistics, we can choose to obtain a prediction of landscape connectivity. This is produced by aggregating all of the individual movement paths into a 'movement density surface'. The density surface has the same format and dimensions as the resistance surface. The value of each pixel is given by the total number of times that pixel was traversed across all movement paths. When producing a density surface to predict connectivity, we recommend running the model several times from each source point (or source–destination point pair), so that the resulting density surface averages the stochastic variation across possible movement paths. Figures can also be provided for the individual movement paths and density surface (as seen in Figure 3.3).

3.2.4 Summary of Pathwalker setup

To summarise, we first choose a resistance surface on which we would like the paths to run, together with a list of source coordinates. Optionally, we may also provide destination coordinates and/or a risk surface. Then, we choose one of the seven mechanisms for our movement, and the maximum length of the path. If the energy mechanism is used, we also specify a total energy value.

In addition, we can choose to incorporate spatial scaling into the movement by choosing a scaling function, and a larger scaling window than the default size of 1×1. We can also incorporate autocorrelated movement and destination bias into our walk, by choosing a nonzero value for the parameters C and D.

Finally, we choose how to pair the source and destination locations, how many times to run the algorithm from each point, and whether we would like our output to include the coordinates for the individual movement paths, the statistics for each path, the movement density surface, and any figures. See Figure 3.7 for an illustration of this schematic.

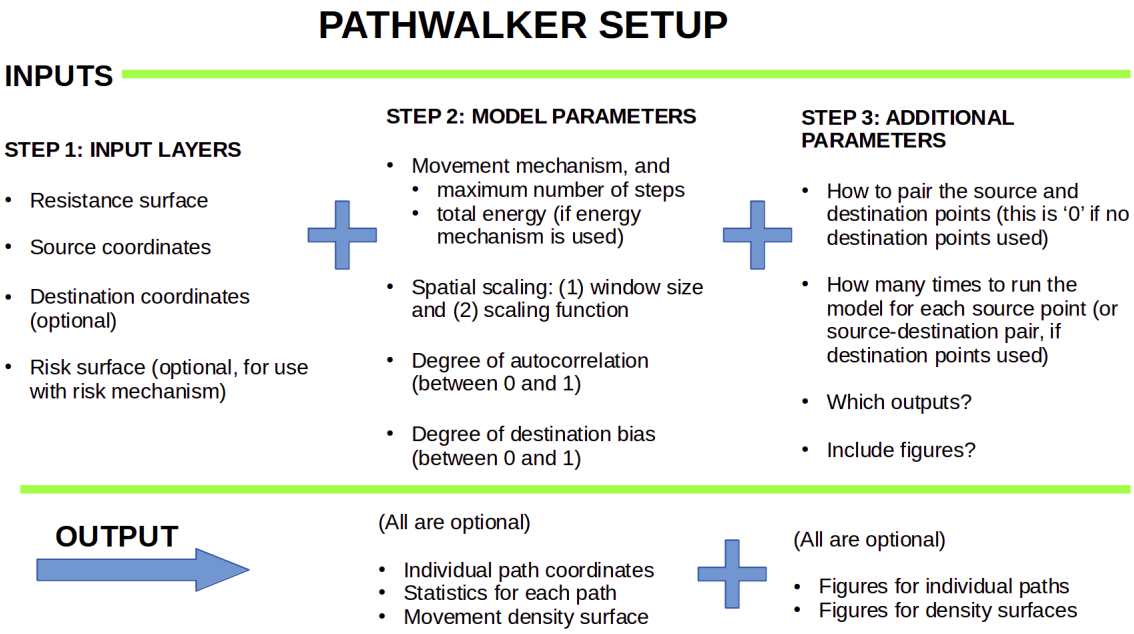


Figure 3.7: Schematic for configuring Pathwalker.

3.3 Case study

In this section, we provide a rudimentary study of how the various movement parameters of Pathwalker interact, and the extent to which each component influences Pathwalker's connectivity predictions. We do this by analysing and comparing the density surfaces resulting from different parameter configurations. All analyses in this chapter are performed in Python 3.8.

3.3.1 Analysis methodology

Producing the density surfaces

We first provide a chosen resistance surface, together with 100 source points distributed uniformly randomly across the resistance surface. For the cases in which we include destination bias, we use the same 100 points as destination locations.

Then, we compute the density surfaces from $4 \times 2 \times 2 \times 2 = 32$ different configurations of the model. These combinations are comprised of: four movement mechanisms (energy, attraction, risk, or all three combined), two spatial scales (1×1 or 7×7) with the focal mean scaling function, two degrees of autocorrelation (0 or 0.35), and two degrees of destination

bias (0 or 0.35). In producing the density surfaces, we run the model 100 times from each source point, in order to average the stochastic variation in the movement paths.

Comparison of density surfaces

We perform four Mantel tests (Mantel 1967) to compare the influence of each of the four movement parameters (movement mechanism, scale, autocorrelation and destination bias) on the movement simulated by Pathwalker, as follows.

Once the 32 density surfaces above are produced, we build a 32×32 matrix M whose i, j-entry is given by the root mean squared error between surface i and surface j. The error matrix M thus provides a measure of similarity between the 32 different density surfaces, where the smaller values in the entries of M correspond to the pairs of surfaces which are more similar.

To then quantify the extent to which the four different parameters influence the movement across the resistance surface (and hence the extent to which they explain the variation of the entries of M), we perform four Mantel tests, each one comparing the error matrix M with a 'model matrix' corresponding to one of the four different parameters. We label these model matrices M_1, M_2, M_3, and M_4 corresponding to the movement mechanism, scale, autocorrelation, and destination bias, respectively.

We now give an example to see in more detail how one of these model matrices, say M_3 (which corresponds to the autocorrelation parameter), is constructed and then compared with M. To construct the 32×32 binary matrix M_3, we give the i, j-entry the value 0 if surface i and surface j are produced from differing autocorrelation values – for example, if surface i is produced using $C = 0$ autocorrelation and surface j using $C = 0.35$. We give the i, j-entry the value 1 if surface i and surface j are produced using the same value of the autocorrelation parameter – for example, if both are produced using $C = 0$. Then to compare M and M_3, we perform a Mantel test between M and M_3. This provides a measurement of the similarity of these two matrices, and thus the extent to which changing the autocorrelation parameter explains the variation between the density surfaces.

We enact the above procedure twice, first using a simple simulated resistance surface, and secondly using the empirically derived resistance surface from Elliot, Cushman, D. W. Macdonald, et al. 2014 (Figure 3.8). The first allows us to see clearly how the different

parameters influence movement density on a simplistic resistance surface, and the second shows how the model runs with an actual example of a resistance surface used in practice. In both cases, the surface consists of 256×256 pixels, taking resistance values between 1 and 100, and is surrounded by a barrier of infinite resistance, which ends the walk if touched. When the risk mechanism is involved, we simply take the risk surface to be proportional to the resistance surface (in other words, the risk surface is the resistance surface scaled so that its values lie between 0 and 1). For this analysis, we use the Python 3.8 packages `scipy` and `mantel`, and for the supplementary analysis in the appendix, we use `scipy` and `scikit-learn` (Pedregosa et al. 2011; Virtanen et al. 2020).

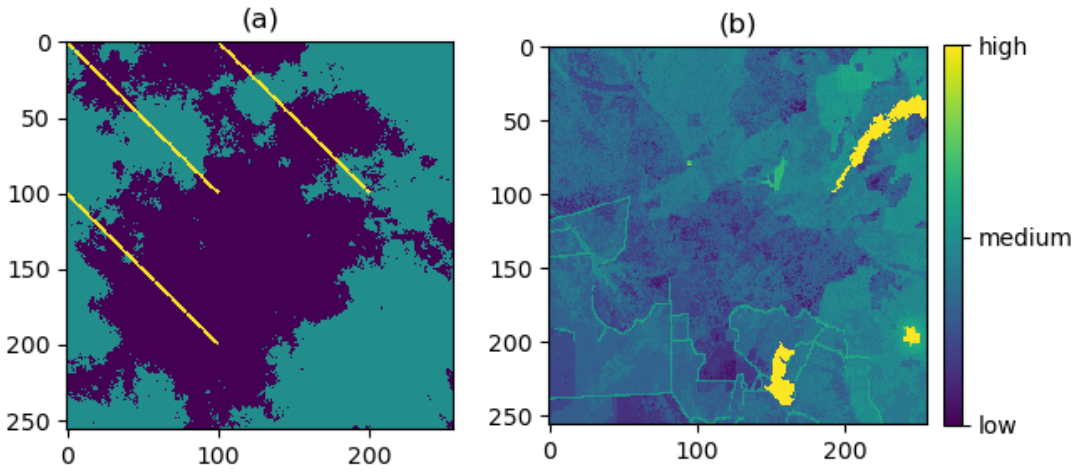


Figure 3.8: The two resistance surfaces used in the case study: (a) the simulated resistance surface (taking only the values 1, 50 and 100); and (b), the empirical resistance surface used for the study in Elliot, Cushman, D. W. Macdonald, et al. 2014. See previous figures in this chapter for instances of these two resistance surfaces, and their usage in Pathwalker and connectivity modelling.

3.3.2 Results

The Mantel test results comparing the influence of the four movement parameters are similar for the simulated and empirical resistance surfaces (Table 3.1). Namely, we find in both cases that the two parameters which explain much of the difference between the density surfaces are the movement mechanism (which varied between energy, attraction, risk, and their threeway

combination) and the degree of destination bias D (which took the values 0 or 0.35).

We can see this from the small p-value (equivalently, high z-score), which indicate that the similarity between M and M_1 and also M and M_4 make it highly probable that these two factors explain much of the extent to which the density surface values differ. In these two cases of movement mechanism and destination bias, the value of the Pearson correlation coefficient ρ, although not close to 1, is typical of Mantel tests in which there is a strong similarity between the two matrices involved.

In comparison, neither the degree of autocorrelation in the movement, nor that of spatial scaling, produced as much overall difference in the density surfaces. However, when configuring the degree of directionality bias in the model, it is important to note the following: while changing the autocorrelation C from 0 to 0.35 did not have as great an effect on the resulting density surfaces as changing the degree of destination bias D from 0 to 0.35, if we had instead changed the autocorrelation parameter C from 0 to a higher value (say, 0.9), then we could expect more dramatic variation in the resulting density surfaces. This case study simply shows that changing the degree of destination bias will have a greater effect on movement density than if we change the autocorrelation parameter *by the same amount*.

The results of this analysis can be anticipated by looking at Figures 3.9 and 3.10. For example, we see that the energy mechanism produces a very different map of density to the attraction mechanism, since the latter causes the movement to often avoid areas of high resistance but does not restrict the extent of movement when in a region of high resistance. Interestingly, in this case study where the risk surface is proportional to the resistance surface, the risk mechanism produces a density of movement similar to that of the energy mechanism, despite the energy and risk mechanisms being theoretically quite different; this similarity would likely be less if the risk surface used is not proportional to the resistance surface.

3.4 Discussion

In this chapter, we have introduced and described Pathwalker, a new spatially-explicit, individual- and process-based model for simulating organism movement through heterogeneous landscapes. Pathwalker incorporates a variety of movement parameters, which allow greater detail in predicting landscape connectivity than do widely used models such as Circuitscape and resistant kernels. Namely, Pathwalker simulates movement as a function of

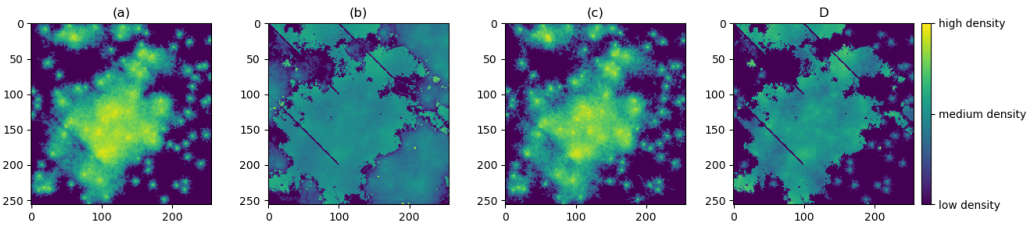


Figure 3.9: These four density surfaces illustrate how the choice of movement mechanism affects the connectivity maps generated by Pathwalker. They are each produced by choosing a different movement mechanism, and then aggregating 10,000 movement paths on the first of the two resistance surfaces in Figure 3.8, in which 100 paths are run at each of the 100 source points and capped at a maximum length of 1,000 steps. The source points are distributed uniformly randomly across the resistance surface. (a) is generated from the energy mechanism, parameterised with a total energy value of 1,000; (b) with attraction; (c) with risk, using the risk surface proportional to the resistance surface; (d) with all three, combining energy, attraction and risk simultaneously. All other parameters are set to their default values. (a) illustrates that, with the energy mechanism, the source locations in areas of high resistance result in small isolated patches of relatively high movement density, in which the walk ends rapidly since the total energy is quickly reached; density is highest in areas of low resistance, and the yellow barriers of high resistance are not completely avoided but do substantially reduce movement. In (b), we see that boundaries between regions of different resistance are largely respected, with the yellow barriers strictly avoided; however, since the length of a walk parameterised by the attraction mechanism is unaffected by resistance values, the areas of medium resistance (coloured by green in Figure 3.8(a)) also have high movement density. Despite risk and energy being theoretically quite different, (c) is quite similar to (a), since both mechanisms produce unbiased random walks whose length are affected by resistance values; however, if a risk surface is used that is not proportional to the resistance surface, then one may expect a much greater difference between density surfaces produced by energy and risk. Finally, (d) may be seen to provide the most 'realistic' connectivity map, integrating how the resistance values affect both the direction (with attraction) and length (with energy and risk) of the movement paths used to produce this surface.

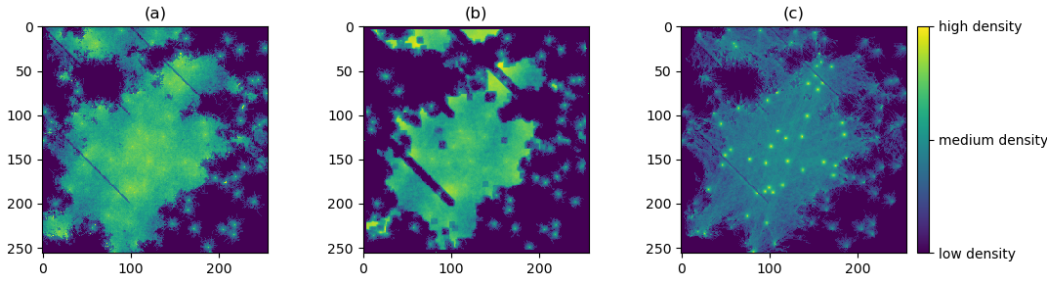


Figure 3.10: These three density surfaces nicely illustrate the effects of the other parameters on the connectivity maps generated by Pathwalker. They are configured with the threeway combination movement mechanism capped at 1,000 steps. As in Figure 3.9, they are produced by aggregating 100 paths at each of the 100 source points on the resistance surface in Figure 3.8(a). With all other parameters set to their default value, they are generated by (a) 0.35 autocorrelation; (b) 7×7 spatial scaling, with the focal mean scaling function; (c) 0.35 destination bias. See Figure 3.17 for an example of how this is configured in Pathwalker.

In (a), we see a similar surface to that in Figure 3.9(d); the slight blurring of the boundaries between regions of different resistance values demonstrates how the inclination to continue in the same direction of travel probabilistically overrides the attraction mechanism directing movement towards area of lower resistance. (b) provides a cumulative picture of the effects seen in Figure 3.5 from increasing spatial scale of movement, whereby the movement density is concentrated in the blue region of the resistance surface, at a greater distance from the green and yellow regions of higher resistance than in the density surfaces where spatial scaling is not incorporated. (c) shows how even a low degree of destination bias ($D = 0.35$) results in a connectivity map where the source and destination locations see high concentration of movement, and regions not between clusters of source and destination points less so.

	M_1	M_2	M_3	M_4
Simulated surface	$\rho = 0.1267$ $p = 0.0001$ $z = 6.3860$	$\rho = -0.0158$ $p = 0.3271$ $z = -0.8178$	$\rho = -0.0158$ $p = 0.3203$ $z = -0.8101$	$\rho = 0.1396$ $p = 0.0001$ $z = 7.2117$
Empirical surface	$\rho = 0.1216$ $p = 0.0003$ $z = 5.6065$	$\rho = -0.0213$ $p = 0.1709$ $z = -0.9896$	$\rho = -0.0166$ $p = 0.3448$ $z = -0.7718$	$\rho = 0.1743$ $p = 0.0001$ $z = 8.0040$

Table 3.1: Results from the Mantel test between the error matrix M and the four model matrices for both the simulated and empirical resistance surfaces, with Pearson correlation coefficient ρ, two-tailed p-value p, and z-score z. M_1, M_2, M_3, M_4 correspond to movement mechanism, spatial scale, autocorrelation, destination bias respectively.

landscape resistance, energetic cost, and mortality risk at multiple spatial scales, whilst simultaneously accounting for autocorrelation and destination bias in the movement.

The importance and utility of simulation techniques for addressing fundamental ecological questions has been established in many branches of spatial ecology: for example, the use of CDPOP in landscape genetics (Cushman, Shirk, et al. 2012; Landguth and Cushman 2010; Shirk, Landguth, et al. 2018), and HexSim in population dynamics (Heinrichs et al. 2016; Stronen et al. 2012). In light of this, we have designed Pathwalker with a simple and highly flexible framework to explore a wide range of behavioural responses to landscape features, enabling evaluations of theoretical and methodological questions in landscape and movement ecology, conservation science and connectivity modelling (as demonstrated in the following chapter and the appendix to this chapter; see also Unnithan Kumar and Cushman 2022).

Relation to popular connectivity models

Popular connectivity models, such as Circuitscape, resistant kernels, and factorial least-cost paths, noticeably do not account for many key drivers of animal movement. This places substantial limitations on their effective use for handling the complexities of many contexts in applied ecology and conservation science. For example, they assume the mortality risk to remain unchanged through different regions of the landscape, and movement choice to occur at a single spatial scale. As noted in McRae et al. 2008, Circuitscape further assumes

a symmetrical movement probability between two adjacent pixels, even though movement from an area of higher to lower resistance (or energetic cost, or mortality risk) is much more likely than the reverse. Moreover, the simplistic random walk mechanisms in these models presume a 'memoryless' walker, despite the established influence of autocorrelation on movement patterns (Cushman, Chase, et al. 2005; Dray et al. 2010).

In contrast, Pathwalker is able to incorporate these important aspects of animal movement into its connectivity predictions. Other recent spatially-explicit, individual-based models, such as HexSim and RangeShifter, also include several parameters which afford greater detail in simulating the factors influencing movement patterns. For example, as with Pathwalker's risk surface, HexSim allows for the use of multiple resistance-like surfaces which approximate landscape features like food and nesting resources, in addition to the spatial input data of landscape resistance. Although HexSim and RangeShifter have seen some recent application in connectivity studies (such as Schumaker, Brookes, et al. 2014), these individual-based models are primarily focused on simulating general population dynamics. Pathwalker has instead been designed specifically for simulating individual movement pathways and predicting connectivity, with an interface similar to UNICOR (which implements resistant kernels and factorial least-cost paths) and Circuitscape, to allow for its immediate and straightforward usage in connectivity modelling.

Conclusion

Modelling and predicting organism movement and landscape connectivity is a fundamental part of modern ecological science. However, the dominant connectivity models currently in use are limited by their simplistic and overly reductionist assumptions of movement behaviour. In this chapter, we work to address this by introducing a new spatially-explicit, individual- and process-based model called Pathwalker. It enables the modelling of individual paths and landscape connectivity as a function of resistance-biased movement choice, energetic cost of movement, mortality risk, autocorrelation, and directional bias towards a destination, all at multiple spatial scales. Moreover, Pathwalker provides a valuable simulation tool for evaluating theoretical and methodological questions in ecological science.

3.5 Appendix A: Effects of autocorrelation on movement density

In this supplementary analysis, we demonstrate a result of theoretical interest for movement modelling, which is to derive the movement density function for different degrees of autocorrelation in the movement. The knowledge of the correct function, which this analysis provides, is essential for accurately configuring movement and connectivity models (such as resistant kernels) which use different kernel functions to represent varying levels of dispersal ability.

Analysis methodology

We look at the average distribution of movement density for four values of the autocorrelation parameter C – 0 (no autocorrelated movement), 0.25, 0.5 and 0.75 – on a landscape with 500×500 pixels and uniform resistance value 1. We configure Pathwalker with the energy movement mechanism and no spatial scaling, noting that the landscape is uniform and thus using a different spatial scale, or using the attraction movement mechanism, results in the same distribution of movement.

For each of the four values of C we simulate 1,000 movement paths from the source point, each of length 500 steps, and aggregate these 1,000 paths into a density surface. We can visualise these movement density surfaces in both two dimensions (as a heatmap) and three dimensions. Then, to these distributions we fit two functions – the exponential function ae^{bx} and the power function $a(x+c)^b$ – and compute the optimum parameters for these two functions, along with the resulting r^2 value of the parameter fit. This allows us to derive a prediction for the kernel shape of movement density under different levels of autocorrelated movement. Since the distribution will be radially symmetric about the source point, we need only perform this computation on the one-dimensional x-axis, rather than on a two-dimensional grid. For this analysis, we use the `scipy` and `scikit-learn` packages for Python 3.8.

Results

The first two columns of Table 3.2 display the extent of the paths and the percentage of total possible area covered on the 500×500 pixel resistance surface, for the four different density surfaces (produced by aggregating 1,000 runs of 500-step paths). We see that both statistics increase as the autocorrelation value increases. Figure 3.11 displays the four density surfaces, with the change in axis values visibly highlighting how the travel extent and autocorrelation increase concurrently.

Figure 3.12 displays the three-dimensional movement density distributions. For ease of visualisation, we remove the source point, since, as we may expect, its density value is much higher than the surrounding points. Taking minor stochastic variation into account, we observe a radially symmetric function resembling a negative exponential or power function. The fit of the power and exponential functions vary depending on whether or not we include the source point in the data: (1) with the source point included, we found the power function to result in a higher r^2 value than the exponential, with the margin between these two r^2 values varying between 0.03 and 0.14, but (2) without the source point, optimum parameters for the power function could not be found, and the exponential is seen to fit much better without, rather than with, the source point. The latter two of the four rows in Table 3.2 provide the parameter and r^2 values resulting from fitting these two functions.

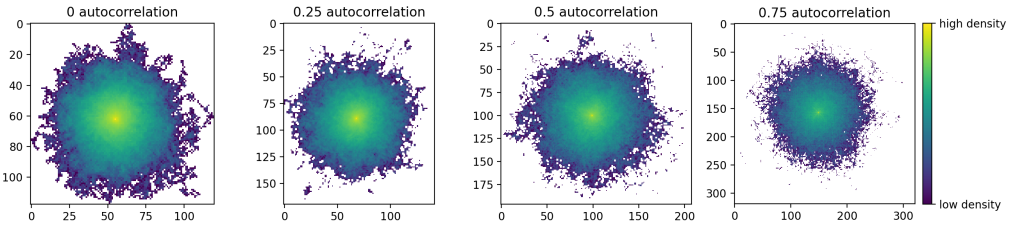


Figure 3.11: This figure displays four density surfaces, produced from a resistance surface of 500×500 pixels with uniform resistance value 1, in which only the autocorrelation parameter in Pathwalker is varied. The source point in these images is the central point of the resistance surface, with the axes displaying the extent to which the paths have spread across the resistance surface. Each surface is produced by aggregating 1,000 paths, configured using the energy mechanism with a total energy of 1,000 and a maximum length of 500 steps. With all other parameters at their default value, these surfaces are generated from autocorrelation values of 0, 0.25, 0.5 and 0.75, from left to right respectively.

As the autocorrelation value C increases, we see that the extent of the resistance surface covered by paths also increases. Moreover, due to the greater proclivity for continuing in the same direction of travel, we observe that the movement density decreases more rapidly when moving away from the source point.

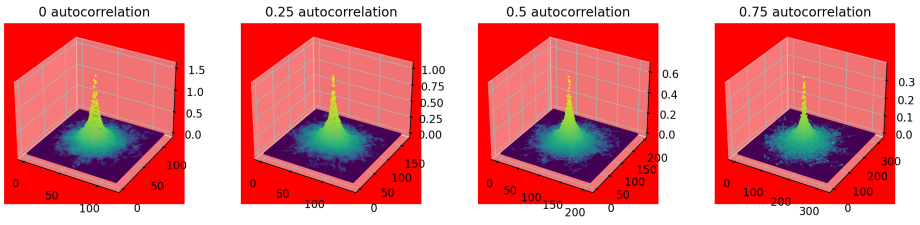


Figure 3.12: The same four density surfaces and colour scheme as in Figure 3.11, now plotted in three-dimensional space. Here we can see more clearly that, as autocorrelation increases, not only does the area traversed grow, but also the distribution of movement density drops more sharply from the source point.

	$C = 0$	$C = 0.25$	$C = 0.5$	$C = 0.75$
Extent of paths	118×120	170×142	197×208	319×320
Percentage of surface covered	3.1268	5.0944	8.1736	15.5456
Power function parameters and r^2 value	$a = 29.975$ $b = -1.751$ $c = 4.240$ $r^2 = 0.991$	$a = 4.3470$ $b = -1.126$ $c = 1.938$ $r^2 = 0.973$	$a = 1.249$ $b = -0.924$ $c = 0.753$ $r^2 = 0.963$	$a = 0.512$ $b = -0.780$ $c = 0.236$ $r^2 = 0.977$
Exponential function parameters and r^2 value	$a = 1.541$ $b = -0.150$ $r^2 = 0.986$	$a = 0.926$ $b = -0.125$ $r^2 = 0.992$	$a = 0.522$ $b = -0.085$ $r^2 = 0.984$	$a = 0.288$ $b = -0.071$ $r^2 = 0.956$

Table 3.2: Statistics for the four density surfaces produced from the four differentautocorrelation values. The first row gives the overall extent of the movement paths on the 500×500 resistance surface, and the second row gives the percentage of the total area covered by these paths. The latter two rows give the parameters and r^2 value for the fitted power and exponential functions respectively.

3.6 Appendix B: Pathwalker technical details

In this second appendix, we present technical details for Pathwalker which are relevant to the material of this chapter. This information is adapted from the documentation available at `https://github.com/siddharth-unnithankumar/pathwalker`.

Program setup

Pathwalker is run from the command line, and requires Python 3, together with the basic packages `numpy` and `matplotlib`. Some computer platforms (such as Linux) come with Python 3 already installed, but others (such as Windows) will require Python 3 to be installed by the user. There are many online tutorials for how to install Python 3 and the packages `numpy` and `matplotlib`.

Once these have been installed, the Pathwalker program can be downloaded from `https://github.com/siddharth-unnithankumar/pathwalker`. We extract the `pathwalker` folder from the `pathwalker.zip` file to our preferred directory. The `pathwalker` folder contains

the executable program `pathwalker.py` together with the documentation, and also a folder called `demo` which contains the data for a demo run of Pathwalker (Figure 3.13). We are now ready to configure the input data and then run Pathwalker!

Input and output data

We create a folder inside the `pathwalker` directory, and name it according to our chosen session name (just as the demo session is contained in a folder called `demo` in the `pathwalker` directory). In this folder, three files are required: (1) a `.txt` file called `settings.txt`, (2) a resistance surface in ascii format, and (3) a `.txt` file specifying the source point coordinates, under the same projection as the resistance surface. Two further optional inputs may be specified. First, if we would like the model to run with destination points, and if these are chosen to be different from the source points, then a fourth file is required: (4) a `.txt` file specifying the destination point coordinates, in the same projection as the resistance surface and source points. Second, if a risk surface is used which is different to the resistance surface, then we require (5) a risk surface in the same ascii format as the resistance surface. See the `demo` folder for an example of the correct file formats (Figure 3.14).

To set the model parameters, configure the settings file according to the options in list below. With all inputs configured, we are now ready to run Pathwalker. Open the command line, navigate to the `pathwalker` directory, and enter the text 'python pathwalker.py'. We will then be prompted to enter our session name. Once we do this, the model will run according to the specified input data, and the terminal will display the time taken for each stage of the program to run. If we have named our session `xx`, then a folder called `xx_results` containing the output data will be created in the `pathwalker` directory (Figure 3.15).

1. `session_name`. A chosen name for the session, the same as the title of the folder containing the `settings.txt` file.

2. `mechanism`. 1 – energy (default); 2 – attraction; 3 – risk; 4 – energy and attraction; 5 – energy and risk; 6 – attraction and risk; 7 – energy, attraction and risk.

3. `scale`. An integer $n > 0$, where $n \times n$ is the window size for the scaling neighbourhood. The default is $n = 1$ (no spatial scaling).

4. `scaling_function`. 1 – focal mean scaling (default); 2 – focal max scaling; 3 – focal min scaling.

5. `correlation`. A number between 0 (default) and 1. The sum of `correlation` and `destination_bias` values should be at most equal to 1.

6. `destination_bias`. A number between 0 (default) and 1. The sum of `correlation` and `destination_bias` values should be at most equal to 1.

7. `steps`. An integer greater than 0 (default 1,000).

8. `energy`. An integer greater than 0 (default 1,000).

9. `resistance_surface`. The name of the resistance surface file, including the file extension. This file should be placed in the folder titled with the session name. For example, in the `demo` folder, we have `res_surface.asc`.

10. `risk_surface`. The choice of risk surface. If either no risk surface is required, or we would like to use the default risk surface (which is the resistance surface first rescaled to take values between 1 and 100, and then divided by 1,000), then the input for this parameter is the number 0. Otherwise, the input is the name of the risk surface (with file extension), which should be in the same format as the resistance surface, and placed in the session folder.

11. `source_points`. The name (with file extension) of the file containing the source coordinates, which must be a `.txt` file, and placed in the session directory. See the file `source_coords.txt` in the `demo` folder for an example of the correct format for the coordinates.

12. `destination_points`. If no destination points are required, this input is 0 (default). Otherwise, the input is the name (with file extension) of the file containing the destination coordinates, which must be a `.txt` file, and placed in the session directory. See the file `dest_coords.txt` in the `demo` folder for an example of the correct format for the destination point coordinates.

13. `source_destination_pairing`. 0 – no destination points are provided in the input (default). 1 – paths for all source-destination pairs will be computed; so if there are k

source points and m destination points, then km paths will be generated. 2 – if there are the same number of source and destination points, then this will pair up the source and destination points (in the order given in the source and destination `.txt` files), and compute the path for each pair; so if there are k source points and k destination points, there will be k paths generated. 3 – if the destination points are the same as the source points, then this computes paths for all source-destination pairs, but excludes the pairing of a point with itself; so if there are k locations, used as both source and destination points, there will be $k(k-1)$ paths.

14. `runs`. The number of times to run the simulation for each source point. The default value is 1. If destination points are included, then this will be the number of times the simulation is run for each source-destination pair.

15. `output`. 0 – no output data provided. 1 – a matrix `.csv` file, with each pair of columns giving the x, y-coordinates for each path; thus, if there are k total paths, this will be a matrix with $2k$ columns (see below for how these columns are ordered). 2 – a matrix `.csv` file, with each column providing the 'additional information' for each path (see below for details of the additional information). 3 – the movement density surface, calculated from the cumulative sum of the paths from all runs, provided in the same ascii format as the original resistance surface. 12 – both 1 and 2, so that for each run, the output is a `.csv` file containing the x, y-coordinates of all paths, together with a separate `.csv` file containing the additional information for each path. 13 – both 1 and 3, so that the output is a `.csv` file containing the x, y-coordinates of all paths, and also the density surface in ascii format. 23 – both 2 and 3, so that the output is a `.csv` file with the additional information for each path, and also the density surface in ascii format. 123 – all three together: coordinates, information, and density surface.

16. `figures`. 0 – no figures provided. 1 – figures provided for each path. 2 – figure provided of the movement density surface, with an additional figure of its log transform, for ease of visualisation; the pixel values of the log density surface is given by $\ln(x+1)$, where x is a pixel value on the original density surface. 12 – figures provided of each path, together with figures of the original and log density surfaces. Figure size and colour can be altered by modifying the code for the output figures in `pathwalker.py`.

Information on output format

In the output data, the paths are ordered by source point first, then destination point, then run number. For example, run 2 computed from source point 4 and destination point 1 will be labeled 'path_4_1_2'. Thus, if we have chosen to output the x, y-coordinates for the individual paths, then the coordinates for this path will be given by the columns with headers 'path_4_1_2_x' and 'path_4_1_2_y' (Figure 3.16).

If we have chosen to output additional information for each path, then we will obtain a file with up to three rows of output data. From top to bottom, these rows provide: (1) the total number of steps taken in the walk, (2) the total energy accumulated from the walk, and (3) the total risk accumulated from the walk. The first row (total number of steps) is always provided, and the remaining two rows will be provided depending on the choice of mechanism specified in the `settings.txt` file. For example, if mechanism 6 (corresponding to 'attraction' and 'risk' together) is chosen, then 'energy' does not feature in this setup; hence, the output will contain two rows of data, the first corresponding to the total number of steps, and the second to the total accumulated risk. The demo session is configured to run mechanism 7 ('energy', 'attraction' and 'risk' together), and so there are three rows of output data, in the order specified above.

Illustrative figures

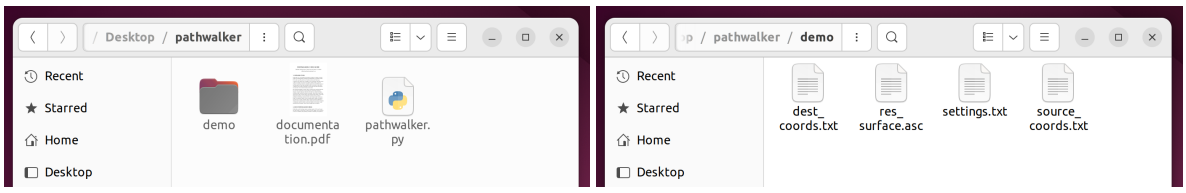


Figure 3.13: (Left) The contents of the `pathwalker` directory, containing the `demo` folder, documentation, and open-access Python script for Pathwalker. (Right) The contents of the `demo` folder, containing the input data for the demo run of Pathwalker; namely, the settings file, the resistance surface, and the source and destination coordinates. This is obtained directly from `https://github.com/siddharth-unnithankumar/pathwalker`.

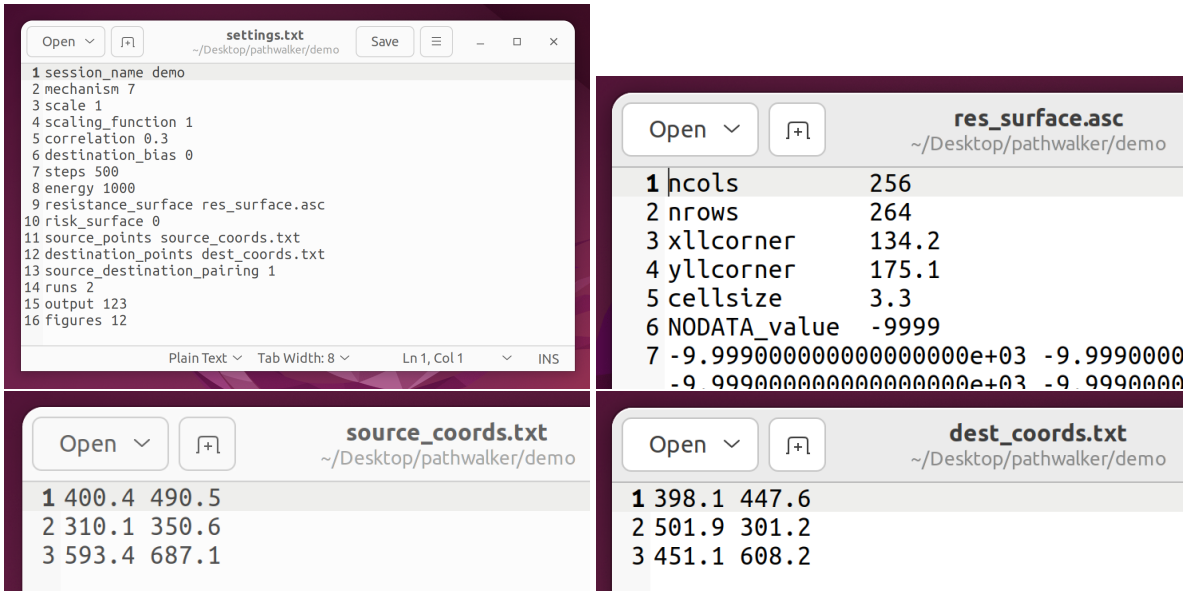


Figure 3.14: The contents of the four input files in the `demo` folder. (Top left) The settings file provides the interface for configuring how Pathwalker will run. (Top right) The resistance surface is in ascii format, with the 6 headers providing the meta-data and the subsequent rows giving the values for the resistance surface. (Bottom left) The x, y-coordinates for the three source points, parameterised by latitude and longitude under the same projection as the resistance surface. (Bottom right) The three destination point coordinates, provided in the same format and projection as the source points.

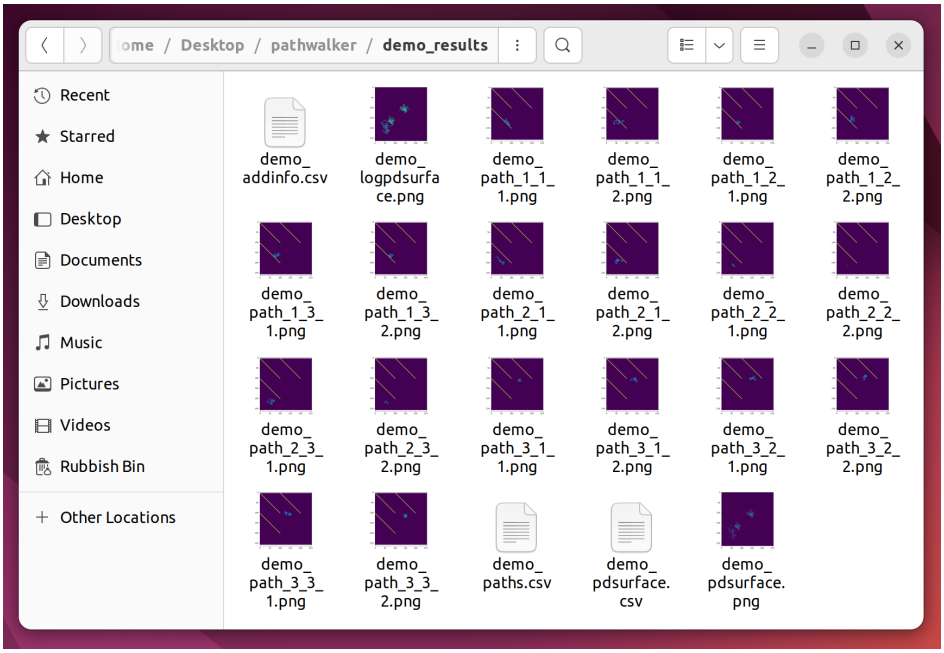


Figure 3.15: The contents of the `demo_results` folder. Here, we see the files for: (1) the path coordinates, in `demo_paths.csv`; (2) the additional information for the paths, in `demo_addinfo.csv`; (3) the density surface, in `demo_pdsurface.csv`. They are produced alongside one figure for each of the 16 individual paths, and figures for the density and log density surfaces.

A	B	C	D	E	F	G	H
path_1_1_1_x	path_1_1_1_y	path_1_1_2_x	path_1_1_2_y	path_1_2_1_x	path_1_2_1_y	path_1_2_2_x	path_1_2_2
399.85	490.25	399.85	490.25	399.85	490.25	399.85	490
399.85	493.55	399.85	490.25	399.85	486.95	399.85	493
399.85	490.25	403.15	490.25	396.55	490.25	399.85	496
399.85	486.95	406.45	490.25	393.25	486.95	399.85	493
403.15	486.95	409.75	490.25	396.55	483.65	403.15	493
403.15	486.95	413.05	490.25	393.25	483.65	406.45	493
406.45	486.95	413.05	490.25	389.95	483.65	409.75	493
409.75	483.65	413.05	490.25	393.25	483.65	413.05	493
406.45	483.65	413.05	486.95	389.95	483.65	409.75	496
406.45	486.95	416.35	486.95	386.65	480.35	409.75	500
403.15	486.95	419.65	486.95	389.95	483.65	413.05	500
403.15	483.65	419.65	490.25	389.95	486.95	416.35	500
406.45	480.35	416.35	490.25	389.95	486.95	419.65	500
409.75	477.05	413.05	490.25	393.25	490.25	422.95	500

A	B	C	D	E	F	G	H	I	
path_1_1_1	path_1_1_2	path_1_2_1	path_1_2_2	path_1_3_1	path_1_3_2	path_2_1_1	path_2_1_2	path_2_2_1	pa
462	476	240	471	500	409	500	500	120	
858	1070	240	669	797	607	500	500	120	
0.858	1.07	0.24	0.669	0.797	0.607	0.5	0.5	0.12	

Figure 3.16: (Top) We see the first rows and columns of the output path coordinates from running Pathwalker with the demo data provided; this is recorded in the `demo_paths.csv` file, whereby each pair of columns corresponds to the x, y-coordinates of an individual path, and each row to an individual step. (Bottom) The contents of the `demo_addinfo.csv` file, which displays the additional information for these same individual paths; namely, each column corresponds to an individual path, and the three rows from top to bottom give the total steps, total cumulative energy, and total cumulative risk.

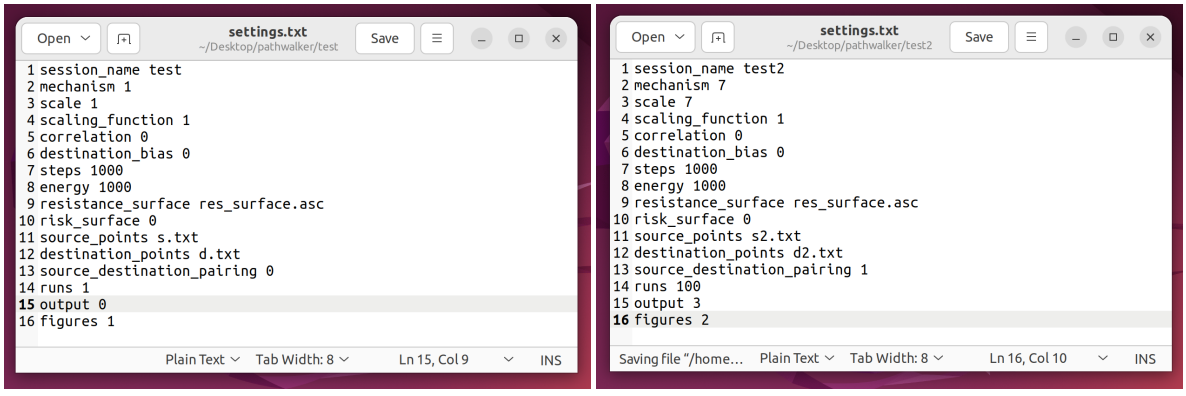


Figure 3.17: These two images display the Pathwalker configurations used to produce two of the images from earlier in this chapter: on the left, for Figure 3.4(a); on the right, for Figure 3.10(b).

Chapter 4

Evaluating landscape connectivity models



Figure 4.1: This chapter is closely adapted from the *Scientific Reports* article *Connectivity modelling in conservation science: a comparative evaluation* (Unnithan Kumar and Cushman 2022). I wrote this piece during the winter of sleeping in the tent glade beside Port Meadow, walking into town before sunrise and some days returning over the meadow amongst shining stars and sleeping horses. Photograph by Siddharth Unnithan Kumar, 9th December 2022.

4.1 Introduction

In the previous chapter, we entered the context of organism movement, and described the concept of 'landscape connectivity' as a framework with which to understand and map the pathways through a landscape most important for facilitating dispersal, gene flow, shifting habitats, and other drivers of animal movement. We mentioned that landscape connectivity has grown in recent years to become a central focus of several ecological disciplines, and that the major connectivity models currently use the concept of a 'resistance surface' to provide spatial input data, which is a technique to quantify how landscape composition affects animal movement choice. Having set the scene as such, we then introduced Pathwalker, a new individual-based model which simulates animal movement and provides a more detailed approach to estimating landscape connectivity. As with the widely used connectivity models mentioned, Pathwalker uses resistance surfaces to provide a measurement of spatial heterogeneity, but also involves several other parameters to map animal movement paths, such as mortality risk, autocorrelation, and varying spatial scales of movement choice.

4.1.1 Chapter overview

In this chapter, with Pathwalker now developed, we use its capabilities to assess the performance of three connectivity models – Circuitscape, resistant kernels, and factorial least-cost paths – which we described in the introduction to the previous chapter. The investigation of this chapter uses simulated data from Pathwalker to address the following question in the field of connectivity modelling: how accurate are (1) factorial least-cost paths, (2) resistant kernels, and (3) Circuitscape, in predicting landscape connectivity, as we vary movement behaviour and spatial complexity over a wide range of parameters? As explained in more detail in Section 4.2, we do this by first simulating a series of resistance surfaces, and then, by choosing different parameter combinations with which to run Pathwalker, we generate movement data on these resistance surfaces from a large variety of possible behavioural scenarios. From this, we obtain a collection of simulated connectivity maps, and measure the ability of the above three connectivity models to accurately predict the patterns of connectivity in the maps generated by Pathwalker.

4.1.2 An introduction to simulation experiments

Simulation experiments are essential for assessing the performance of computational models in ecology. This was briefly touched upon in Chapter 2 in the realm of community ecology and species distribution models, when we compared the predictive abilities of the smoothing function with those of the generalised linear model and random forest machine learning algorithm. To motivate and contextualise the material of this chapter, we begin by discussing the utility and techniques of simulation more fully, now in the setting of animal movement.

Simulated versus empirical data

At present, there exist a wide range of studies using empirical data which evaluate the abilities of connectivity models to match the frequented pathways which emerge from observed movement patterns (for example, Laliberté et al. 2020; Pullinger et al. 2010; Sawyer et al. 2011; Zeller, Jennings, et al. 2018). These analyses typically assess model performance by measuring the degree of correlation between empirical movement data and connectivity model predictions. However, in an empirical analysis, the relationships between observed movement and its biotic and abiotic environmental drivers, which are inferred from the empirical data to build the resistance surface, remain unknown.[1] Moreover, these connectivity model predictions require configuring values for parameters such as dispersal ability, and the density and distribution of the studied population, which are also not empirically known.

As a result, the degree to which a connectivity model prediction matches observed movement paths *does not necessarily demonstrate the model's accuracy relative to other methods in general*. This is because the many uncontrolled factors in an empirical study mean that the 'underlying' relationship shaping movement patterns need not be reflected in the observed data.[2] Thus, although empirical connectivity analyses can give tremendous insight in many contexts, they are limited in their ability to comparatively evaluate the performance

[1] Further technical details on how resistance surfaces are created are given in Chapter 5.

[2] In contemporary connectivity modelling, this quantitative relationship is presumed to exist in order to build the resistance surface, and it seeks to capture how each individual environmental variable influences movement behaviour. As in Chapter 2, the quotation marks are used here because, from a broader ecological perspective, there is no evidence or reason to assume that such an underlying universal relationship (which isolates the response to each individual environmental variable) exists. Thus, we distinguish its methodological use in this context from any ontological claims about nonhuman behaviour.

of different connectivity models. Working instead with suitably generated simulated data allows us to compare model predictions with a 'known truth' – namely, the connectivity map generated by simulated movement paths resulting from a controlled set of known parameters – and thus enables a more definitive assessment of model performance.

The utility of simulation techniques

Simulation frameworks have been instrumental for testing key hypotheses in many branches of spatial ecology. For example, in landscape genetics, simulated data generated by models such as CDPOP have been used to study central questions in this field which cannot be addressed with empirical data alone (Cushman and Landguth 2010; Landguth, Cushman, et al. 2010). Simulation techniques have also recently been used in species-specific landscape connectivity studies, such as with the Sunda clouded leopard (E. A. Macdonald et al. 2018), and northern spotted owls (Schumaker, Brookes, et al. 2014). Yet there has been no published comparative evaluation which utilises a simulation framework to measure the relative performance of the connectivity models themselves. Given the widespread usage of Circuitscape, resistant kernels and factorial least-cost paths across an enormous range of connectivity analyses in recent years, a rigorous evaluation of their predictive abilities using simulation techniques is essential for guiding the appropriate and effective application of these connectivity models for environmental policy and practice.

The flexibility and detail of Pathwalker enable us to test a variety of hypotheses concerning the patterns of landscape connectivity which result from differing movement choices and spatial complexities. Of course, no amount of parameters could enable a model to capture every detail of how animals move, and thus the movement paths generated by Pathwalker are simply an approximation to empirical movement patterns and their possible drivers. Yet, rather than detracting from the comparative analysis of these connectivity models, using movement paths simulated by Pathwalker rather than those gathered from empirical telemetry data *actually lends itself* to evaluating their relative performance. This is because the algorithmic rules which generate the movement paths in Pathwalker use and elaborate upon the very same movement rules presumed by Circuitscape, resistant kernels, and factorial least-cost paths. Hence, the movement paths and connectivity maps simulated by Pathwalker for this investigation encompass the best possible scenarios for how accurate these three

connectivity models can be. In other words, their performance in the analysis to follow will include the cases in which these three models are at their most accurate.

4.2 Methods

4.2.1 Creating the connectivity model predictions

For our comparative simulation analysis, we begin by first simulating 7 resistance surfaces of 256×256 pixels, which increase in complexity, from a simple uniform landscape with three barriers, to surfaces with more continuous and varied simulated landscape features (Figure 4.2). We also randomly select 100 points in a 256×256 grid, which act as the starting locations for the movement on the resistance surface. Each of these 7 surfaces, together with the 100 source points, is then given to our three connectivity models – factorial least-cost paths, resistance kernels and Circuitscape. For each of the 7 resistance surfaces, we thus obtain three predictions for landscape connectivity, one from each model. In the analysis described below, we measure the extent to which the outputs of each of the three models matches the actual connectivity pathways generated from the movement data simulated by Pathwalker, across a wide variety of scenarios arising from different simulated movement behaviours.

4.2.2 Creating the simulated connectivity maps

As we have seen in the previous chapter, Pathwalker outputs individual movement paths generated by these parameter combinations, and it can then aggregate these movement paths into a 'density of movement' surface, providing the simulated connectivity maps to which we compare the three connectivity model outputs (Figure 4.3). In our analysis, for each parameter configuration (which represents one possible combination of movement behaviours), we run Pathwalker 100 times from each of the 100 randomly selected source points, and we then aggregate these 10,000 movement paths to create a single connectivity surface which results from the movement choices of this particular set of behavioural parameters. The length of each path in the analysis is capped at 500 steps.

In order to provide a comparative evaluation of factorial least-cost paths, resistance kernels and Circuitscape, we perform two comprehensive analyses. First, we test their accuracy with each of the 7 resistance surfaces across 252 possible configurations of movement be-

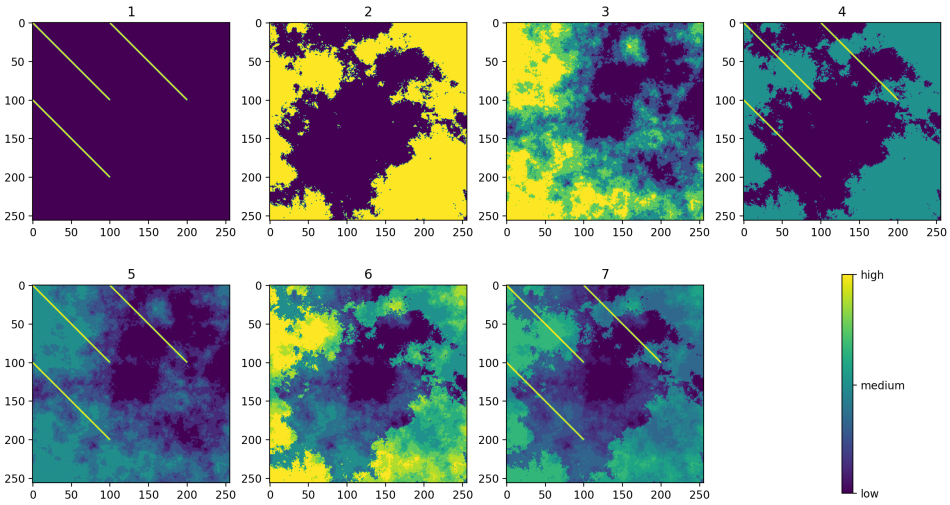


Figure 4.2: The seven resistance surfaces used in the analysis. Resistance values range from 1 to 100, with blue indicating low resistance and yellow indicating high resistance.

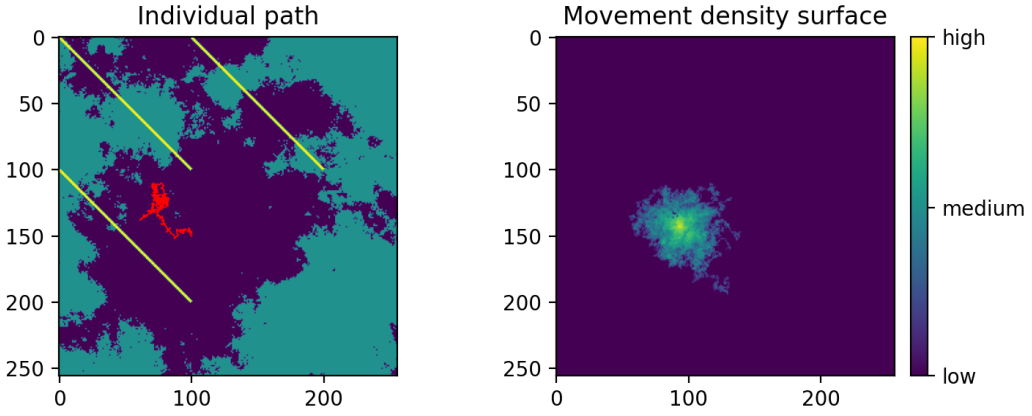


Figure 4.3: On the left, an example individual stochastic path in red on the fourth resistance surface used in this analysis; yellow is high resistance and blue is low resistance. On the right, an example density surface produced by aggregating 100 paths from the same source point and with the same movement parameters; yellow is high density and blue is low density. In this manner, the colour bar applies to both figures.

haviour, sampling the full parameter space of movement mechanism, spatial scaling and degree of autocorrelation. Specifically, for each of the 7 resistance surfaces, we run 7 different movement mechanisms, 4 degrees of spatial scale, 3 types of scale response, and 3 degrees of autocorrelation, giving a total of 1,764 simulated connectivity scenarios (Table 4.1).

For a second analysis, we then test the effect of 3 degrees of destination bias on the model accuracies, by varying this parameter together with the 7 different movement mechanisms while keeping the spatial scale, scaling function and autocorrelation fixed, providing an additional 21 movement scenarios for each of the 7 resistance surfaces (Table 4.1). This gives a further 147 connectivity scenarios, resulting overall in 1,911 simulated connectivity surfaces with which to compare the predictive abilities of factorial least-cost paths, resistant kernels and Circuitscape.

	First analysis	Second analysis
Resistance surface	All resistance surfaces	All resistance surfaces
Movement mechanism	All movement combinations	All movement combinations
Spatial scale	1×1, 3×3, 5×5, 7×7	1×1
Scaling function	All scaling functions	Focal mean
Autocorrelation	0, 0.35, 0.75	0.2
Destination bias	0	0.1, 0.3, 0.6
Total combinations	1,764	147

Table 4.1: The selection of parameters used to produce the simulated connectivity maps with Pathwalker. In both analyses, all 7 resistance surfaces are tested, and all 7 movement combinations are used (energy, attraction, risk, and their pairwise and three-way combinations). In the first analysis, the spatial scale, scaling function and degree of autocorrelation are varied; in the second analysis, these three parameters are fixed whilst the degree of destination bias is varied.

4.2.3 Measuring the accuracy of the connectivity model predictions

To measure the accuracy of these connectivity models in each of the 1,911 scenarios, we use three statistics: (1) the root-mean-squared error between the true and predicted surface, (2) the Pearson linear correlation coefficient between the true and predicted surface, and (3)

the degree of spatial overlap between the areas of 10% highest connectivity in the true and predicted surface. For (1), we divide the total error by the number of pixels on the resistance surface, in order to obtain a scaled value between 0 and 1.

We subsequently perform a variance partitioning and a set of canonical correspondence analyses (CCAs) on these three statistics, supported by appropriate boxplots and an analysis of variance. We do this first for the 1,764 surfaces which do not include movement biased towards a destination, and then separately for the 147 surfaces which do incorporate destination bias. These multivariate analyses allow us to synthesise our results over the whole collection of different parameter configurations, and thus provide a thorough evaluation of the model accuracies across these behavioural scenarios.

4.2.4 Summary of analysis methodology

To summarise, we first simulate 7 different resistance surfaces, together with 100 source locations on these surfaces. We run the three connectivity models – factorial least-cost paths, resistant kernels and Circuitscape – on these 7 surfaces, giving three different connectivity predictions for each resistance surface.

For each resistance surface, we then stipulate a range of possible movement behaviours, which sample the full parameter space of mechanisms, spatial scales and degrees of autocorrelation – and use the Pathwalker software to simulate one connectivity map from each parameter configuration, giving us 1,764 simulated connectivity surfaces. Additionally, we test the effect of destination bias on model performance by varying this parameter together with the movement mechanisms for each resistance surface, while fixing the scaling and autocorrelation parameters, generating a further 147 connectivity surfaces.

We then measure how closely the three connectivity models compare with each of the 1,911 simulated connectivity maps, by calculating the average error, linear correlation and degree of spatial overlap between the true (simulated) and predicted surfaces in each case.

Finally, we synthesise these statistics using variance partitioning, canonical correspondence analyses and analysis of variance, supported by appropriate boxplots. From this we obtain a definitive picture for the accuracy of each of the three models across the possible movement behaviour parameters and resistance surfaces.

All computations in this study are performed using Python version 3.8 with the `SciPy`

package (Virtanen et al. 2020), except for the redundancy analysis and variance partitioning, which are performed using R version 3.6 with the `vegan` package (Dixon 2003).

4.3 Results

4.3.1 Connectivity model performance without destination bias

For the first analysis, the variance partitioning in Figure 4.4(a) shows that the dominant factor in the accuracy of predicting connectivity is the choice of model used. More specifically, Figure 4.4(b) shows that predictions using Circuitscape result in the least root-mean-squared error between the predicted and simulated connectivity maps. Resistant kernels are seen to be the most accurate method in terms of the linear correlation and spatial overlap between the predicted and true connectivity maps. The factorial least-cost paths model is the least accurate in all three statistics. This is shown numerically in Table 4.2. A key to the CCA figure labels is provided in Table 4.5.

Figure 4.4(c) demonstrates that variation in landscape structure can have a substantial effect on model performance: on average, as spatial heterogeneity increases, the models display much higher error but also substantially higher overlap, with little effect seen on the degree of linear correlation. Moreover, the four-way analysis of variance (Table 4.4) shows very strong interaction between model accuracy and the choice of resistance surface. The boxplots in Figure 4.7 show that the difference in model performance is much greater at lower levels of spatial complexity. As the spatial heterogeneity becomes more complex, all three models display higher error; but, simultaneously, the correlation and overlap of factorial least-cost paths and Circuitscape increase, while those of resistant kernels remain consistently high across the variation in spatial complexity.

Figure 4.4(d) shows that these connectivity models are overall much less accurate if the movement is parameterised only by landscape resistance values, without any limit on dispersal capabilities or mortality risk, as seen by the position of the attraction mechanism (labelled as 'm2'). More detail on the effects of movement mechanism on model performance is illustrated by the boxplots in Figure 4.8. Namely, with the presence of energy or risk, resistant kernels has much higher correlation and overlap than Circuitscape, and similar levels of error; without any threshold for dispersal or mortality risk, Circuitscape has substantially lower error, and

similar levels of correlation and overlap, in comparison with resistant kernels.

The variance partitioning suggests that the effects of spatial scaling and autocorrelation, in contrast with movement mechanism and connectivity model choice, are not seen to be major factors affecting the accuracy of the three connectivity models, as shown in the additional CCA diagrams in Figure 4.6.

Method	Average error	Linear correlation	Spatial overlap
Factorial least-cost paths	0.0095	0.3943	0.3897
Resistant kernels	0.0071	0.6736	0.6070
Circuitscape	0.0062	0.5876	0.4503

Table 4.2: Results from the first study, in which we test the accuracy of factorial least-cost paths, resistant kernels and Circuitscape across 1,764 connectivity scenarios without destination bias. This table displays the overall (1) average root-mean-squared error, (2) linear correlation and (3) degree of spatial overlap, between the simulated connectivity surfaces and the predictions given by these three models.

4.3.2 Connectivity model performance with destination bias

For the second analysis, the variance partitioning in Figure 4.5(a) shows destination bias to be the main driver in variation of model accuracy across the different connectivity scenarios, approximately three times as influential as the choice of model used. Figure 4.5(b) illustrates a very clear trend in model accuracy: as the degree of destination bias increases, the error increases and the correlation and overlap decrease. A key to the CCA figure labels is provided in Table 4.5.

In Figure 4.5(c), we see factorial least-cost paths to still be the least accurate by all three metrics, and, as before, resistant kernels display the highest spatial overlap and Circuitscape the lowest average error. This trend is in fact consistent over all degrees of destination bias, as seen with the boxplot diagrams in Figure 4.9(a) and 4.9(c). However, the boxplot diagram in Figure 4.9(b) shows that, for higher levels of destination bias, the connectivity predictions by Circuitscape produce the strongest linear correlations with the simulated connectivity maps; this results in the overall higher correlation seen with Circuitscape in Table 4.3. And in comparison with the first study, the presence of destination bias results in a stronger link

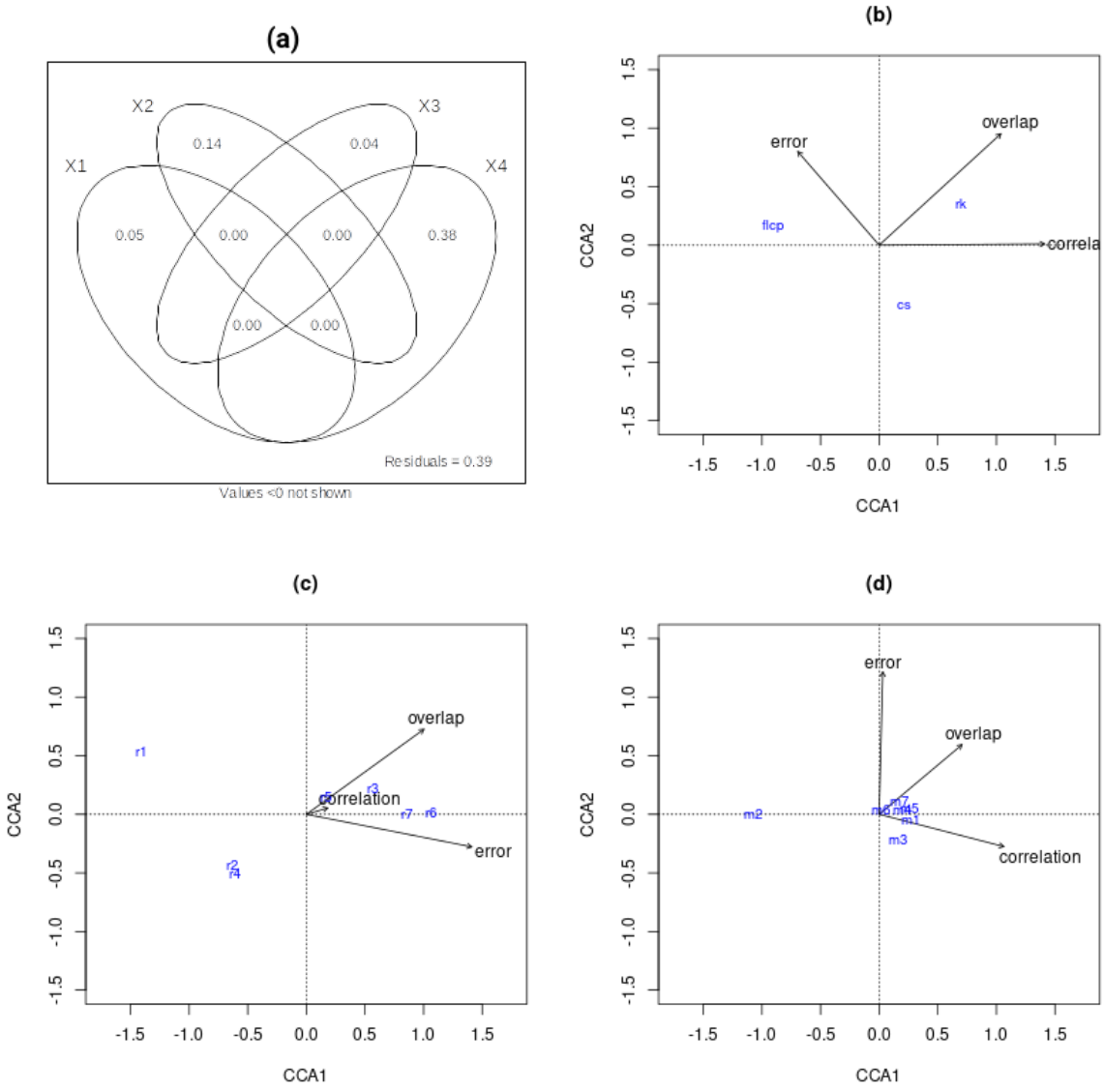


Figure 4.4: Variance partitioning (a) and canonical correspondence analyses (b-d) for the first investigation. The variance partitioning shows model choice (X4) to be the major factor affecting predictive accuracy, more than twice the strength of the effects of spatial complexity of the resistance surface (X2), which in turn is roughly triple that of the mechanism (X1) and the remaining parameters – autocorrelation, scale and scaling function – combined (X3). In (b) we see that predictions by resistant kernels overall give the highest correlation and overlap, and those by Circuitscape result in the least error, whereas factorial least-cost paths is seen to be the least accurate with all three statistics. (c) shows that higher levels of spatial complexity result in great model error and overlap, with little effect on correlation. (d) demonstrates model performance to be much lower when using only the attraction mechanism.

between higher spatial complexity and greater model accuracy, as inferred from Figure 4.5(d).

Method	Average error	Linear correlation	Spatial overlap
Factorial least-cost paths	0.0150	0.3318	0.4160
Resistant kernels	0.0139	0.4627	0.5675
Circuitscape	0.0127	0.5276	0.4801

Table 4.3: Overall results from the second analysis, which tested the accuracy of factorial least-cost paths, resistant kernels and Circuitscape across 147 connectivity scenarios.

4.4 Discussion

Analysis results

The results of our simulation analysis show particular patterns in model performance which remain constant across the various combinations of movement mechanism, spatial scaling, autocorrelation, destination bias and spatial complexity. Centrally, factorial least-cost paths proved the least accurate of the three models, consistent in having the highest error and lowest correlation and spatial overlap. This demonstrates that, despite being a widely used approach to modelling connectivity, the precise least-cost path (or corridor) between two locations on a resistance surface may dramatically not reflect the actual pathways of animal movement.

We also find resistant kernels to consistently produce predictions which result in the greatest degree of spatial overlap with the simulated connectivity maps, substantially higher than both Circuitscape and factorial least-cost paths. In terms of the other two statistics measuring accuracy – root-mean-squared error and linear correlation – the comparative predictive abilities of resistant kernels and Circuitscape vary according to two factors: primarily, the degree to which movement is inclined towards a known destination; and to a lesser degree, the spatial complexity of the resistance surface. Other movement parameters in Pathwalker did not affect model performance to the same extent as destination bias and spatial heterogeneity.

Without destination bias, resistant kernels produced connectivity predictions which correlated and overlapped more strongly with the simulated connectivity scenarios than those given by Circuitscape, across all degrees of spatial complexity, suggesting resistant kernels to

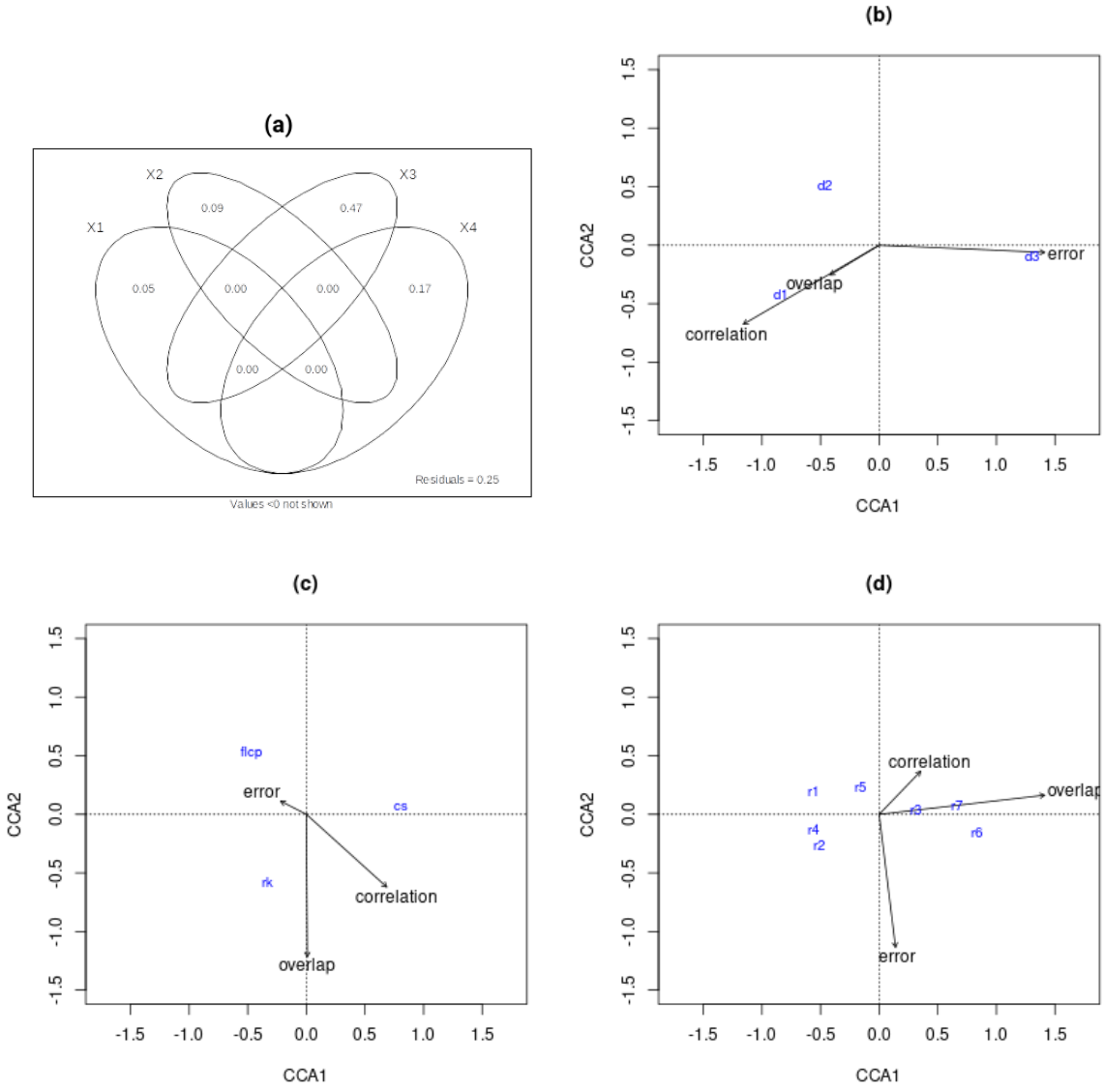


Figure 4.5: Variance partitioning (a) and canonical correspondence analyses (b-d) for the second investigation. The variance partitioning now shows destination bias to be the primary factor determining the accuracy of connectivity predictions, approximately thrice as influential as model choice (X4), which in turn has a much greater effect on predictive accuracy than movement mechanism (X1) and spatial complexity (X2). In (b), we see a lower degree of destination bias gives predictions which are more accurate across all three statistics. In (c) we see that predictions by resistant kernels overall give the highest overlap, and those by Circuitscape result in the least error, whereas factorial least-cost paths is seen to be the least accurate. The increase in correlation and overlap in (d) suggests that, with destination bias, higher spatial complexity now results in more accurate model predictions.

be the most robust model regarding variation in landscape structure. Moreover, between these two models, the outputs from resistant kernels resulted in a smaller error for lower degrees of spatial complexity, with the reverse being true for higher spatial complexity. However, when the movement was strongly biased towards a known destination on the resistance surface, the connectivity predictions of Circuitscape typically correlated more strongly than those of resistant kernels. Additionally, in this case the error from these two models roughly doubled, and the spatial overlap in the predictions from Circuitscape increased but still remained less than those from resistant kernels.

Importantly, we note here that in many applications of connectivity modelling, knowledge of the precise destination of movement is often very difficult to obtain, particularly with dispersing animals. This limits the effectiveness of models such as Circuitscape which require knowledge of a place towards which the movement is inclined. In contrast, this is a strength of resistant kernel modelling, which does not require the knowledge or assumption of a destination prior to movement.

Conclusion

The widespread usage of landscape connectivity in ecological theory and application has led to the development of many predictive algorithms, with Circuitscape, resistant kernels and factorial least-cost now amongst the most popular. Despite the influential usage of these three models, there is at present no published analysis which comprehensively evaluates their relative predictive abilities with simulated data. Although many studies to date have tested and validated their predictions using empirical data, such analyses are limited in their capacity to comparatively evaluate the accuracy and performance of these connectivity models, due to the unknown variables and relationships driving the movement patterns in empirical data.

In this chapter, we have used the spatially-explicit individual-based movement model Pathwalker to generate different connectivity scenarios from a large variety of simulated movement behaviours and spatial complexities, and then measured the extent to which the three models are able to predict these simulated patterns of landscape connectivity. Thus, we are able to provide a thorough evaluation of the performance of three of the dominant connectivity models in conservation science, giving important information for their effective use and application across different contexts.

4.5 Supplementary figures and tables

Parameter	DF	SS	MS	F-value	P-value
Mechanism	1	2.30	2.299	111.808	<2e-16
Resistance	1	10.54	10.539	512.602	<2e-16
Scale	1	1.11	1.115	54.220	2.07e-13
Model	1	19.07	19.073	927.675	<2e-16
Mechanism:Resistance	1	0.46	0.460	22.390	2.28e-06
Mechanism:Scale	1	0.00	0.000	0.005	0.94554
Mechanism:Model	1	0.01	0.007	0.359	0.54924
Resistance:Scale	1	0.15	0.147	7.170	0.00744
Resistance:Model	1	3.49	3.490	169.726	<2e-16
Scale:Model	1	0.11	0.108	5.237	0.02215
Residuals	5281	108.58	0.021		

Table 4.4: Four-way analysis of variance table for movement mechanism, resistance surface, spatial scale and model choice. Strong interaction is seen between model choice and resistance surface, suggesting the three models to differ in effectiveness as spatial complexity varies. Mechanism and resistance surface also show substantial interaction.

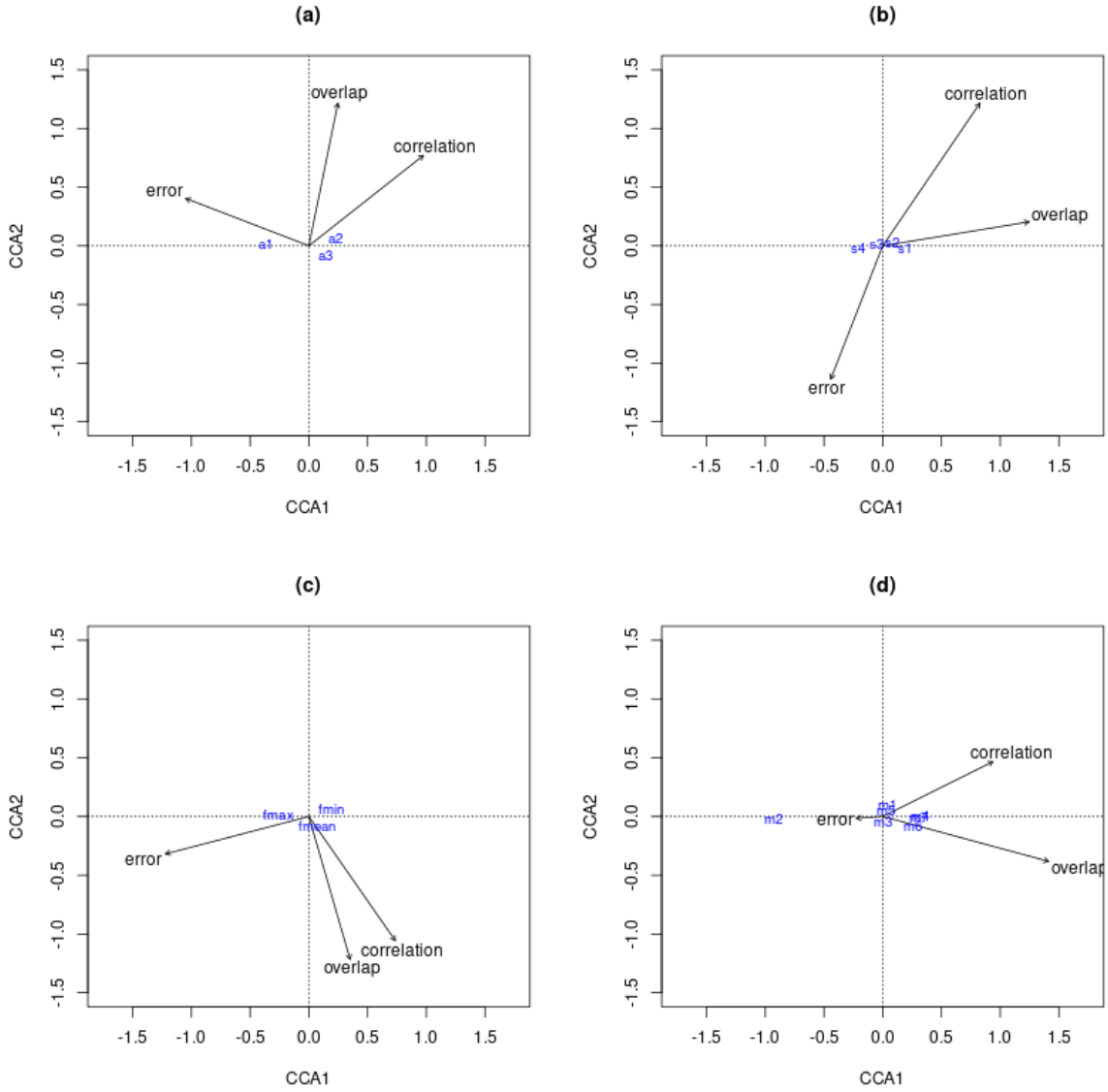


Figure 4.6: Additional CCA diagrams: (a-c) are from the first study, (d) is from the second study. A key to the CCA figure labels is provided in Table 4.5. (a) shows that higher degrees of autocorrelated movement resulted in lower model error, but had little effect on correlation and overlap. Variation in spatial scale (b) and scale response function (c) had little overall effect on accuracy. However, the relatively low impact of spatial scale seen in (b) may reflect the small range of movement scales used in the simulation study; larger spatial scales of movement behaviour may result in a more substantial effect on model accuracy. The spread of points in (d) is similar to that in Figure 4.4, suggesting the effects of movement mechanism on model accuracy to be fairly consistent over different degrees of destination bias.

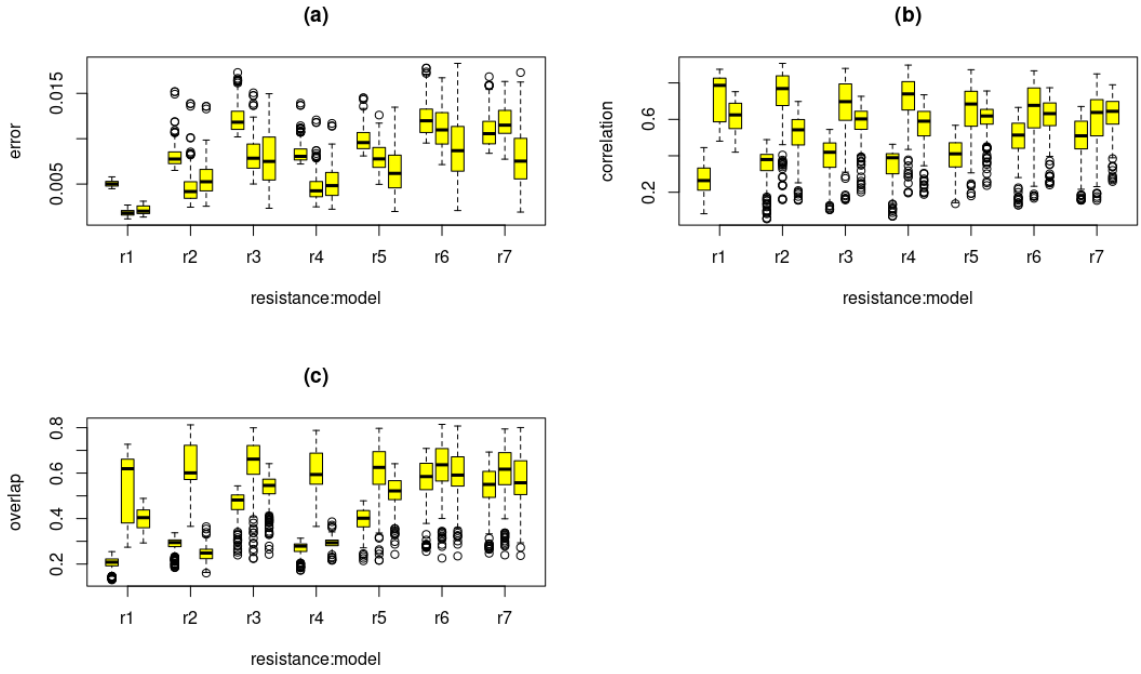


Figure 4.7: Boxplots illustrating the effects of landscape structure on model accuracy from the first study, displaying the error (a), correlation (b) and overlap (c). Each triplet of boxes represents factorial least-cost paths, resistant kernels and Circuitscape, from left to right, respectively. Across all three statistics, the three models perform more similarly as spatial complexity increases. For the simpler surfaces (r1, r2 and r4), resistant kernels is substantially more accurate than factorial least-cost paths and Circuitscape. For the more complex surfaces (r3, r6 and r7), error increases for all three models. However, the correlation and overlap for factorial least-cost paths and Circuitscape also increase, while resistant kernels remain consistent with high correlation and overlap.

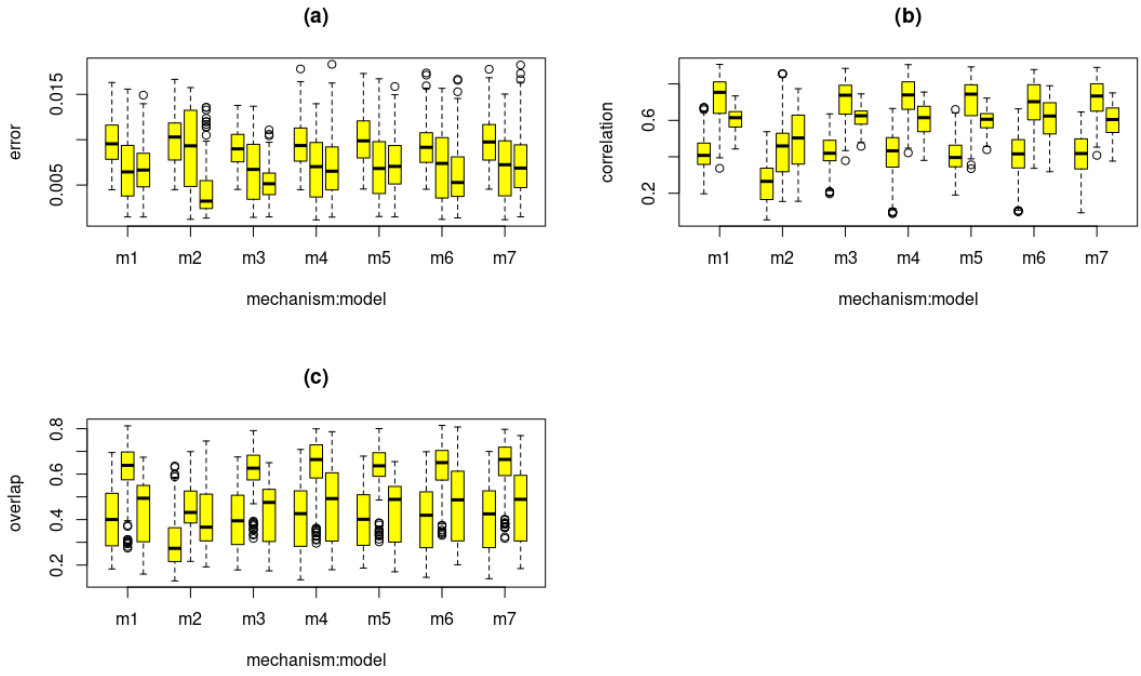


Figure 4.8: Boxplots illustrating the effects of each movement mechanism on model accuracy from the first study, displaying the error (a), correlation (b) and overlap (c). Each triplet of boxes represents factorial least-cost paths, resistant kernels and Circuitscape, from left to right, respectively. Aside from the attraction mechanism without energy or risk (m2), each model maintains fairly consistent accuracy across the movement mechanisms: resistant kernels has substantially higher correlation and overlap than Circuitscape, and these two models produce predictions with similar levels of error; factorial least-cost paths is the least accurate in every case. With the attraction mechanism, in the absence of energy or risk, Circuitscape has much lower error and similar levels of correlation and overlap to resistant kernels.

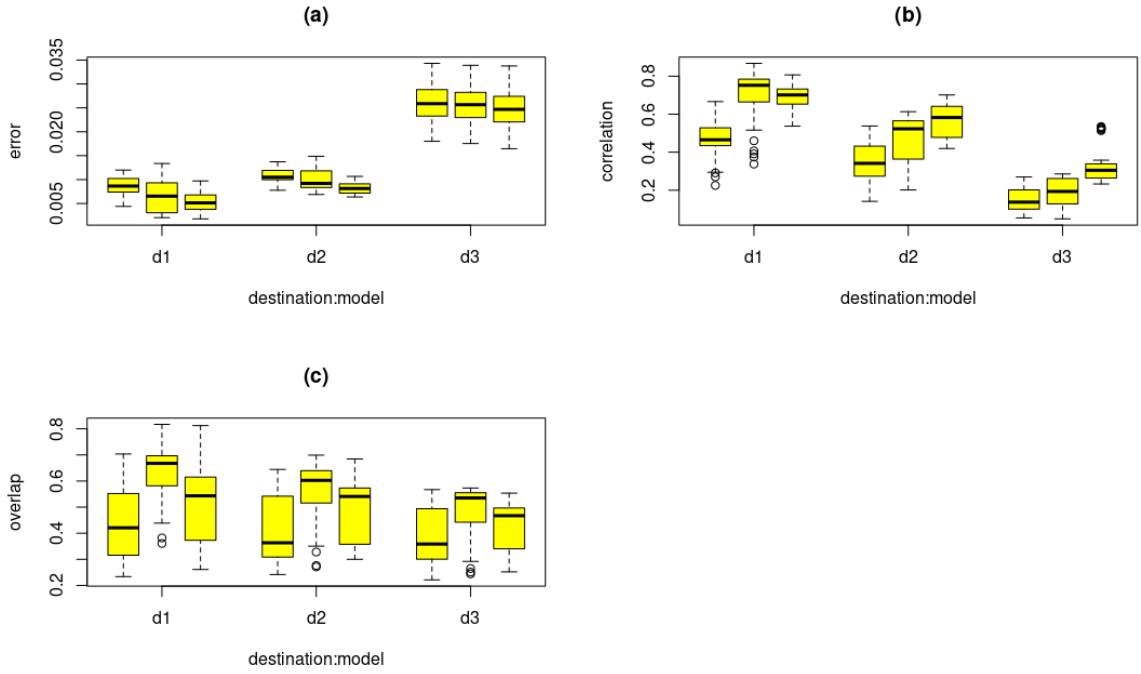


Figure 4.9: Boxplots illustrating the interaction between model accuracy and the degree of destination bias from the second study, displaying the error (a), correlation (b) and overlap (c). Each triplet of boxes represents factorial least-cost paths, resistant kernels and Circuitscape, from left to right, respectively. (a) shows Circuitscape to produce predictions with the lowest error across all levels of destination bias, although the difference between the three models is only marginal. (b) demonstrates that, at low levels of destination bias, predictions by resistant kernels correlate most strongly with the simulated connectivity maps; for higher degrees, CircuitScape gives predictions with greatest linear correlation. In (c), we see resistant kernels to consistently result in the highest spatial overlap.

Parameter	Label	Value
Model	flcp	factorial least-cost paths
	rk	resistant kernels
	cs	Circuitscape
Resistance surface	r1	resistance surface 1
	r2	resistance surface 2
	r3	resistance surface 3
	r4	resistance surface 4
	r5	resistance surface 5
	r6	resistance surface 6
	r7	resistance surface 7
Mechanism	m1	energy
	m2	attraction
	m3	risk
	m4	energy + attraction
	m5	energy + risk
	m6	attraction + risk
	m7	energy + attraction + risk
Autocorrelation	a1	0
	a2	0.35
	a3	0.75
Spatial scale	s1	1×1
	s2	3×3
	s3	5×5
	s4	7×7
Scaling function	fmean	focal mean
	fmax	focal maximum
	fmin	focal minimum
Destination bias	d1	0.1
	d2	0.3
	d3	0.6

Table 4.5: Key to figure labels for diagrams in main text and supplementary material.

Chapter 5

Moving beyond landscape resistance



Figure 5.1: This chapter is closely adapted from the *Landscape Ecology* article *Moving beyond landscape resistance: considerations for the future of connectivity modelling and conservation science* (Unnithan Kumar, Turnbull, et al. 2022b). The journey of this piece unfolded through the entirety of my year in the tent glade. Photograph by Siddharth Unnithan Kumar, 5th October 2022.

5.1 Introduction

As we have seen in the previous two chapters, the concept and methods of 'landscape connectivity' have grown to become a central focus of ecological science, with widespread use in policy and management. The dominant paradigm for mapping connectivity uses 'resistance surfaces' to reflect the influence of landscape features on organism movement. Its major appeal lies in its ability to provide a spatially-explicit framework for connectivity models while requiring relatively few parameters (Cushman, McRae, et al. 2013). However, as we argue in this chapter by synthesising material from conservation science and environmental geography, the simplistic assumptions and high degree of reductionism inherent in resistance surfaces severely limits the ability of connectivity algorithms to account for many fundamental aspects of animal movement, to the extent that they greatly reduce the effectiveness and relevance of connectivity models for environmental theory and practice. But, unlike previous critiques of resistance-based connectivity models (such as Moilanen 2011), this chapter is also upbeat and offers promising avenues for future research, emphasising how currently existing models can be expanded and enriched with newly available techniques and methods.

5.1.1 Chapter overview

We begin by providing a technical and historical overview of the development of connectivity modelling and resistance surfaces, which necessarily repeats some of their details mentioned in the two previous chapters. We then discuss several important drivers of movement behaviour which are absent in resistance-based models, with a focus on the context-dependent and spatiotemporally dynamic nature of animal movement, and we examine a range of recent empirical scientific studies which demonstrate the significant effects these have on connectivity predictions. This opens us to a huge and rich area of research, full of unexplored hypotheses which we believe to be central to the future of connectivity modelling. We conclude with a discussion of how we may look to newly emerging technologies and interdisciplinary work to develop methodologies, models and conversations which move beyond the limitations of the landscape resistance paradigm, so that connectivity models can better reflect the patterns of animal movement in their lively reality.

5.2 Landscape connectivity and resistance surfaces: a brief history

5.2.1 The emergence of landscape resistance

Early models for predicting connectivity were developed in the 1990s and 2000s, based on simple adaptations of random walk theory (Codling et al. 2008). Although these individual- (or agent-) based models did incorporate a handful of basic parameters into simulating movement – such as autocorrelation and differential mortality risks (C. M. Bergman et al. 2000; Kareiva and Shigesada 1983) – they paid little attention to the heterogeneity of the landscape. Where spatial variation did appear, it involved no more than simple barriers or homogeneous landscape patches (Dunning Jr et al. 1995; Schumaker 1996). Soon afterwards, the concept of the resistance surface (explained below) was introduced from transport geography as an attempt to quantify how landscape features differentially affect movement, and to provide a greater degree of spatial complexity in connectivity modelling. This was made possible by the availability of increasingly high-quality and fine-scale geospatial satellite data, which allowed for more detailed parameterisation of the landscape than the simple habitat patches used in earlier models (Cushman and Huettmann 2010). Since its introduction, the paradigm of landscape resistance has swelled to become the dominant framework with which to model and predict connectivity (Zeller, McGarigal, and Whiteley 2012).

5.2.2 Estimating landscape resistance

A resistance surface is a pixelated map of the landscape, in which each pixel is assigned a numerical value which reflects the estimated 'cost of movement' through the region of the landscape corresponding to that pixel. These were originally developed according to 'expert opinion' (Adriaensen et al. 2003; Beier, Majka, and Spencer 2008), but this approach had major disadvantages due to the lack of empirical evidence for its predictions (Cushman 2006). Hence, in the last decade, ecologists have sought to craft methods for creating resistance surfaces which are explicitly informed by empirical data. The first such efforts began by assuming landscape resistance to be directly proportional to the inverse of habitat suitability data (Beier, Majka, and Newell 2009). However, because habitat suitability primarily reflects the ability of a landscape to support the needs of an organism dwelling there, whereas

connectivity is concerned with *movement through* a landscape, habitat suitability has since been established as an insufficient proxy for estimating resistance to movement in many cases (Keeley et al. 2017; Wasserman et al. 2010).

The most recent attempts to create resistance surfaces have focused on developing methods which optimise a functional relationship between the landscape (represented by a collection of chosen GIS layers) and data on animal movement patterns, for which telemetry or genetic data are often used (Cushman and J. S. Lewis 2010; Shirk, Wallin, et al. 2010). This approach typically employs a resource selection function (Boyce et al. 2002). In more detail, this means that a regression model is used with the empirical movement data to estimate the coefficients of a particular linear function. This mathematically expresses resistance to movement as a function of the different chosen environmental variables, where the coefficients reflect the degree to which each variable is predicted to assist or impede movement (Thurfjell et al. 2014). The resulting linear combination of these GIS layers produces a new layer, which is the resistance surface. Figure 5.2 illustrates a resistance surface used in Elliot, Cushman, D. W. Macdonald, et al. 2014, created using a path-selection function with telemetry data gathered from the Hwange National Park locale in Zimbabwe.

Several studies have since shown this functional relationship approach to perform stronger than the earlier methods of expert opinion and habitat suitability (Mateo-Sánchez et al. 2015a,b; Shirk, Schroeder, et al. 2015). Yet there are limitations to the rigour and utility of the telemetry- and genetics-based methods too. Fundamentally, as with all applications of resource selection function theory, the practitioner must decide *a priori* which environmental factors are considered influential for movement, and thus which variables are included in predicting landscape resistance (Burnham et al. 2004; Manly et al. 2007).

5.2.3 Resistance-based connectivity modelling

Landscape resistance is point-specific: each pixel reflects the estimated difficulty of moving through that specific location in the landscape, and hence does not account for the emergent routes through the landscape as a whole, which is the central focus of landscape connectivity. Resistance-based connectivity models thus typically work by applying a chosen movement algorithm to a resistance surface in order to obtain predictions of landscape connectivity (Cushman, McRae, et al. 2013). Alongside now briefly charting the historical developments

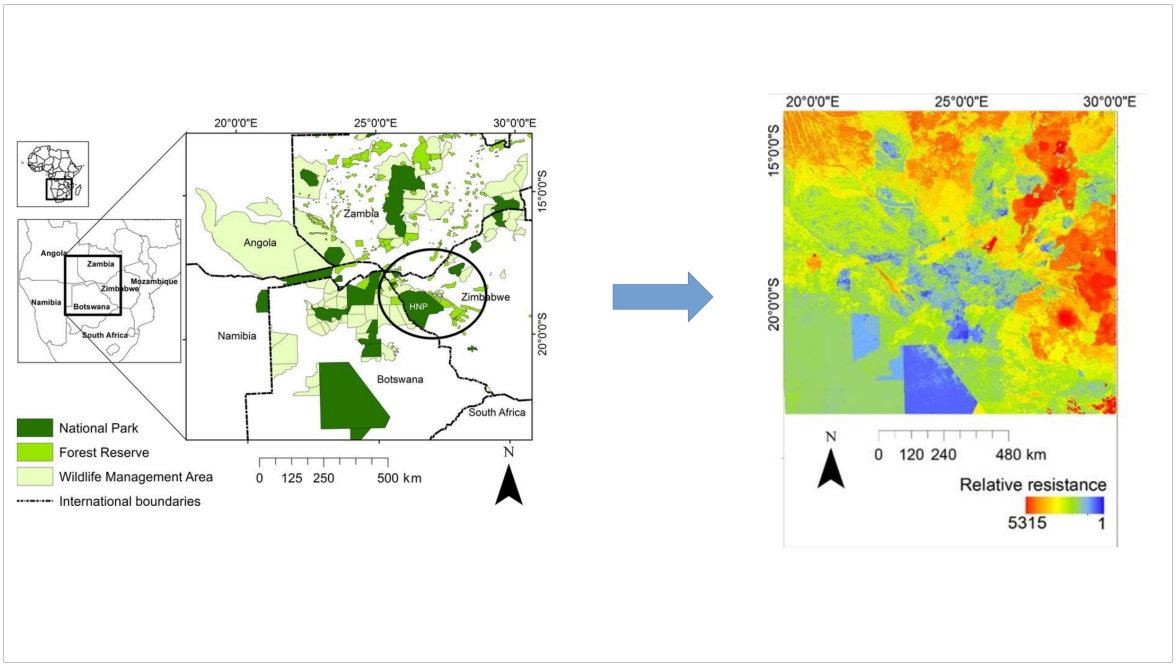


Figure 5.2: Example of a resistance surface used in Elliot et al. (2014a). The surface was created using a path-selection function with telemetry data gathered from dispersing lions.

of certain major connectivity models in conservation science, we revisit some of their details mentioned in Chapter 3.

The first resistance-based models of landscape connectivity calculated the 'least-cost path' between two points on the resistance surface, as an approximation to the most favourable movement paths in a landscape (Adriaensen et al. 2003). In other words, they computed the route which minimises the accumulated 'cost of movement' between two locations. This was later extended to produce a network of least-cost paths between all combinations of any number of source points (Cushman, McKelvey, et al. 2009); similar multiple-path approaches are presented in Rayfield et al. 2010 and Pinto et al. 2009. However, there are substantial limitations to these least-cost path approaches in practice. There is little reason to assume that an animal knows (or even thinks in terms of) the route of the least-cost path. Moreover, the destination point may not be known to the animal prior to or during movement – and even if this were so, obtaining the knowledge of their precise destination can be very difficult in practice, especially with dispersing animals.

Further algorithms for predicting connectivity have since been developed, with the most

popular still using the framework of landscape resistance. Presently, two major connectivity models in use are 'resistant kernels' and 'Circuitscape' (Compton et al. 2007; McRae et al. 2008). Resistant kernels is a cost-distance approach based on Dijkstra's algorithm, which estimates connectivity as a function of landscape resistance and dispersal thresholds, producing a map of connectivity by summing together the expected dispersal density in the pixels around each source point. In contrast, Circuitscape uses electrical circuit theory, in which the resistance surface is treated as a circuit and animals are modelled as electrons 'flowing through this circuit', with mortality and connectivity quantified by the mathematical relationships of circuit theory. This algorithm produces a map in which the current flowing through each pixel of the resistance surface is assumed to reflect the degree of connectivity. In both cases, animals are modelled as automatons moving according to simple rules from graph theory or random walk theory.

5.2.4 Combining individual- and resistance-based approaches to connectivity

These connectivity models use resistance surfaces to parameterise the energetic cost of moving through the landscape, but this is only one of many factors influencing movement. For example, resistance-based connectivity models do not account for the autocorrelated nature of animal movement (Cushman 2010a) – as acknowledged with Circuitscape in McRae et al. 2008 – despite the present state of an animal's movement being strongly influenced by their immediate past direction of travel (Dray et al. 2010). As mentioned above, the earlier agent-based algorithms (such as Kareiva and Shigesada 1983) in contrast did incorporate greater detail into simulating individual animal movement, and the mechanisms for individual movement parameters have been developed theoretically since then (DeAngelis et al. 2005; M. A. Lewis et al. 2013). However, the spatially homogeneous nature of these early individual-based algorithms greatly limited their effective use in landscape ecology and conservation science, in which spatial complexity plays a central role (McGarigal and Cushman 2005).

This directed attention towards crafting detailed individual-based models which also attend to variations in landscape composition. Such examples include: simulating individual movement using geospatial data on old-growth forest distribution in the Pacific Northwest in order to assess the effects of habitat fragmentation on dispersal (Schumaker 1996), and

developing an algorithm to detect dispersal corridors which used geospatial data to provide the locations of habitat patches (Hargrove et al. 2005). Although these models did weave a degree of spatial heterogeneity into their studies of connectivity, they worked only with a binary quantification of landscape structure (namely, whether a location could be considered as habitat or not).

Thus, subsequent work has combined the detail of the individual-based approach with the more continuous measure of spatial patterns given by resistance surfaces, like the Pathwalker model which we have seen in the previous two chapters. Other such algorithms include HexSim and RangeShifter, which model movement based on the interplay of population dynamics and individual characteristics in a spatially-explicit framework (Bocedi et al. 2021; Schumaker and Brookes 2018). For example, HexSim allows for the use of multiple resistance-like surfaces which approximate landscape features such as food and nesting resources, in addition to a measure of the energetic cost of movement from a traditional resistance surface. These spatially heterogeneous individual-based models thus incorporate details which are missing in the simplistic assumptions used by the dominant resistance-based connectivity algorithms.

5.3 The trouble with resistance surfaces: or, getting back to the wrong landscape

As discussed above, certain important aspects of animal movement which are absent in popular resistance-based algorithms like Circuitscape and other least-cost path approaches are addressed to some degree by recent spatially-explicit individual-based models such as Pathwalker. Yet it may be apparent that several fundamental drivers of movement and connectivity are not accounted for in any currently available model which uses the framework of landscape resistance. Centrally, there is a conspicuous lack of spatiotemporal variation and contextual detail in the modelling of animal movement behaviour and their relationship with the landscape.

All scientific models inherently require a simplification of ecological complexity and dynamics. But does the extent of the reductionism involved in current resistance-based connectivity models, and their simplistic assumptions about animal behaviour, render them

inappropriate for application to the realities of conservation practice and landscape ecology? And if this is the case, then can this issue be addressed effectively by a conceptual reframing of the objectives and assumptions used in building these models – a better-informed understanding of which complexities to reduce, and the techniques for doing so – rather than simply creating parameter-heavy models which become unwieldy for widespread usage?

The remainder of this chapter is devoted to working with these two questions. In this section, we discuss conceptual arguments and look at a range of empirical studies which establish the importance of spatiotemporal nonstationarity and context dependence in understanding and modelling landscape connectivity. The influence of these effects on the actual patterns of animal movement has been largely unexplored in the scientific literature. Recent works, mentioned below, are only just beginning to scratch the surface of this question, but already they point towards the enormous effect these factors can have on movement and connectivity predictions.

5.3.1 Spatiotemporal effects

Temporal variability

The landscape resistance paradigm assumes that an animal's movement decisions do not change over time, and thus is unable to account for the migratory, diurnal, seasonal and life-history cycles which greatly influence the way animals move through the landscape. Of these temporal changes, it is most obvious that connectivity for migratory species is inherently variable over time (Webster et al. 2002). What about the broader effects of seasonal cycles of animal and landscape on connectivity predictions?

From a year-long study of African elephant movement in southern Africa, Kaszta, Cushman, and Slotow 2021 found dramatic variation in landscape resistance and connectivity predictions in different months, highlighting a 'potentially serious problem in using movement models from a particular temporal snapshot to infer general landscape effects on movement'. In a different study of African elephants, Osipova et al. 2019 conclude that 'models disregarding seasonal resource fluctuations underestimate connectivity for the wet and transitional seasons, and overestimate connectivity for the dry season'. The temporally static nature of a resistance surface ignores the dynamism of the landscape itself, which is a process always in flux rather than a fixed entity (Ingold 1993). Temporal landscape variation, such as seasonal

rainfall and vegetation change, often alters animal movement pathways, as demonstrated in Cushman, Chase, et al. 2005.

Additionally, the broader timescale of an animal's life history does not appear in the widely-used connectivity models, despite its established importance in patterns of movement and connectivity for many species. For example, in a decade-long study of African lions in southern-central Africa, Elliot, Cushman, D. W. Macdonald, et al. 2014 found connectivity predictions for young males to be vastly different than for adults, concluding that ignoring demographic variation when 'parameterizing resistance surfaces intended for connectivity modelling may lead to erroneous conclusions about connectivity and potentially unsound management strategies'. Particularly with intra- and interspecific relationships, these dispersal and home range movement patterns interact with diurnal variation (Hearn et al. 2018), and the temporality of the landscape itself (Schwartz et al. 2009).

Spatial variability

The question of spatial nonstationarity refers to whether the relationship between animal and landscape varies across space; and if so, to what extent does this variability affect resistance-based connectivity models? In other words, does the spatially unchanging functional relationship used to build a resistance surface from empirical data result in models whose predictions do not accurately reflect the actual pathways of movement and connectivity in different landscapes?

In ecological science, the biotic or abiotic variables which ostensibly have the greatest impact on the viability of animal movement or dwelling in a particular region are known as 'limiting factors' (Cushman, Shirk, et al. 2013). Vergara et al. 2017 found that the limiting factors which most strongly influenced stone marten genetic connectivity varied vastly across Iberia. Their results highlight the importance for landscape models to be developed *specific to the region of interest* as a precursor to conservation management decisions, and for the effects of spatial nonstationarity to be carefully considered and evaluated in any application of connectivity modelling. In a study through both central and western India, Reddy et al. 2019 found tiger movements to be primarily related to topographic roughness and secondarily to diffuse disturbance. However, the relationship between the tiger and these two limiting factors was inverted between western and central India, suggesting that a resistance surface

built from a spatially constant functional relationship would at best be appropriate for only one of these two regions.

In some cases, such as the study of the American black bear in Cushman, J. S. Lewis, and Landguth 2014, resistance surfaces may provide adequate information to explain observed movement patterns. Yet the above recent works are among others (e.g. Cushman, Raphael, et al. 2011; Reding et al. 2013; Shirk, Schroeder, et al. 2015) which give strong evidence that the movement choices made by animals in relation to different landscape features will vary through space, and that these behavioural changes substantially impact connectivity predictions. This spatially dynamic relationship between animal and landscape also interacts with human presence: for example, the sparse cover of hedgerows may be preferred in arable landscapes without forest, but not when more continuous forest is present (Tree 2018). Certain dense forest patches may be entirely avoided, or highly desirable, dependent on the many possible effects of human presence on nonhuman movement (Hearn et al. 2018; Mathur 2021). We discuss this further in the section on human-nonhuman interactions below.

Noise or fundamental driver?

Cushman 2010b asked whether spatiotemporal complexity in ecological systems is merely noise around a stable, equilibrium state; or is this variability in space and time instead a core driver of such systems, so that 'ideal' models which are spatiotemporally homogeneous do not represent the fundamental dynamics of ecological processes?

As described earlier, resistance surfaces are created from a functional relationship with a chosen set of environmental factors, and this relationship (which is typically linear or logistic) is modelled as stationary in both time and space. The above studies on spatiotemporal variation are mostly very recent, and thorough investigations into these effects are only just beginning in ecological science research. In some cases, such as the aforementioned empirical study of the American black bear, landscape resistance may provide a sufficient explanation of observed movement patterns. Yet in the majority of studies published to date which analyse spatiotemporal effects on movement and connectivity predictions, they are found to have a significant impact to the degree that the equilibrium and stationary assumptions in the landscape resistance paradigm result in connectivity models which are often inadequate for conservation practice and management.

This growing body of work points towards embracing that an animal's relationship with a landscape is not composed of a universal and unchanging set of separate factors (such as elevation, terrain slope, forest cover, and so on), as chosen and isolated by the modeller. Instead, it is dynamic on multiple scales, local in nature, and experienced in relation to the composition of the landscape as a whole (Abram 1996; Ingold 2000). In other words, this inherent spatiotemporal complexity is central to understanding the relationship between an animal and the landscape of which it is part, to the extent that much of animal movement through a changing landscape cannot be understood using only a pixelated map created from a weighted sum of static geospatial image layers.

Recent ecological work has started looking into incorporating spatiotemporal variability into a resistance-based framework. For example, by adapting connectivity models so that the coefficients of the geospatial layers used to create the resistance surface vary with time, or with the location of the animal (Jennings et al. 2020; Zeller, Lewsion, et al. 2020). However, the topic of nonstationarity in space and time is part of a broader issue of the many ways in which animal movement is thoroughly 'context-dependent'. We now turn to study examples of context dependence and its implications for connectivity modelling, examining how it calls into question the paradigmatic assumptions of resistance surfaces and the simplistic cost–benefit approach to quantifying animal movement.

5.3.2 Context dependence

Intraspecific and interspecific interactions

The pathways travelled by an animal are shaped by their relationships with the changing presence and movements of other animals. Intimacy, territoriality, hunger, love, competition, curiosity, dialogue, a web of social dynamics, and countless other relational bonds, can be fundamental drivers of movement patterns. What influence do these interactions have on connectivity predictions?

The decade-long study of African lions in Elliot, Cushman, Loveridge, et al. 2014 provides 'the first investigation of seasonal movement patterns during dispersal in conjunction with territorial adults and how this varies depending on group size', in which they found intraspecific group size to have a substantial impact on the choice of route taken by the lions. Social relations between demographic categories were seen to explain radically different predictions

of connectivity (Elliot, Cushman, D. W. Macdonald, et al. 2014). Broekhuis, Madsen, et al. 2019 analyse the relational movement of male cheetahs, and its link with territoriality and mortality, 'giving a first detailed insight into intraspecific interactions in cheetah[s].' As mentioned earlier, these effects on movement interlock with the spatiotemporal heterogeneity of the landscape (Gorini et al. 2012).

A similar argument applies to interspecific interactions, in which the details of a predatory or coexistive relationship play a key role in movement behaviour, as demonstrated in Broekhuis, Cozzi, et al. 2013. Studying the relationships between cheetahs, lions and spotted hyaenas, they found cheetah movement routes to be highly influenced by the changing presence of lions; in conclusion, they encourage 'a more dynamic approach to investigate interactions between species'. In a seven-year study using 'the largest Bornean felid detection dataset to date', Hearn et al. 2018 investigate the dynamic coexistence of five felids and their spatiotemporal distribution, finding intra- and interspecific interactions to play a central role in explaining observed occurrence and movement patterns.

Perhaps due to the complexity of such empirical investigation, few field-based analyses have emerged in the ecological science literature which look at the impact of creaturely interactions on connectivity predictions. Moreover, these relational drivers of spatial distribution also mix with the effects of human presence (discussed in the next section). For some species, understanding these interactions may not be so important for mapping their movement patterns. However, because connectivity is calculated directly from the cumulative movement choices made by individual animals, these above studies and others suggest connectivity predictions to be highly sensitive to many intra- and interspecific relationships (as explicitly shown in Elliot, Cushman, D. W. Macdonald, et al. 2014).

This gives rise to many interesting hypotheses, which could be tested and explored using simulation techniques. For example, flexible existing individual-based models like Pathwalker could be used (or straightforwardly adapted) to include parameters for simulating particular interactive effects and subsequently assessing their impacts on connectivity. More broadly however, the degree of theoretical reductionism inherent to the landscape resistance paradigm does make it a rigid framework in which to perform such investigations (Moilanen 2011). These limitations come into sharp focus when becoming cognizant of the many different ways in which creatures interact with each other, which Unnithan Kumar, Turnbull, et al.

2022a highlight as a fundamental limitation to the 'animal economicus' approach to scientific movement modelling. This raises the following question, to which we return in the final section of this chapter: can we develop ways to measure and quantify ecological processes which do not force them into this enormously simplistic assumption of animal behaviour, which does little to reflect the complex and rich reality of these lively relationships?

Human-nonhuman interactions

Humans have long been (and still are) part of the interconnected ecological flows of this living and breathing world. However, the earth's ecosystems are now increasingly shaped by anthropogenic presence. Conservation science thus inherently requires attention to be given to human-nonhuman relationships; for the effective modelling and application of landscape connectivity, it is obvious that these influences on movement patterns must be adequately accounted for. Traditional, ideal movement models which ignore the complexities of human influence on animal behaviour for the sake of theoretical and algorithmic simplicity are thus growing increasingly unreliable (Benson 2014; Berkes et al. 2008; Pooley, Barua, et al. 2017). Ecological processes in reality do not follow a neat distinction between 'nature' and 'society' (Cronon 1997; Lorimer 2015). Indeed, Boettiger et al. 2011 show in a study with African elephants that predictions with existing movement models 'were most frequently inaccurate outside protected area boundaries near human settlements, suggesting that human activity disrupts typical elephant movement behavior.'

In producing a resistance surface, human presence is typically reduced to a static geospatial image layer, with each pixel given a positive or negative value according to the estimated push–pull effect of that region on animal movement. Many of the connectivity studies mentioned above point towards the impacts of human settlements on movement patterns and connectivity predictions, and the complex yet key ways these also govern how animals move in relation to other animals. Can the reality of these interactive effects be adequately captured by the spatiotemporally fixed, push–pull quantification of human presence used in resistance surfaces?

Penjor et al. 2022 show in their empirical analysis of carnivore groups in Bhutan that human settlements strongly shape movement patterns and spatial distribution, but that the effects are contrasting and varied. Integrating several methods from landscape ecology and

landscape genetics in studying the anthropogenic impact on Sunda clouded leopards in Borneo, Kaszta, Cushman, Hearn, et al. 2019 find that management decisions using resistance-based connectivity models 'might be misleading and may in some cases lead to decrease in population size', if other factors like mortality risk are not accounted for. Rostro-García et al. 2016, in an empirical study showing how the relative movements of tigers, humans and leopards are varied and complex, conclude: 'it should be realized that all maps are partial truths, and their ability to approach reality can only be judged when ground-truthed.' This provides an important reminder that maps are representations of a region, built with particular methodologies and values, and are not the landscape itself (Ingold 1993; Patel et al. 2017).

Many other studies reach similar conclusions, showing that resistance surfaces alone account for little of the complexities of how human presence—which itself is often dynamic—influences nonhuman movement patterns. Some, such as Elliot, Cushman, D. W. Macdonald, et al. 2014 and Elliot, Cushman, Loveridge, et al. 2014, demonstrate how particular animals which may generally avoid human settlements are found to move in close proximity with humans due to intraspecific social dynamics. Others, such as Ash, Cushman, et al. 2020, highlight the importance of temporally varying mortality risk on species movement.

Rigorous and detailed analyses of how human-nonhuman interactions affect animal movement can be found in the overlapping disciplines of the conservation and environmental social sciences (Bennett et al. 2017). For example, in a study of Asian elephants, Barua 2014a uses telemetry measurements and GIS data, together with data on land use change and interviews with local farmers, to obtain a more complete understanding of elephant movement patterns. In doing so, the multifaceted nature of human-elephant interactions is found to influence movement patterns in unexpected ways (Barua 2014b).

The utility of more interdisciplinary approaches to understanding animal movement and connectivity, and their compatibility with the diverse scientific analyses mentioned above, is being widely established in conservation science and landscape ecology, and we discuss this further below. Interactions are often fundamental drivers of movement patterns, whether with humans or other animals, and these fluid encounters are rarely captured by the binary cost–benefit framework of resistance surfaces, which collapses these dynamics into a single,

static number (Frank et al. 2019; Peterson et al. 2010; Pooley, Barua, et al. 2017).

Dynamic individuation: internal states and movement behaviour

We now address one final aspect of context dependence, which has been a key focus in the growing field of movement ecology: the central importance of an animal's internal states – physiological, emotional, physical – for understanding their movement patterns. Resistance surfaces, and the widely-used connectivity models based upon them (such as Circuitscape and resistant kernels), inherently assume an unchanging and universally applicable caricature of animal behaviour, in which animals are typically modelled as mindless automatons following simple random walk rules. However, the internal state of an individual creature, varying through space and time – which we call *dynamic individuation* – has been increasingly recognised as a core component of movement ecology and its application to conservation science (Jeltsch et al. 2013; Nathan et al. 2008). For example, in their study of puma movement patterns, Zeller, McGarigal, Beier, et al. 2014 found landscape resistance estimates to be sensitive to both spatial scale and movement behaviour, with different behavioural states inverting the puma's relationship with several landscape features. As a result, they 'recommend examining a continuum of scales and behavioral states' when estimating landscape resistance.

There is ostensibly little room in the framework of landscape resistance for understanding the ways an animal's internal state affects predictions of movement, and thus, connectivity. Although it is of demonstrable importance as a core driver of animal movement patterns (Holyoak et al. 2008), incorporating such information into connectivity modelling appears challenging, and until recently may not have been plausible. However, newly emerging technologies, particularly in the recent field of conservation physiology, provide a rich and promising place from which to creatively develop methods to address this. See Cooke, Sack, et al. 2013, who note that '[w]hen physiological knowledge is incorporated into ecological models, it can improve predictions of organism responses to environmental change and provide tools to support management decisions.'

For example, Cooke, Hinch, et al. 2012 link physiological and migratory data to provide valuable insights into the movement and survival of Pacific salmon, concluding that 'the best and only way to address complex conservation problems is through interdisciplinary research,

of which conservation physiology is certainly becoming a recognized and important contributor.' Sherub et al. 2017 survey the development of biologging sensors in conservation practice, and use these sensors with GPS telemetry data to study the flight paths and mortality of Himalayan vultures.

Intuitively, ecologists may expect a creature in a state of fear to respond to the landscape very differently to one in a state of calm, joy, sexual arousal or hunger. The emerging availability of biologging sensors in conservation practice is beginning to help understand how emotional and physiological states affect movement patterns (Bograd et al. 2010; Wilson et al. 2015). Further examples for integrating physiology, behaviour and conservation practice can be found in Cooke, Blumstein, et al. 2014. Ellis et al. 2012 provide an extensive discussion of the value of conservation physiology for landscape ecology and conservation science, and their possibility for compatibility and integration. These newly available conservation technologies are also inseparable from the politics and power dynamics involved in their production and usage, raising crucial questions for wildlife management like those discussed in Arts et al. 2015; C. Bergman 2005; Parreñas 2018.

More broadly, the assumption that animals behave as random walking automatons is also challenged by a question of vital importance for conservation practitioners across all disciplines: are we concerned only with maintaining the numbers of a population, or do we also place importance on the *quality* of the lives lived by the animals we study? These two priorities must be considered together, and both are essential for effective and resilient conservation practice (Hooks 2001; Sekar et al. 2020; Wallach et al. 2018). Focusing solely on population numbers to the exclusion of other such considerations has led to serious unintended consequences and harm in conservation efforts (Adams and Mulligan 2012; Paquet et al. 2010; Parreñas 2018; Pooley, Barua, et al. 2017). The reduction of animal liveliness to simplistic adaptations of graph theory or random walk theory, modelled within the attraction-aversion framework of landscape resistance, is not only a poor methodology for reflecting the actual movement patterns relevant to conservation practice and landscape ecology; as historian of wildlife tracking technologies Benson 2016 explains, this 'behavioural minimalism' also leaves no scope for attending to the quality and richness of individual lives. Developing methods to account for dynamic individuation thus seems to be a promising, exciting and vital aspect of the future of movement and connectivity modelling.

5.4 Moving beyond landscape resistance

Thus far, we have seen that landscape connectivity has become a central focus of theoretical and applied ecological research. The paradigm of landscape resistance has become the dominant framework with which to develop connectivity models, providing a spatially-explicit foundation requiring relatively few parameters. Resistance surfaces and resistance-based connectivity algorithms typically model animals as random-walking automatons, moving in relation to the landscape according to a simplistic set of movement rules which do not vary in space and time.

However, connectivity is fundamentally a phenomenon which emerges from cumulative animal movement patterns. As we have argued in this chapter, animal movement behaviour is dynamic in space and time, is inherently shaped by their internal states, and is thoroughly influenced by their rich and complex interactions with other creatures. Through both conceptual discussion and a survey of recent empirical studies of movement and connectivity, we have demonstrated that ignoring these fundamental drivers of movement often greatly limits the effectiveness and reliability of resistance-based connectivity algorithms. We acknowledge that all models require a simplification of ecological processes, and a choice of which biotic and abiotic effects on movement are considered significant enough to include as parameters. However, the analyses presented and discussed in this chapter highlight that the degree of reductionism inherent to the landscape resistance paradigm, and the rational-choice, cost–benefit assumptions made on animal movement behaviour, rarely provide an adequate basis for connectivity models to have appropriate and useful application in conservation practice and policy.

Nonetheless, we still believe that resistance surfaces can be very helpful for connectivity analyses, and will likely continue to have widespread application in landscape ecology and conservation science. Rather, the focus of this chapter has been to show that accurately understanding and predicting movement and connectivity requires methods which account for aspects of animal movement other than just landscape resistance alone. Yet conceptually and in practice, it appears a challenging task for ecological practitioners to integrate spatiotemporal variability and context dependence into workable and effective models. In light of this, we have intended here to stimulate and draw attention to what promises to be a rich field of research, and one which we believe will be crucial for the development of many

ecological disciplines. We thus end by revisiting the following question, which has been raised throughout this chapter: as an ecological community, how are we to approach and develop techniques and methodologies which allow models to better reflect the realities of movement and connectivity?

5.4.1 Hypothesis testing, validation and simulation experiments

The studies discussed in this chapter which evaluate and validate connectivity models have only just scratched the surface of an important set of hypotheses. Through decades of investigations and analyses, ecological science established the importance of scale as a fundamental aspect of ecosystem dynamics and animal movement (Levin 1992; Wiens 1989; Zeller, McGarigal, Beier, et al. 2014) – attending to the temporal, spatial, and other context-dependent drivers of movement and is now long overdue. The empirical studies discussed in earlier sections highlight their often substantial impacts on connectivity predictions, suggesting the inadequacy of current models which are often too simplistic to appropriately inform conservation in practice. However, as previously discussed in this thesis, empirical data alone are typically insufficient to assess the performance and accuracy of connectivity models in response to hypotheses and questions concerning drivers of movement.

We recall from earlier chapters that working instead with simulated data reverses this process, since we are able to compare connectivity predictions to the 'known truth' of the connectivity pathways generated by simulated movement data. The importance and utility of simulation techniques for addressing key ecological questions has been established in many branches of spatial ecology. Simulation tools thus provide a powerful and tractable framework with which to explore hypotheses concerning the influence of spatiotemporal variability and context dependence on connectivity predictions.

In particular, flexible spatially-explicit individual-based movement algorithms like Pathwalker which are used for connectivity modelling provide an excellent place from which to evaluate a wide range of theoretical and methodological questions in this area, as demonstrated in the previous chapter. Although such models still make use of resistance surfaces to provide spatial input data, they afford greater complexity to animal movement behaviour than models like Circuitscape and resistant kernels, and can straightforwardly be adapted to include additional parameters. For example, by simultaneously varying spatial input data

with mortality risk, spatial scaling and directionality bias, Pathwalker provides a highly capable framework for investigating the precise effects of simulated drivers of movement patterns beyond landscape resistance.

5.4.2 Interdisciplinary collaboration: models, methodologies, practice

Earth's landscapes are increasingly shaped by anthropogenic presence, to the extent that ecological models which do not adequately attend for these impacts are likely to be ineffective and inappropriate for use in applied ecology. Moreover, since landscape ecology and conservation science are inherently interdisciplinary (Farina 1998; Kareiva and Marvier 2012), this is an excellent opportunity in which to draw upon the conservation social sciences. In recent years, contributions from these overlapping fields have been recognised as vitally important for conservation theory, modelling and practice (Bunnefeld et al. 2017). While disciplinary boundaries are often useful for focusing study and investigation, they must not become rigid categories which prevent the collaborations and conversations that fundamentally stimulate development of ecological science (Campbell 2005; Johnson et al. 2016; Parathian et al. 2018; Pooley, Mendelsohn, et al. 2014). Attending more fully to the human dimensions of conservation practice is essential for such efforts to be successful (Adams, Aveling, et al. 2004; Bull et al. 2020; Ntuli et al. 2019). See Bennett et al. 2017 for a succinct and helpful overview of the utility and value in engaging with concepts and models from the conservation social sciences.

The context-dependent effects on animal movement discussed in this chapter, while demonstrated to often have a substantial influence on movement and connectivity predictions, may be difficult to address with business-as-usual quantitative techniques. In this regard, our intention is not to prematurely prescribe the exact methods for expanding the current field of connectivity modelling; instead, we aim to stimulate research and exploration into the many promising possibilities which arise from working to address the issues raised in this chapter. Recent analyses in interrelated fields, such as ethnobiology, conservation geography, and multispecies ethnography, bring more relevant and powerful complementary techniques to landscape ecology and conservation science than previously available, as discussed in Parathian et al. 2018. These disciplines offer valuable material which would enable scientists to identify new parameters and objectives for models to fit better with the realities of conservation

practice.

For example, the aforementioned study in which Barua 2014a tracks elephant movements using telemetry, ethnographic and historical data together produces much greater insight into elephant movement patterns than with any one data type alone. Similarly, Parathian et al. 2018 synthesise primatology science with multispecies ethnography to give crucial information on the spatial distribution and conservation of western chimpanzees. Hodgetts and Lorimer 2015, 2020 introduce the concept of animals' mobilities, and discuss methodologies and studies involving tracking and genetic technologies (e.g. Cantor et al. 2012), which may help to address the spatiotemporally varying effects of social dynamics on individual and collective movement. Holistic approaches to connectivity are necessary for considering the many factors required for effective and resilient conservation practice (Hodgetts 2018; Milner-Gulland et al. 2021). Paltsyn et al. 2019 integrate traditional ecological knowledge with remote sensing technologies to produce more robust and democratic maps of vegetation dynamics for governance and management. The seminal work of Berkes 2017 provides a comprehensive account of how scientific modelling and traditional ecological knowledge can greatly enrich and complement each other, addressing several key contemporary issues in environmental management (see also Kimmerer 2013; Salmón 2000). Scientists and modellers who are willing to engage with this interdisciplinary literature may find themselves at the forefront of revolutionary advances in theoretical and applied ecological research.

5.4.3 Conclusion

Connectivity modelling is a rich and rapidly growing subdiscipline which lies at the heart of theoretical and applied ecology. Two decades ago, 'landscape resistance' emerged as the dominant paradigm for mapping connectivity because it provided the best spatially-explicit framework available at the time. However, the reductionism and simplistic assumptions inherent to resistance surfaces do not account for many fundamental drivers of animal movement and connectivity, such as spatiotemporal variation, species interactions and other context-dependent effects. Through conceptual discussion and a range of recent empirical studies, we have highlighted how resistance-based connectivity models can thus be ineffective and unreliable for application to conservation practice. In light of this, we have drawn on emerging research across ecological disciplines to look at how to expand methodologies and techniques

in conservation science so that our models can better reflect the complexities of animal movement in this mysterious and beautiful world.

Chapter 6

Conclusion: Ecological mathematics

6.1 Crossing the threshold

> Will ecology be the last of the old sciences, or the first of the new?
>
> –Theodore Roszak, *Where the Wasteland Ends*

6.1.1 The path we have walked

This thesis has been centered around the fundamental inquiry of ecology, which is to understand the relationships between organisms and their environment. In a scientific context, this involves studying their patterns of movement, distributions across space and time, and interactions with other organisms and the landscape itself. Mathematical techniques abound in ecological science, and are typically held as the prized tool for distilling these complex relationships into knowledge that informs environmental theory and practice. Yet despite their established utility, these applications of mathematics and statistics are often reductionist to a degree which loses many vitally important dimensions of ecological dynamics, as discussed earlier in the context of animal movement.

Indeed, the major analytical material of the previous chapters has been concerned with developing and testing novel mathematical methods which attend more fully to the many contextual details which fundamentally shape ecological processes. We began in the realm of community ecology and species distribution models, looking into insights provided by advanced areas of mathematics like topology and geometry. In doing so, we introduced the concepts of the smoothing function and the environmental manifold for working with the nonlinear patterns emerging within and strongly influencing the relationship between environmental conditions and species abundance. The utility of these novel mathematical tech-

niques quickly became clear: the smoothing function performed very strongly in comparison with the widely-used generalised linear model and random forest machine learning algorithm as a method for recovering spatial distribution patterns from noisy and sparse occurrence data, and the environmental manifold produced (and holds great potential for) fundamental new understandings of species-environment relationships and the Hutchinsonian niche.

The following three chapters then shifted focus to animal movement and connectivity modelling, each working from a different angle to provide more depth and breadth in addressing salient questions from this increasingly influential field of ecology. The first of these chapters developed a new computational model for mapping animal movement, called Pathwalker, which synthesises the spatially-explicit foundation of resistance surfaces used in modern connectivity models with the behavioural detail in simulating individual animal movement allowed by agent-based methods. Pathwalker enables a powerful approach to mapping landscape connectivity and movement routes, overcoming established limitations of existing methods and providing a flexible and capable framework for investigating a wide range of hypotheses relevant to ecological science. This utility is demonstrated in the second of these three chapters, in which Pathwalker is used to generate connectivity maps from a large variety of simulated movement behaviours and spatial complexities, providing the data for a thorough comparative evaluation of Circuitscape, resistant kernels, and factorial least-cost paths, which are three major connectivity models currently in use in conservation science.

These two chapters then provided the ground for the penultimate chapter, which involved an interdisciplinary investigation into the limitations of the landscape resistance paradigm as a basis for modern connectivity modelling. We started with a technical analysis to shine a light on how resistance surfaces introduce a 'bottleneck' of reductionism into connectivity modelling, through which little of the information in empirical movement data is retained for subsequent predictions of landscape connectivity. Having established this, we integrated recent empirical studies in conservation science with adjacent work in environmental geography to elucidate the many levels at which resistance-based connectivity modelling fails to capture some of the key dimensions of animal movement. Opening the lens of inquiry to then touch the broader epistemological questions and philosophical assumptions which are at play behind the scenes, we are led to call into question the relevance and effectiveness of resistance-based connectivity models for application to environmental work in theory and practice. Drawing

on the richness of interdisciplinary research in this branch of ecology, we closed the chapter by moving beyond critique to suggest promising avenues of exploration for overcoming these constraints and developing modelling techniques which give greater attention to the lively realities of animal movement.

6.1.2 The landscape before us

Environmental concerns are emerging as a central focus across academic disciplines, guiding the imperative for thoughtful and interdisciplinary approaches to ecological questions. The mathematical models and techniques developed in this thesis join similarly motivated efforts emerging across all levels of environmental research, which attempt to speak more fully to the rich and multifaceted nature of ecological phenomena. However, while the applications of mathematics in ecology have grown more advanced and elaborate in recent years, the limitations *at the foundations of mathematics itself*, for its use as a lens through which to understand ecological relationships – the possible incongruence of principles at the root of mathematics with the living and breathing dynamics of ecological reality – still remain hidden, heretofore unexplored by environmental scientists.

With a motivation borne of a love for the wonders of both ecology and mathematics, and also from a sense which has grown through the previous chapters that we have been knocking on the door of some deeper questions concerning the interplay of these two subjects, I will conclude this thesis by presenting a potential path, off the beaten track, to take mathematics and science into deeper conversation with the environmental humanities and social sciences, and to help them touch the ecologies of this world in their fullness. Implicit hierarchies of disciplines result in mathematics always as the prefix: we have mathematical ecology, mathematical biology, mathematical physics, to name a few. Now, I hope to instead paint the possibility of an *ecological mathematics*.

6.2 Mathematical histories and the ethnosphere

Many of the structures and abstractions of mathematics in recent centuries have developed in close reciprocity with advances in physics. Hence, Newtonian mechanics, Riemannian geometry, matrix algebra and Lie groups all provide powerful and bespoke tools to capture

the experimental and theoretical findings of the physical sciences. Motivated thus by the ability of mathematics to elegantly crystallise phenomena at scales from the subatomic to the cosmic, 'an overwhelmingly large part of ecology tries to adhere to the tenets of conventional science. It tends to be quantitative, reductionist, and not at all sacred or spiritual' (Berkes 2017).

In contrast to its harmony with theoretical physics, the current usage of mathematics in ecological science stumbles over mismatches and tensions: the rigid adherence to established notions of objectivity, independence and mechanistic relationships fundamentally jars with the many subjective, relational, and embodied dimensions of ecological processes, which we discuss further below. One example from the previous chapter is the 'animal economicus' – the assumption animals respond to their environment according to a rational-choice, cost-benefit attitude. This neoclassical economic epistemology is a mode of quantification so firmly entrenched in ecological science that it has become an ontology for nonhuman behaviour, the impossibility of other relationships left implicit by the broader worldviews of conventional Western thought,[1] which remain unquestioned in this scientific context but nonetheless delineate the methodological boundaries deemed appropriate for ecological analysis.

Several of the social sciences – including geography, anthropology and sociology – have critically examined their disciplinary strait-jackets constraining the study of nature and the human place within it, and have recently begun to 'ecologise' in their methodological and conceptual scope (Greenhough 2014). This has involved the investigation and deconstruction of false dichotomies, such as those between nature and society (Cronon 1996), subject and object (Ingold 2002b), the interiority of human cognition and constitution from the enfolding terrain of the exterior world (Abram 1996; Alaimo 2010), and the withholding of agency and intelligence from the sensate world beyond our human bodies (Kimmerer 2013; Lorimer

[1]The term 'Western' appears often in this concluding chapter, sometimes interchanged with words like 'Enlightenment' for a similarly intended purpose. Unfortunately, this term is laden with no end of misnomers: for example, it is geographically incorrect, and is utterly homogenising of human difference, both in so-called Western societies and also with those for whom this term is used in contrast. Acknowledging this, and while still hoping to find a more suitable word someday, I use the term 'Western' here to refer broadly to the multifaceted matrix of cultural values and legacies which, at their core, include: seeing and speaking about human and nature as distinct, privileging rational logics over intuition and embodiment, and the evolutionary mindset of progress from traditional to modern.

2015). Reflecting threads from the vastness of ecological knowledge long practiced by a variety of human cultures, these contemporary turns in the environmental social sciences have created space within such disciplines for attending more fully to the dimensions of ecological phenomena which are excluded from the narrow lens of Enlightenment ideologies of nature, but which evidently constitute the animate and relational world in which we dwell.

Mathematics, however, is typically presented and taught as a system of timeless truths, divorced from the everchanging flux of human concerns and environmental conditions. Yet the branches of modern mathematics, although diverse in their theories and techniques, share a common formalisation of principles which have developed from mathematics' very much human history. These established practices have been guided and constructed inextricably from the cultural, political, economic and geographical contexts in which mathematicians from a handful of colonial nations have lived and been conditioned to think and see the world (d'Ambrosio 1985). As we discuss throughout this chapter, the resulting lens through which mathematics is applied to ecology remains firmly situated within Western Enlightenment worldviews of nature, which, implicitly and explicitly, carry an outdated set of philosophies for studying the natural world.

6.2.1 Ethnomathematics

> One of the major differences between the twenty-first century and the twentieth century will be the degree of intermingling of people of different cultures. Every day, more aspects of the lives of all of us are being affected by this. Just as in any other realm, participants in the world of mathematics cannot be adequately prepared for the future without an understanding of the past and of the present. Western mathematical ideas have changed through time; so, too, have our philosophies and histories of mathematics. Not the least of these changes has been the definition and redefinition of the boundaries of mathematics. It is important to once again revise our philosophy and history in recognition of the fact that mathematical ideas are cultural expressions and that our Western ideas are intimately linked with Western culture. And, moving beyond our own Western mathematics, a broader global ongoing history must acknowledge and include the ideas of other cultures.

–Marcia Ascher, concluding chapter of *Ethnomathematics: A Multicultural View of Mathematical Ideas*

The insights of anthropology, centered around the fundamental revelation that there is no singular or privileged human experience of cognition, behaviour or external world, have provided the ground for traditional scientific fields to complement conventional methodologies with the richness of knowledge outside the Western canon, giving rise to disciplines such as ethnobotany and ethnoastronomy. But mathematics has to a great degree eluded this expansion beyond the confines of its privileged position at the top of established hierarchies of knowledge, perhaps because of tightly held notions of intellectual purity, and a deeply ingrained belief in the universality of its expression in human thought (Ascher 2017). Not only did colonial worldviews obscure the possibility for modes of ecological relationship beyond their scientific-capitalist rationale,[2] but – believing in a linear evolution of humanity from 'savagery' to 'civilisation' – the mathematical ideas of cultures deemed 'primitive' were assumed to exist only as simple forms of numeracy, effectively writing out of history the mathematical sophistication of much of humanity (Ibid). This is particularly the case for those oral cultures whose depths of embodied mathematical knowledge were either unsettling or invisible to the colonial eye, such as the unrivalled geometric and astronomical expertise of the Polynesian wayfinders, whose mastery of the Pacific waters so confounded European sailors as to be deemed an impossibility for the capacities of human skill (Davis 2009).

Even mathematics, though, cannot be presumed to float immaterially above the histories and social contexts of its mathematicians. The recent emergence of *ethnomathematics* has investigated the diverse practices of mathematical ideas found, for example, in the symmetric rafter patterns of the Maori in Aotearoa (New Zealand), the spatiotemporal orderings of the Diné in the southwestern United States, the dihedral group structure in the kinship relations of the Warlpiri in Australia, and the topological abstractions in the artwork of the Malekula in Vanuatu (Ascher 2017). Marcia Ascher's excellent book, *Ethnomathematics: A Multicultural View of Mathematical Ideas*, and other works in this realm serve to illustrate that, while mathematical ideas do manifest in every human society, there is no singular or inherent expression of mathematics, nor a universal linear path along which mathematical ideas develop or can be compared.

[2]For example, see Ghosh 2021, or the words of Christopher Columbus in Patel et al. 2017.

Moreover, the routes along which such ideas evolve are inextricable from the emphases and priorities of the culture in which they are nurtured: the material encoding of histories, songs and edicts in the knot-theoretic *quipus* of the Incas in South America reflect their value of bureaucracy and orderly processing of multiple data types, and the importance of certain aesthetics in the political power of the Bushoong in southern Africa motivated their developments of graph theory, just as biopolitics and the desire to govern and classify human populations led directly to the prevalence of statistics, and concerns with efficient material distribution during the second World War guided the rise of optimisation and linear programming. Even the notion that counting with an arithmetic base of ten is 'natural', because of having ten fingers and toes, falters over the example of the Yuki of California, who count with a base of eight for precisely the same reason, the only difference being counting the spaces *between fingers*, rather than the fingers themselves (Ibid).

Making sense of the true diversity of mathematical practices shared by humanity necessarily raises the question of what mathematics actually *is*, the pertinence of which for this discussion is the acknowledgement that, just as certain mathematical developments in Western formalisations need not have analogues in the mathematics of another culture, so too will we be blind to the fullness of mathematical expression in another culture if we limit ourselves to selecting only those instances with which we can draw direct correspondence to our own particular systems of mathematics. Indeed, any metric placing the culturally differentiated constellation of mathematical ideas on a scale from 'simple' to 'complex' would carry an inherent bias, since the elaboration and developments of Western mathematical theories are themselves driven by a cultural value placed on abstraction and generalisation. Hence, by defining and attending to *mathematical ideas* rather than *mathematics*, Ascher's work on ethnomathematics circumnavigates philosophies of mathematics, which, steeped in their own sociopolitical nuances and intellectual exclusivity, are given substantial treatment elsewhere. This approach opens us to a multiplicity of mathematical expressions touching all facets of human life, such as those we would typically categorise as agricultural practice, artwork, genealogy, navigation – and most of all, language.

These revelatory works of ethnomathematics have, with good reason, been primarily concerned with restructuring mathematical pedagogy, seeking to decolonise and move beyond the cultural barriers which inhibit engagement with mathematics for peoples whose values and

understandings of the world do not fit well with the ideological underpinnings of traditionally taught Western mathematics. However, the potential of these ethnographic accounts – of mathematical ideas in cultures who live and breathe different worldviews and relationships with nature – for reframing mathematical practice in ecology remains unexplored. By opening to subjective and embodied understandings of ecology, still held as the primary source of environmental knowledge by a great variety of peoples in this shared world, could we arrive at an interplay between mathematics and ecology which moves beyond the subdivision of interconnected phenomena into component parts, and the quantification of life processes into mechanistic systems without agency or intelligence?

6.2.2 Abstraction and direct experience

Earlier in this thesis, we saw that the 'animal economicus' mode of measurement has become synonymous with the practice of quantification itself in ecological science, yet is manifestly an expression of particular economic-political thought. Similarly, Descartes' philosophical abstractions, which have foundationally guided the evolution of Western mathematics and science, may carry a residue of his doctrine that European civilization must become 'the masters and possessors of nature' (Patel et al. 2017). Indeed, we may suspect that the implicit but pervasive assumption in ecological science of a mechanistic relationship between animal and landscape bears some resemblance to the Cartesian thesis that humans alone (but, crucially, excluding women, nonwhite peoples, Indigenous Peoples, among others) are privileged with higher faculties of thought, whereas those not in the human category are simply automata who function in relation to their environment as machines without perception or agency. Furthermore, we may wonder which dimensions of ecological understanding hide themselves from a scientific lens founded in the worldviews of Francis Bacon, who proclaimed that 'science should as it were torture nature's secrets out of her', and that the 'empire of man' should penetrate and dominate the 'womb of nature' (Ibid).

The capacity and inclination for abstraction – the literal root of which is to 'pull away' – both lends Western mathematics its ability to universally approximate physical phenomena, and also detaches its methodologies from being able to attend to the uniqueness of any one ecological system. But a route through this impasse, to finding a practice of mathematics which speaks more fully to the liveliness of corporeal reality, need not take issue wholly with

the process of abstraction itself, ostensibly a necessary element of navigating and making this vibrant world (McCormack 2012). For abstraction is, of course, not unique to Western thought, and is also found in cultures whose worldviews do not presume humans to be outside the material flows and relations of nature. Describing an instance of abstraction in the story *Raven Travelling*, told by Skaai of the Qquuna Qiighawaai, Edward Doolittle of the Indigenous Mathematicians relates:[3]

> Now when the Raven had flown a while longer, the sky in one direction brightened. It enabled him to see, they say. And then he flew right up against it. He pushed his mind through and pulled his body after.[4]

However, logics of abstraction do indeed hold a prized position in conventional scientific approaches to ecology, where they are favoured and accepted over 'base' modes of knowledge more directly involving perceptual and embodied experience, which are often seen as derivative or secondary to the 'universal truths' of mathematical generalisations. Viewing ecological processes only through the lens championed by Western science, however, would be to don red-tinted glasses and conclude that the world is red. In this light – rather than mathematical abstraction as simply an approximation to, but never touching the entirety of, the multiplicity of living expression – the boundless variety of material forms are conversely seen as the physical manifestations of generalisable underlying laws encoded by mathematics (Ingold 2006), with their 'irregularities' explained away as 'random variation', ostensibly more a reflection of unacknowledged epistemological limitations than a sincere comment on ecological difference. As David Abram writes in *The Spell of the Sensuous*, this detachment from our direct perceptual connection with the more-than-human earth, withdrawing into reliance on established scientific-political theories and narratives as our primary means of knowing the world, serves to isolate us from the dimensions of living reality which are not so easily captured by the usual techniques of scientific analysis. Just as we cannot know the crisp taste of an apple until biting into its flesh, or the magic of the full moon rising until bearing it witness with our own eyes, so too are countless facets of the animate landscape hidden to us until we bring our direct experience of sensory perception to the foreground of our attention.

[3] https://indigenousmathematicians.org

[4] I expect that anyone who has studied abstract algebra will be able to relate to this feeling.

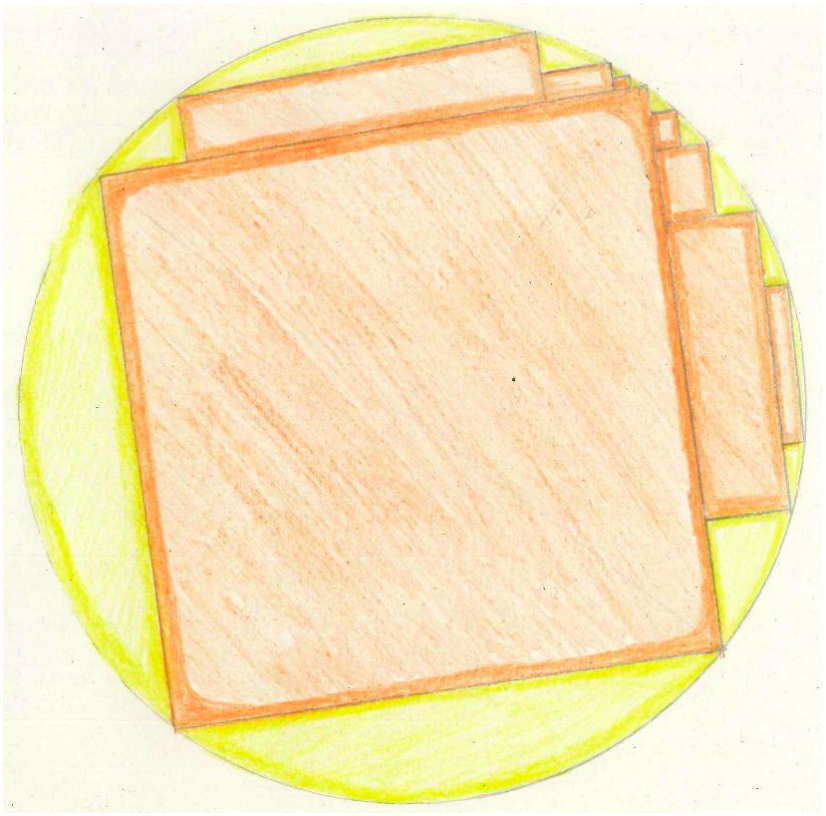


Figure 6.1: Sometimes the current applications of mathematics in ecology feel like this drawing of squares in a circle. Mathematical methods have indeed grown more sophisticated in trying to describe ecological phenomena. But just as the linearity of the squares can only approximate yet never realise the encompassing circularity, so too do the prescribed separations by mathematical models of ecosystems into component parts never touch the wholeness and interdependence of ecological reality. All models necessitate degrees of reductionism and abstraction, but I do wonder if this can be done in such a way which, rather than starting by breaking ecologies into fragments, is instead grounded at the outset in an understanding of wholeness. Drawing by Siddharth Unnithan Kumar, 1st December 2022.

6.3 Ecologising mathematics

> *Take yourself outside and rest your eyes upon something with visual detail at medium distance from you – a tree or leaf is a good choice, particularly if there is a slight breeze. Place some part of that object in the centre of your visual field, and keep your gaze rested there. Let your attention be soft, being open to and receiving the experience rather than examining with focused intensity. Without putting words on what you find, see if you can notice the details of its form, the way the light falls, the qualities of colour and texture. There may be a stream of thoughts that will try to pull you away: 'why am I doing this', 'what will someone else think if they see me', 'what will this lead to' – and then more subtle: 'am I doing this right', 'perhaps I didn't choose the right spot'. When you notice them, just return to the gentle giving of attention to the place you have been observing. Just as it can take a few moments resting your gaze upon the grass to suddenly see the community of ants and other insects roaming the ground, notice if, perhaps after a minute, you begin to see forms appearing that present themselves to you only after you have given your loving attention for a period of time – an emergent figure or pattern, perhaps with fluidity and character, that is hidden to a cursory glance but arises with unshakable solidity and depth in response to your sustained receptivity.*[5]

Thus far, we have touched upon some of the cultural underpinnings which have traditionally guided Western scientific engagement with the more-than-human world, and made mention of the mathematical practices found in non-Western peoples with different worldviews of nature. In the brief journey of this concluding chapter, to develop a sense of the possibilities for reorienting the interplay of mathematics and ecology that may arise from stepping outside the cultural legacy of Enlightenment approaches to nature, we turn our attention to the relationship with space and time experienced by certain oral societies, particularly those such as the Diné (Navajo) in the western United States, where I have been

[5]This exercise for seeing spirits is inspired by my beloved friend and teacher, Hugo Shakeshaft. Spirits, not as immaterial beings of fantastical realms, anthropomorphised onto forms external to our human bodies. But rather, as David Abram writes in *The Spell of the Sensuous*, the animate aliveness of material existence itself – if only we have the eyes to see it.

fortunate to spend some space/time during the last two summers.

A thorough and respectful investigation, of substance, into different understandings of ecological relationship and the human place in nature which could help to reframe practices of mathematics in ecology, would be the premise of a new thesis, rather than the concluding lines of this one. Indeed, I cannot here present to you a definitive example of what ecological mathematics would look like, not because it is 'beyond the scope of this study', but simply because I have not yet come to a clear understanding of it myself. Many of the interlocking twines of knowledge mentioned in this conclusion deserve entire chapters for their own exploration and clarification, such as distinguishing between 'mathematics' and 'mathematical ideas' (which is given substantial attention in Ascher's book on ethnomathematics).

Nonetheless, drawing on the writings of David Abram and Marcia Ascher, I will try to convey some of the value and inspiration I have felt from accounts of the experiences of peoples who perceive the richness and vibrance of this dynamic world differently to the dominant cultural matrix in which I have been embedded, the engagement with which I believe holds the key for developing ways of doing mathematics which can speak more fully to ecological reality in all its wonder. Thus, I hope you will be able to take the indistinctions and unclarified threads of this chapter in your stride, and enjoy the broader journey upon which we are embarking together. I will attempt to share with you my lens, which I am still gradually adjusting into focus, on what ecological mathematics could be, and perhaps your eyes and animal senses will catch on to something too.

6.3.1 Spacetime in the oral universe

Although the paradigm shift precipitated by Einstein's theory of relativity brought to modern physics the understanding that space and time are not only inextricable, but also nonlinear in their unfolding – with the gravity of material presence exerting distortions on the lines traveled by light itself – the cultural legacy of absolute space as a homogeneous three-dimensional void and absolute time as a straight line continue to shape much of our 'commonsense' approach to the world.[6] In doing so, the present moment is to be found only in an infinitesimal moment in time, a single point speeding on a line and forever at the cusp of being relegated

[6]The ideas in this paragraph, and the following two, are largely drawn from *The Spell of the Sensuous*, Chapter 6: *Time, Space, and the Eclipse of the Earth.*

to the fixtures of the historical past. Yet, how is it so that this relentless model of temporal reality, reinforced by the ticking of clocks and schedules in our minds, speaks nothing to the unshakable solidity and stillness of the present moment when we take a few deep breaths and feel our bodies corporeally rooted amongst the surrounding material forms which suddenly reveal themselves to be unconcerned by all this hurry filling us moments ago?

This spatiotemporal partitioning stands in contrast to the indistinction between space and time made by many oral cultures. Without the medium of alphabetic writing to delineate a historical time lacking reference to a particular place, the temporality and collective memory of an oral society is necessarily grounded in the textured forms and sounds of their enfolding landscape – indeed, among others, the Diné and Hopi of the southwestern United States and Pintupi of the Western Desert in Australia do not have separate words for space and time in their languages. Moreover, the human experience of time in these contexts is often cyclical at many scales, whereby events are understood as happening within the arc of unfolding processes which, rather than collecting dust amongst the annals of history, continually emerge to bring the physical present into being. Lame Deer of the Miniconjou Lakota explains that 'the Lakota define the year as a circle around the border of the world', and Heȟáka Sápa (Black Elk) of the Oglala Lakota describes how 'everything the Power of the World does is in a circle' (Lame Deer et al. 1994; Neihardt 1996).

From this perspective of the world, the colonial notions of evolutionary societal progress from 'savagery to civilisation' are quite peculiar, believing origin stories to have no place in modernity and thus severing their power to give resonance, meaning and guidance to the experiences which we meet in daily life. Instead, with language and cognition grounded in the corporeal dynamism of the landscape itself, the temporal dimension of existence is inseparable from the materiality of space. Thus, the present moment, rather than some impossibly momentary phenomenon whose incessant course along a linear timeline forever eludes our human sensibilities, now takes on the tangible solidity and rooted tranquility in the totality of the forms and textures constituting our surrounding environment. As David Abram writes:

> The 'present' itself expands to become an enveloping field of *presence*. And this presence, vibrant and alive, spontaneously assumes the precise shape and contour of the enveloping sensory landscape, as though this were its native shape! It is

> this remarkable fit between temporal concept (the 'present') and spatial percept (the enveloping presence of the land) that ... prompts me to wonder whether 'time' and 'space' are really as distinct as I was taught to believe. There is no aspect of this realm that is strictly temporal – for it is composed of spatial things that have density and weight, and is spatially extended around me on all sides, from the near trees to the distant clouds. And yet there is no aspect, either, that is strictly spatial or static – for every perceivable being, from the stones to the breeze to my car in the distance, seems to vibrate with life and sensation. In this open present, I am unable to isolate space from time, or vice versa. I am immersed in the world.

Seeing mathematics as part of the way we orient to the flow of daily life – and, hence, freeing this term from the cloistered confines of 'professional mathematics' – it becomes apparent that our relationship with cultural notions of space and time (in planning our day, or planning our route) fundamentally constitute how we navigate the world each day. For example, demonstrating the Diné experience of spatial phenomena as both embedded with circularity and also inherently dynamic, in a twenty-minute documentary of weaving practices described in Ascher's *Ethnomathematics*,

> fully fifteen minutes ... showed the weaver walking – walking to collect materials; walking to shear the wool; walking to the loom; and, always, beginning and ending the walking by leaving and returning to her hogan. The process of weaving, then, is the interrelation of many processes that emanate from a center, spread out from the center, and return back along the same path.

Drawing on Abram's thesis that language in oral societies arises from the unique physicalities and rhythms of their surrounding ecologies, together with Ascher's explanation that language provides the primary lens through which mathematical ideas in different cultures can be understood, we arrive at the understanding that the mathematical expressions which emerge in different regions are not distinct from the ecologies of those places. Thus, if homogeneous space and rectilinear time are not absolute facets of reality, but simply one perspective of engaging with the world, reinforced by terraforming our external environment to reflect our internal orderings of reality; if they are an *experience* which is not universal

but instead differentiated to the extent of being scarcely comprehensible to human cultures which do not separate these dimensions of existence; then why should we expect nonhuman life to subscribe to this one particular model of the animate earth? And so, we may ask, along which practices of spatial navigation and temporal dynamism do the diverse lives of our nonhuman neighbours unfold, guided by sensibilities thoroughly different to our own?

6.3.2 Embodying topology

Questions of this kind have been asked before in the humanities and social sciences (Philo et al. 2004), but modelling different spatiotemporal modes of experience in ecological science appears challenging. Indeed, Ascher notes that 'notions of space and time are so crucial to the framework we use to perceive, structure, and interpret experience that it is extraordinarily difficult to even conceive of others.' Fortunately, however – albeit motivated not so much by an awareness of differing cultural perspectives of existence, but nonetheless driven, particularly from experimental findings in physics, by an acknowledgement of the limitations carried by these entrenched notions of space and time – many theoretical developments of Western mathematics itself have in the last century sought to attend more deeply to other possible approaches to spatiotemporal relationships.

Of the formal mathematical disciplines, it is *topology* which provides the concepts and methods for working with the underlying patterns within and between the nonlinearities of spatial and temporal structures, revealing qualitative descriptions of relationships not otherwise discernible to the Euclidean eye. Moreover, topology enters into perspectives of space which, although dressed in the attire of formal mathematical logic and abstraction, do actually step out of the viewpoint of the detached observer, and *into the situated relationship with space arising from the direct experience of being immersed within the spatial structure being studied.* The omniscient Euclidean lens, for example, would see two parallel lines which skim the surface of a sphere floating in featureless space as traveling to infinity without ever meeting. In contrast, there are core techniques in topology and non-Euclidean geometry from which one can mathematically deduce that two lines which begin as parallel, but which travel *along the surface of the sphere*, will cross, like meridians at the North Pole; moreover, these lines may continue indefinitely on their path upon the sphere without wavering from their original direction, yet in doing so will be tracing circle after circle after circle. Thus, even in

this simple setting, that which the placeless observer and situated earthling both experience in their own cosmology as a straight line is seen to the detached perspective as the contrast between line and circle.

In topology, more so than any other area of mathematics, the exclusivity of symbolic formulae often gives way to the primacy of visual expression as a mode of understanding and communicating, whether it be gesticulated or drawn on the page, but in a manner which is integrated with all the established formalities of Western mathematics.[7] Hence, whilst still wrapped up in layers of conceptual abstraction away from the fullness of situated experience in embodied reality, topology does open both a conceptual *and* a methodological doorway for Western mathematics to mix with other modes of knowledge in the earthy basin of ecology. Here, for example, mathematical topology meets its doppelgänger in the environmental social sciences, clothed instead in relational approaches to socioecological systems, and reframings of the spatialities of power structures and urban mobility (Martin et al. 2014; Prager et al. 2009).[8] Importantly, this is not merely a coincidental matter of common terminology - it is a shared cognizance, emerging across academic disciplines, of how different spatiotemporal models of reality reveal patterns and relationships otherwise hidden to the Euclidean eye, echoing in conceptual and analytical language the experiential insights afforded by attending to relationships with the animate earth lived by peoples such as the Diné and Pintupi.

6.3.3 To be continued

Now, sadly, and perhaps abruptly, I must bring this case study to a close, since I have not yet alchemised the above material into a new substance to give you which I could call 'ecological mathematics'. But by collecting these threads together – the lens of placeless space

[7] Diné artist Bajé Whitethorne, Sr. distils generations of embodied relationship with the high desert landscapes in the nondualitistic constitution of his vibrant paintings; Wassily Kandinsky captures the essence of vitality of a moving fish in his dynamic stroke of a line on canvas (Ingold 2010). Just so, a topologist seeks to convey the essential qualitative information of a shape or process beyond the capacity for human visualisation with a suggestive interplay of a variety of lines, loops, colours, and shading techniques (Francis 1987; Milnor 2015).

[8] Many of these characterisations of networks and assemblages do only represent a sliver of the scope of topology in its fullness as developed in mathematics – and even those efforts (such as the 'Deleuzian manifold') to stretch conceptual limbs into the richness of its spatiotemporal theories are still laden with the baggage of certain modes of abstraction which do not cross the threshold into embodied reality.

and linear time as simply one perspective of reality which not all humans share, let alone nonhumans; the return of temporality back into the material forms of a landscape, leading to different ways of navigating the world; and topology as an established mathematical system for attending to temporal unorthodoxy and spatial nonlinearity which carries promise of lively rapport with the environmental social sciences and humanities – I hope that I have shared with you the sense of a genuinely new interplay of mathematics and ecology I am sure to be possible; one which speaks more fully to rich diversity of human and nonhuman engagement with the world, and which can be of service in contemporary environmental work by bringing disciplines together across their long-presumed impasses to provide the holistic synthesis of knowledge needed for healing the ecologies of our inner and outer worlds.

6.4 Love, truth, and the mystery

> It is a question, practically of relationship. We must get back into relation, vivid and nourishing relation to the cosmos and the universe. For the truth is, we are perishing for lack of fulfillment of our greater needs, we are cut off from the great sources of our inward nourishment and renewal, sources which flow eternally in the universe. Vitally the human race is dying. It is like a great uprooted tree, with its roots in the air. We must plant ourselves again in the universe.
> –D. H. Lawrence

I believe that at the heart of the environmental challenges of the present day is the question of relationship - of how we relate to ourselves, to fellow humans, and to the more-than-human world which we all call home. Fundamentally, will we relate to our experience of the world out of fear, or out of love? Perhaps this is why I am sure that mathematical and scientific methodologies grounded in logics of control and domination, leaving respect and emotion as an afterthought, cannot ultimately take us to the depths of ecological healing needed in this time. I have also grown increasingly aware of the extraordinary wisdom of the body – a perfectly respectable (and often primary) site of knowledge in most cultures, although seen as base and derivative in Enlightenment epistemological hierarchies. Embodied experience not only knows and reveals aspects of reality far beyond the reach of our cognitive processes, but also provides the very ground for the 'higher thought' of logic and reason which is held so

dear in Western science and its cultural legacy (Abram 1996; Merleau-Ponty 1965). Myriad ecological relationships hidden to the traditional scientific lens sparkle brightly when met at the doorway of sensory perception, and the rich variety of embodied mathematical practices found throughout the world invite us to rethink the conceptual exclusion of the body in our approach to mathematics.

This is not to deny the tremendous value of conventional mathematical models for guiding effective environmental work. Nor do I mean to romanticise, or extract without reciprocity, the possible value that mathematical practices from other cultural contexts could have for illuminating the somewhat myopic lens of mainstream ecological science. Indeed, I think there is also extraordinary potential in simply bringing existing mathematical models into greater conversation with the methods and insights of other environmental disciplines and structures of governance, particularly in combination with efforts to decolonise and democratise these knowledge systems and practices, as many people are already doing so powerfully. As such, this investigation into ecologising mathematics is not guided by the desire to find an expression of mathematics which can stand alone to illuminate the totality of the ecological relationships which shape the forms and patterns of this living planet, for I think such insights can come only from our personal intimacy with the world – someone can point us towards the moon, but it is with our own eyes that we must see it.

Instead, this exploration takes as its premise the knowledge that mathematical ideas are inextricable from their situated cultural contexts, and that the practices of mathematics and their guiding philosophies have changed through time in relation to the human and more-than-human environments in which they have evolved. The work of ethnomathematics has shown us that mathematical ideas need not be grounded in the worldviews with which this dominant culture is so familiar, and that differing relationships with nature give rise to diverse expressions of mathematics, each of which intersects uniquely with other facets of human existence. The possible forms which an ecological mathematics could take – how embodiment and direct experience are accounted for, which mathematical formalisations are kept or modified, the place of axioms and abstractions, and how to synthesise a greater variety of knowledge practices – that is for us to discover. I do not mean to advocate pursuing this route of inquiry to the replacement of current mathematical models in environmental work, many of which are so deeply needed at this time in research, policy, communication, and many

other intertwining spheres of life. Rather, supported by growing motivation and material found across and far beyond academic disciplines, I do believe that exploring this potential of mathematics in ecology with an open heart and mind, and overcoming the confining and outdated worldviews in which mainstream ecological science has long been situated, could help find a fruitful route through the increasingly ossified impasses built from those very same ideologies of nature and the human place within it.

6.5 Epilogue: Ecology and the Dhamma

> Enlightenment is intimacy with all things.
>
> –Dogen

Becoming conscious of the narratives and stories that fundamentally guide our engagement with the world, and realising the choice of love and grace over greed and fear in relationship with ourselves and others, is a process which inevitably requires attention to both inner and outer realms of experience (Unnithan Kumar 2022; Zambucka 1978). The teachings of the Buddha (the *dhamma*) provide a systematic way to widen the sphere of our awareness and shine a light on habitual patterns of thought which keep our world small and rigid. They also present methods to cultivate the intrinsic qualities of undiscriminating love and compassion, which are our deepest essence and without which no true healing work could happen (Brach 2004; Gyatso 2012). These teachings, as the Dalai Lama says, are a science of mind, but one which can examine our conditioned ways of seeing the world without falling into the confining separations of mind and body, and which takes our embodied experience of the world as the essential ground of knowledge and insight (Kornfield 2008).[9]

Central to the dhamma is an experiential awareness of the ways in which our minds and bodies are thoroughly interwoven with the world beyond our bounded selves, and of how all

[9]It is important to note here that, while the terms 'mind' and 'body' are used throughout the Buddha's teachings, they do not correspond to the usual Cartesian distinction between, respectively, immaterial cognition located in the brain and corporeal matter without sentience (Hanh 2016). Instead, they more closely resonate with understandings of mind and body found in many oral cultures, and also within the phenomenological school of Western philosophy, whereby body and mind share an inextricable symbiosis in which the former both provides the ground for and is also an extension of the latter (Abram 2010). Simply put, rather than being confined to the human skull, the mind is seen as thoroughly continuous with the body and the world beyond.

conditioned phenomena are everchanging – an imminent universe continually brought into being by all the aliveness of the present moment. Here, there is no prescribed or written truth of reality to be imbibed; rather, the method for investigating the relevance of these teachings in the corporeal richness of our own lives is the practice of *bhāvanā*, usually called meditation but perhaps better translated as 'cultivation' or 'bringing into being'. In a manner which closes the gap between the subject and object of perception, the *Satipatthāna sutta* (the discourse on the four foundations of mindfulness) cultivates this embodied awareness by guiding attention first to the sensory experience of the body, which creates the space for then attuning to the flow of feeling and emotion through our bodies, and in turn this provides a stable vessel for seeing the contents, patterns and states of our mind. The gentle understanding which emerges from this engagement with body, feeling, and mind, then develops a lens through which to see, with clarity and loving curiosity, the fourth foundation of mindfulness – namely, the processes and relationships which shape our living world (Hanh 2008).

This sense of the world and its ecosystems, which comes alive through directly experiencing these teachings on impermanence and interdependence manifest in ecological phenomena, are echoed not only in the emerging shifts within the environmental social sciences and humanities mentioned earlier in this chapter, but also by many ethnographies of and works by Indigenous Peoples. For example, see Tim Ingold's detailed description of ecological relationship in the Ojibwa universe (Ingold 2002a); and the works of Umeek (E. Richard Atleo) on *Tsawalk*, in which he develops an indigenous ontology for guiding contemporary environmental work, grounded not in the Western 'historical notions of civilisation and scientific progress', but in the interdependence of existence presented by Nuu-chah-nulth origin stories (Atleo 2007, 2012).[10]

These perspectives on ecology are, of course, not specifically 'Buddhist'. Rather, their appearance in these different worldviews and recent turns in academic disciplines points towards an approach to the world, which, aided by a set of teachings untethered to any one livelihood or label, is simply an understanding that can arise within us when attending to our embodied experience of existence, as if returning to something we already know to be true but which we have perhaps forgotten. Many such attitudes, whether expressed in

[10]See also Joan Halifax's essay *The Third Body: Buddhism, Shamanism, and Deep Ecology*, one of the few essays I have found and appreciated which explicitly looks at ecology and the Buddha's teachings together.

the words of Christian mystic Thomas Merton, phenomenologist-magician David Abram, or Lakota medicine man Lame Deer, serve to reinstate the presence of the sacred and divine (in whichever way those words make sense to us) back into the landscapes and beings with whom we shared this uniquely brilliant world. I am realising this spiritual dimension as vital for ecology, and the Buddha's teachings on the middle way – grounded in love and wisdom, nonviolence and nonjudgement, and an acknowledgement of both the countless joys and sorrows of being human in this world – give me a refuge and companion in ecological and healing work for which I am eternally grateful.

Wildfires choke and burn the bodies of deer and bears, pigs and chickens live and die in the violence of industrial farms, my kin from low-lying island nations are losing all they hold dear to the rising seas, and my brothers and sisters everywhere are dying with empty bellies in the burning sun, while I have the privilege to sit here and write these words in the Old Bodleian Library in Oxford. As the shadows of suffering born from world-devouring logics lengthen, it is the task for each of us to become more conscious, to find out who we really are and what gifts are ours to uniquely and collectively bring into the world, and to do so with love. When love meets the pain of the world, it becomes compassion, like the sun at sunset – closer to darkness, but more beautiful because of it. I dedicate this work and its merits for the benefit of all beings. May all beings be well and happy, and may all beings be free from suffering.



Figure 6.2: 'And above all these, put on love, which binds everything together in perfect harmony.' Words at the base of the yew tree by the church at the end of Binsey Lane, near Port Meadow, Oxford. Photograph by Siddharth Unnithan Kumar, 1st December 2022.

Acknowledgements



Figure 6.3: (Left) Allegra with a nonalcoholic ginger beer at the Medley in Port Meadow, 29th June 2022. (Right) Hugo on a dhamma walk down Binsey Lane, 25th May 2022. Photographs by Siddharth Unnithan Kumar.

I heard it said that Ananda, the Buddha's most beloved disciple, at one time went to the Buddha and shared his reflection that friendship constitutes half of a fulfilling life, to which the Buddha replied instead that friendship makes up the entirety of a fulfilling life. Just so, the journey of this work has come from nothing but friendship – with my family, friends and teachers, with my inner world and ancestors, and with the dancing forms and wonders of this more-than-human earth. Mitakuye Oyasin.

To my elders and teachers

Blood ancestors aside, there are four people who have particularly graced this journey with their loving presence and cosmic wisdom. I feel honoured to call you my elders and to you first I bow in gratitude. I do not know whom or where I would be without you.

To my beloved acupuncturist Allegra Wint, who produced the artwork for the final page

of this thesis; for feeding and transforming the demons and making the darkness conscious, returning me to my heart and my connection with the universe and my ancestors, helping me discover who I really am and what I am here in this precious lifetime to bring into the world, and being my friend. To my meditation teacher Hugo Shakeshaft, who produced the artwork for the title page of this thesis, so beautifully weaving together the earthly magic of the tent glade with my favourite Buddhist imagery; for so much laughter and friendship, for teaching me the practice that has become a refuge of unshakable strength and the steady path to boundless truth and goodness, and for being a true companion on the journey of existence.

To my doctoral supervisor Sam Cushman, whose love and extraordinary wisdom brought this thesis into being, gave it skilful direction and substance, and kept it steadfast and alive through my times of darkness. Thank you, for being my mentor for the wild and bringing me to intimacy with the astounding powers of this more-than-human earth, for road trips and poetry and our cosmic rapport, and for having faith in me and being a great friend. To earth wizard and kindred spirit David Abram, for the unrivalled gift of transmission of a connection with the world I had long forgotten but knew in my heart to be true all along, and for the magic and aliveness and wild resonance and conversations about ecological mathematics which we shared during my few days with you in the foothills of the Rocky Mountains.

I now turn in gratitude to those other elders and teachers whose guidance and encouragement forms part of the vital substance of this thesis and will remain with me in the adventures to come. To Tarquin Grossman, my mathematics teacher at the end of high school; for reinstating the place of wonder, astonishment and potent curiosity back into my engagement with mathematics, and for seeing my value and believing in me. To Dennis and Rainie Evans, whom I met in the summer amongst the sun-soaked beauty of the Canadian Pacific; for conversations about love, spirituality and ecology, and the singularly invaluable gift of a soul connection so magical it confounds explanation. To Wade Davis, whom I met in those same landscapes that summer; for the stories I listened to which filled me with inspiration and possibility, embodying the nonlinear and extraordinary magnificence of the potential of human existence, and those simple yet timeless instructions on living a true and fulfilling life. And to Tim Ingold, for showing me how to write one's truth with sublime

precision and unwavering heart in the established realms of academic scholarship.

To those remarkable figures with whom I have not yet had the privilege of a bodily encounter but who nonetheless have graced and shaped my life with their writings and teachings. Tara Brach and *Radical Acceptance*, Jack Kornfield and *The Wise Heart*, Adyashanti and *The Most Important Thing*, Thich Nhat Hanh and *Old Path White Clouds* (among many other works), the Dalai Lama and *Beyond Religion*, and all those who have brought the Buddha's teachings into the infinite richness of the present world, whose prose now pulsate in my bloodstream and orient the compass of my heart to daily give me direction and courage. The poet Jalaluddin Rumi and those masters of language, whether literary or not, who have so beautifully woven the eternal truths of human experience into the precious gift of words whose reassurance and power resonate through the depths of eternity. Michelle Paver and Brian Jacques, authors of my childhood favourite books, the *Wolf Brother* and *Redwall* series; for your lyrical prose and magical worlds which helped ignite and keep alive the flame of adventure and love for the animate earth and its more-than-human beings that brought so much beauty to my life, and gave me intimacy with those ecological sensibilities to which I returned and rediscovered when the universe led me to David Abram and his writing.

And to Siddhartha Gautama the Buddha, for developing the ten perfections and having the resolve to sit down right in the middle of this human existence in search of truth and freedom, and bringing the dhamma into this world which we all call home.

To my seniors in Oxford University

Beyond my elders with whom I connect on the level of soul and spirit, there have been many university staff whose guidance and insight has been invaluable and necessary for this research to begin, to metamorphose in consonance with the evolution of my interests, and to finally come to fruition in this thesis.

First, to the faculty of the Mathematical Institute, most of all Philip Maini, my doctoral supervisor whose consistently gentle and supportive presence has made effortless the handling of many hurdles in doctoral study; to Sandy Patel, whose clear compassion and skilful action were a bastion of help at critical moments in this journey; to André Henriques, whose concurrent familiarity with the most abstract realms of mathematics and also matters of nature and the heart provided inspiration during the early stages of this thesis; to Michael

Monoyios, my mathematical mentor from undergraduate who saw promise in me and spoke words of encouragement which I greatly valued; and to Maria Nemțanu, whose delicious Romanian food nourished me during my year in the tent, and whose efforts alongside all the maintenance staff at the Mathematical Institute create an environment which allow members of department to carry out their work.

To the faculty of the Wildlife Conservation Research Unit: David Macdonald, whose remarkable insight and experience proved instrumental during important moments of transition, and whose every utterance makes me laugh; Żaneta Kaszta, whose friendship and refreshing honesty I have cherished from the very beginning of this research; and to Paul Johnson and Andy Hearn, whose warmth and encouragement have helped me to flourish.

And to those many other university faculty whose conversations and presences have woven themselves into this thesis. Most memorably: Andrew Teal, whose gentle words carried blazing compassion which helped me see my luminosity during times of darkness in my second year of study; Sarah Shaw, for her sage presence and guiding words on meditation and the dhamma; Matt Ives, for good vibes and stimulating conversations; Tim Hodgetts, a beacon of encouragement, wisdom and friendship on my journey into the realms of geography; and to Jamie Lorimer and Yadvinder Malhi, whose geography lectures helped opened my world and put me more deeply in touch with the work I love.

To my friends

My whole being reverberates with the fullness of love as I turn to thank my friends, old and new – who knows after how many lifetimes we are meeting again. To Gonzalo Gonzalez de Diego and Imi Dobie, companions and allies from beginning to end in the metamorphic journey of doctoral research. To Austin Barber, a gorgeous man and kindred soul, may our paths to connect with faith and the divine forever intertwine. To my friends from the Geography department and the Nature, Society and Environmental Governance course, whom I met in the third year of this doctoral research: Katie Polkinghorne, with whom I have learned so much; Elvie Crowe, treasured companion in finding our truths and bringing them into the world – you also give the best hugs; Andrew Fowler, may I continue to enjoy the magnificence of your company and stunning good looks over lunches by the bank of the river in Port Meadow for endless sunny days to come; Jenny Harker, your luminous presence brings

great energy into this world and your astounding dexterity with language blows my mind, you must write a book and I'll be the first to read it; Jamie Hinch, whose more-than-human sensibilities and rapport with love and the wild gives me resonance and inspiration; and to the other wonderful friends from this class, particularly Sonakshi Srivastava and Flora Campbell.

To my Sangha, sisters and brothers in the dhamma: my soul friend Lindsey Thompson, may we continue to meet the challenges and beauties of opening heart and mind to the cosmos together; Theodore Leigh, for smuggling me into your college room during my year in the tent so that I could nap and be warm in the depths of midwinter; Aamir Khaderbhai, for our astonishing karmic resonance and timeless walks in Port Meadow; Alex Georges, who helped open my spirit to so much embodied richness and knowing; Annie Obernoster, may we together develop our connection to the earth beings and continue to synthesise ecology and the dhamma; and to Nikita Ostrovsky, Rory Bedford, Jago Bruce, Mrinank Sharma, Toby Ralph, Stefano Gandolfo, Sachintha Dias, and others. May our journeys in space and time forever interlock as we continually discover and bring into being the dhamma in the wildness and everchanging mystery which calls us to follow the truths in each of our hearts. Sangham saranam gacchami.

To Celia and Tim Bickersteth and Francesca Rigg, and to Hannah Parks and Sam Bickersteth, for sharing swims in the meadow, and the great privilege of having me in your home and the gift of a beautiful room – each day I am deeply thankful for your generosity and kindness. To my childhood friends, particularly Will Burton and Will Bridgland, my brothers in arms through the darkness and light, and Rafferty Lindon, soul friend and companion in adventuring the timeless mystery. To my friends from undergraduate, particularly Ollie French, Simon Cooper, Guy Steed and Joe Burns, may we forever make mischief. To Isla Duporge and Luca Chiaverini, and to Jonny Turnbull and Kayla Schulte, whose friendship proved invaluable for helping and guiding this research. To Kate Hunt, Oakley Loudon, Kevin Hobbs, and the other gardeners of Lady Margaret Hall, with whom I celebrated on the day of receiving the offer to undertake this doctoral study, and who have been a constant source of love and encouragement throughout this journey. To those women in Oxford who have given me counsel, support and friendship: Laura Evers, Lorraine Orders, Emily Carson, and beloved yoga teacher Mariella de Martini. To Harrison Fannon, Corina Smith, Emma Ashdown and company, who opened my heart and mind to the landscapes and lore of the

West Country. To Josephine Reynell and family, a warm and welcoming presence in Oxford since my childhood. To those countless others I have met here during my studies whose paths I have been grateful to interlock with mine, including Henrik Diamant, Shati Patel, Georgia Crowther, Alex Saad and Lila Brustad. And to the light and promise of new friendship: Marits Luinenberg and the many luminous souls I met in Canada last summer, Sam Cornish, Ajay Thakur and family, Lauren Laing-Buisson, Astrid Blystad and company, Callie Maron, Sammi Bennet, Ginya Marr, and more - may we share many good stories and adventures in the years to come!

To my land ancestors

If there were to be a coauthor for this thesis then it would be Port Meadow, the landscape of my heart. Not a day goes by where I do not feel the call to return to the meadow and bear witness to the blazing sunsets and star-studded midwinter skies, agog with wonder and held by an unshakable belonging that steadily grows as I have hefted upon the meadow and in turn let the contours of my inner world be slowly shaped over the seasons by its quietly magical rhythms and textures. The stand of poplars I call the spirit of the meadow, which presides over the stretch of river where I would swim with my friends in every season, skin steeled by snowy winds and licked by the warm sun; the many spots along the eastern bank of the river where I have shared countless lunches with beloved friends; the gentle grassy bank which shoulders the floodplain where I would meditate in the spring and summer; the fields along Binsey lane, my favourite road in Oxford, and the mystical church which lies at its end; the little glade where for a year I slept in a tent alongside the badgers and hooting owls and kindly horse chestnuts; and the vastness of the meadow's enfolding sky, the gateway to connection with my ancestors and the luminous friendship growing between myself and the sun and moon and stars; all these realms of Port Meadow have grown rich and deep with their significance to every relationship and creative expression I have been graced to receive during the unfolding of this research. And on this journey with no beginning or end I once again find myself in the meadow after a beautiful evening of friendship and gratitude, now sitting under the snow moon with my bivouac and sleeping bags, feeling the gentle breeze play with my hair and the clouds part to reveal the stars above, waiting for the arrival of midnight to submit my doctoral thesis, and to then spend a night with the meadow and greet

the dawn with my wholehearted presence.

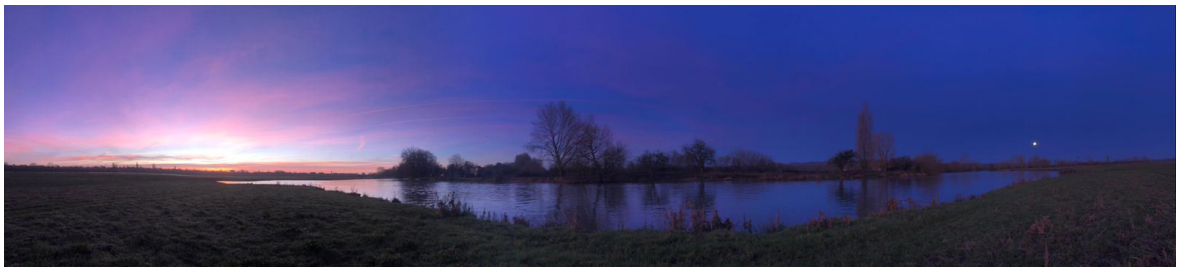


Figure 6.4: Waking with ice on my bivouac by the river in Port Meadow following the midnight submission of my doctoral thesis, with the rising sun and full moon bearing witness to each other across the dawn sky. The words of the prajñaparamita sutra echo in my being – *Regard this fleeting world like so: like the stars fading and vanishing at dawn, like bubbles in a fast moving stream, like morning dewdrops evaporating on blades of grass, like a candle flickering in a strong wind.* Photograph by Siddharth Unnithan Kumar, 5th February 2023.

To the Coconino forest of the high mountain desert in southwesterly Turtle Island, amongst whose ponderosa pines and sunkissed grasses I wandered and felt so held, and home to the deer and elk with whom I exchanged the gift of song. And to the other westerly landscapes of Turtle Island, whose vast beauty blew open my heart and mind and showed me the landscapes of equal numinosity within: the Valley of the Gods, who taught me that the Great Wind is my friend when I slept there overnight on my road trip to visiting David Abram; the dazzling wonder of the mountain forests between the Whulge (Puget Sound) and the Pacific Ocean, who gave me humility and poetry; the islands and salt waters around the Desolation Sound, who graced me with so much human generosity and connection; the Grand Canyon, across whose great buttresses and ravines I watched the sunset in awe with Sam and a dinner of bread, cheese and peanut butter; and that mountain meadow in Colorado shown to me by Callie whose name and location I cannot recall but whose bright blue sky and rolling grassy swards of wildflowers imprinted its serene beauty deep into my consciousness. I hope in this lifetime that I will serve to heal the present wounds of settler-colonial legacies borne by these landscapes and their inhabitants, whose cultural and spiritual practices are so powerful and precious and speak to the depths of my being.

To Oxford, who fills me with gratitude as I bring to mind the countless friendships of past present and future that this place has given me, kindred spirits and magnificent souls that

I find myself carrying in my heart and giving me strength wherever I may be in space and time; beyond Port Meadow, I bow especially to the upper reading room of the Old Bodleian Library, among whose bright wooden aesthetics I have written ninety percent of this thesis, and to the Mathematical Institute, an unexpected refuge where I would cook my oats and take a shower in the year I slept in my tent. And I thank those other landscapes with whom I have lived, and who have so directly given life and love to this doctoral research: most of all, my home town of Lewes and the surrounding hills whose paths I have wandered amongst since childhood; and Todiramzanipura and the desert, whose Rajasthani colours and tranquil magic are woven into my soul.

To my earthly support systems and nonhuman companions

My belly rumbles with delight and my heart explodes with joy as I turn to thank my breakfast – oats with apple banana ginger cinnamon turmeric nuts raisins – which has given me incalculable levels of pleasure and provided me with the soul food necessary for bringing this thesis into being. Pasta and tomato sauce, rice and daal, stewed fruit, fresh bread, honey and tahini, hot tea with something sweet – you give me life and I'll love you forever. How fortunate to be incarnated into a world where the food is so damn good! This leads me to bring to mind all the people who have planted and tended these crops, those who have worked to bring the food from the soil to my hands, the ancestors who cultivated the knowledge and practice of farming and cooking, the nonhuman beings themselves for their life-giving nourishment, and the more-than-human earth encompassing this all. Truly no grain of sand or blade of grass has been separate from the wholeness of the process which has made this research possible.

I turn to thank those other inhabitants of this world who have so greatly helped me during this time of study, in particular: my tent, who sheltered me through the cycling seasons and brought me so much learning; my clothes, who keep me warm and whose colours bring me joy; my meditation cushion, whose willingness to fit the contours of my body aids daily the return to my heart and inner world; Shadowfax and Yakul, my noble steeds old and new; Appa, my faithful companion; and the films and soundtracks of Studio Ghibli, especially *Nausicaä of the Valley of the Wind* and *Princess Mononoke*, whose timeless beauty and visionary power speaks directly to my heart.

To the sun and moon: bearing witness to your celestial dance I continually discover the profound resonance between your cosmic intimacy and the relationships unfolding in my life, and to rest my gaze upon your moments of contact with the earthly horizon brings me to feeling at home in this world. To the stars above, and most of all to Orion, whose presence in the darkness comforts me and connects me to my ancestors. And to the two birds I saw today flying west into the sunset, whose dancing forms in the golden light moved me to tears.

To my family

To Sanjiv Kumar, my dad, who has graciously imparted the wonder and beauty of mathematics since before I can remember, and whose loving and gentle presence gives me immense reassurance and joy in life. To Maya Unnithan, my mum, whose anthropological spirit and curiosity and connection with humanity inspires and guides me. Thank you both for bringing me into this world, and for your love and friendship which keeps me steadfast amongst the winds of storm and tranquility. To Arjun Unnithan Kumar, my brother, may our companionship continue to grow and strengthen as our lives unfold together. And to Gerda and Thottamon Kantan Kesavan Narayanan Unnithan (Oma and Appupan), and Vinod and Sudha Kumar (Baba and Dadima), my grandparents; you teach me so much and leave me wide-eyed with wonder at the lives you have lived, I am honoured to carry you with me and may we continue our conversations through eternity. I love you all so much.

Now I turn to consciousness and the mystery, and as I close my eyes I acknowledge that I am holding in my hand the baton between all my ancestors before me and all my descendents to come. Thank you for the gift of this human existence, and may I do the best I can with the precious time I have been given.



Figure 6.5: One of those rare truly magical days born from the mystical joy of worlds meeting. (Left to right) Dad, Sam, Żaneta with baby Oliver, and Mum, gathered in front of my dwelling place in the tent glade. Photograph by Siddharth Unnithan Kumar, 20th August 2022.

Bibliography

[1] David Abram. *The Spell of the Sensuous: Perception and Language in a More-Than-Human World*. Pantheon books, 1996.

[2] David Abram. *Becoming Animal: An Earthly Cosmology*. Vintage, 2010.

[3] William M Adams, Ros Aveling, Dan Brockington, Barney Dickson, Jo Elliott, Jon Hutton, Dilys Roe, Bhaskar Vira, and William Wolmer. "Biodiversity conservation and the eradication of poverty". In: *Science* 306.5699 (2004), pp. 1146–1149.

[4] William M Adams and Martin Mulligan. *Decolonizing nature: strategies for conservation in a post-colonial era*. Routledge, 2012.

[5] Frank Adriaensen, JP Chardon, Geert De Blust, Else Swinnen, S Villalba, Hubert Gulinck, and Erik Matthysen. "The application of 'least-cost'modelling as a functional landscape model". In: *Landscape and urban planning* 64.4 (2003), pp. 233–247.

[6] Stacy Alaimo. *Bodily natures: Science, environment, and the material self*. Indiana University Press, 2010.

[7] Koen Arts, René van der Wal, and William M Adams. "Digital technology and the conservation of nature". In: *Ambio* 44.4 (2015), pp. 661–673.

[8] Marcia Ascher. *Ethnomathematics: A multicultural view of mathematical ideas*. Routledge, 2017.

[9] Eric Ash, Samuel A Cushman, David W Macdonald, Tim Redford, and Żaneta Kaszta. "How important are resistance, dispersal ability, population density and mortality in temporally dynamic simulations of population connectivity? A case study of tigers in southeast Asia". In: *Land* 9.11 (2020), p. 415.

[10] Eric Ash, David W Macdonald, Samuel A Cushman, Adisorn Noochdumrong, Tim Redford, and Żaneta Kaszta. *Optimization of spatial scale, but not functional shape, affects the performance of habitat suitability models: a case study of tigers (Panthera tigris) in Thailand*. 2021.

[11] Eugene Richard Atleo. *Tsawalk: A Nuu-chah-nulth worldview*. UBC press, 2007.

[12] Eugene Richard Atleo. *Principles of Tsawalk: An Indigenous approach to global crisis*. UBC press, 2012.

[13] Luciano Atzeni, Samuel A Cushman, Defeng Bai, Jun Wang, Pengju Chen, Kun Shi, and Philip Riordan. *Meta-replication, sampling bias, and multi-scale model selection: A case study on snow leopard (Panthera uncia) in western China*. 2020.

[14] Maan Barua. "Bio-geo-graphy: Landscape, dwelling, and the political ecology of human-elephant relations". In: *Environment and Planning D: Society and Space* 32.5 (2014), pp. 915–934.

[15] Maan Barua. "Volatile ecologies: towards a material politics of human—animal relations". In: *Environment and Planning A* 46.6 (2014), pp. 1462–1478.

[16] Paul Beier, Daniel R Majka, and Shawn L Newell. "Uncertainty analysis of least-cost modeling for designing wildlife linkages". In: *Ecological applications* 19.8 (2009), pp. 2067–2077.

[17] Paul Beier, Daniel R Majka, and Wayne D Spencer. "Forks in the road: choices in procedures for designing wildland linkages". In: *Conservation Biology* 22.4 (2008), pp. 836–851.

[18] Nathan J Bennett, Robin Roth, Sarah C Klain, Kai Chan, Patrick Christie, Douglas A Clark, Georgina Cullman, Deborah Curran, Trevor J Durbin, Graham Epstein, et al. "Conservation social science: Understanding and integrating human dimensions to improve conservation". In: *Biological conservation* 205 (2017), pp. 93–108.

[19] Etienne S Benson. "Minimal animal: Surveillance, simulation, and stochasticity in wildlife biology". In: *Antennae* 30 (2014), p. 39.

[20] Etienne S Benson. "Movement Ecology and the Minimal Animal". In: *LA+* 4 (2016), p. 30.

[21] Carita M Bergman, James A Schaefer, and SN Luttich. "Caribou movement as a correlated random walk". In: *Oecologia* 123.3 (2000), pp. 364–374.

[22] Charles Bergman. "Inventing a beast with no body: Radio-telemetry, the marginalization of animals, and the simulation of ecology". In: *Worldviews: Global Religions, Culture, and Ecology* 9.2 (2005), pp. 255–270.

[23] Fikret Berkes. *Sacred ecology*. Routledge, 2017.

[24] Fikret Berkes, Johan Colding, and Carl Folke. *Navigating social-ecological systems: building resilience for complexity and change*. Cambridge University Press, 2008.

[25] Benjamin Blonder, Christine Lamanna, Cyrille Violle, and Brian J Enquist. *The n-dimensional hypervolume*. 2014.

[26] Greta Bocedi, Stephen CF Palmer, Anne-Kathleen Malchow, Damaris Zurell, Kevin Watts, and Justin MJ Travis. "RangeShifter 2.0: an extended and enhanced platform for modelling spatial eco-evolutionary dynamics and species' responses to environmental changes". In: *Ecography* 44.10 (2021), pp. 1453–1462.

[27] Alistair N Boettiger, George Wittemyer, Richard Starfield, Fritz Volrath, Iain Douglas-Hamilton, and Wayne M Getz. "Inferring ecological and behavioral drivers of African elephant movement using a linear filtering approach". In: *Ecology* 92.8 (2011), pp. 1648–1657.

[28] Steven J Bograd, Barbara A Block, Daniel P Costa, and Brendan J Godley. "Biologging technologies: new tools for conservation. Introduction". In: *Endangered Species Research* 10 (2010), pp. 1–7.

[29] Mark S Boyce, Pierre R Vernier, Scott E Nielsen, and Fiona KA Schmiegelow. "Evaluating resource selection functions". In: *Ecological modelling* 157.2-3 (2002), pp. 281–300.

[30] Tara Brach. *Radical acceptance: Embracing your life with the heart of a Buddha*. Bantam, 2004.

[31] Femke Broekhuis, Gabriele Cozzi, Marion Valeix, John W McNutt, and David W Macdonald. "Risk avoidance in sympatric large carnivores: reactive or predictive?" In: *Journal of Animal Ecology* 82.5 (2013), pp. 1098–1105.

[32] Femke Broekhuis, Emily K Madsen, Kosiom Keiwua, and David W Macdonald. "Using GPS collars to investigate the frequency and behavioural outcomes of intraspecific interactions among carnivores: A case study of male cheetahs in the Maasai Mara, Kenya". In: *PloS one* 14.4 (2019), e0213910.

[33] Olivier Broennimann, Matthew C Fitzpatrick, Peter B Pearman, Blaise Petitpierre, Loïc Pellissier, Nigel G Yoccoz, Wilfried Thuiller, Marie-Josée Fortin, Christophe Randin, Niklaus E Zimmermann, et al. *Measuring ecological niche overlap from occurrence and spatial environmental data*. 2012.

[34] Joseph W Bull, EJ Milner-Gulland, Prue FE Addison, William NS Arlidge, Julia Baker, Thomas M Brooks, Michael J Burgass, Amy Hinsley, Martine Maron, John G Robinson, et al. "Net positive outcomes for nature". In: *Nature ecology & evolution* 4.1 (2020), pp. 4–7.

[35] Nils Bunnefeld, Emily Nicholson, and EJ Milner-Gulland. *Decision-making in conservation and natural resource management: models for interdisciplinary approaches*. 1st. Vol. 22. Cambridge University Press, Cambridge, UK, 2017, pp. 1–16.

[36] Kenneth P Burnham and David R Anderson. "Multimodel inference: understanding AIC and BIC in model selection". In: *Sociological methods & research* 33.2 (2004), pp. 261–304.

[37] Lisa M Campbell. "Overcoming obstacles to interdisciplinary research". In: *Conservation biology* 19.2 (2005), pp. 574–577.

[38] Mauricio Cantor, Leonardo Liberali Wedekin, Paulo Roberto Guimaraes, Fabio Goncalves Daura-Jorge, Marcos Roberto Rossi-Santos, and Paulo Cesar Simoes-Lopes. "Disentangling social networks from spatiotemporal dynamics: the temporal structure of a dolphin society". In: *Animal Behaviour* 84.3 (2012), pp. 641–651.

[39] Richard Chandler and Jeffrey Hepinstall-Cymerman. *Estimating the spatial scales of landscape effects on abundance*. 2016.

[40] Luca Chiaverini, Ho Yi Wan, Beth Hahn, Amy Cilimburg, Tzeidle N Wasserman, and Samuel A Cushman. *Effects of non-representative sampling design on multi-scale habitat models: flammulated owls in the Rocky Mountains.* 2021.

[41] Edward A Codling, Michael J Plank, and Simon Benhamou. “Random walk models in biology”. In: *Journal of the Royal society interface* 5.25 (2008), pp. 813–834.

[42] Bradley W Compton, Kevin McGarigal, Samuel A Cushman, and Lloyd R Gamble. “A resistant-kernel model of connectivity for amphibians that breed in vernal pools”. In: *Conservation Biology* 21.3 (2007), pp. 788–799.

[43] Steven J Cooke, Daniel T Blumstein, Richard Buchholz, Tim Caro, Esteban Fernandez-Juricic, Craig E Franklin, Julian Metcalfe, Constance M O’Connor, Colleen Cassady St. Clair, William J Sutherland, et al. “Physiology, behavior, and conservation”. In: *Physiological and Biochemical Zoology* 87.1 (2014), pp. 1–14.

[44] Steven J Cooke, Scott G Hinch, Michael R Donaldson, Timothy D Clark, Erika J Eliason, Glenn T Crossin, Graham D Raby, Ken M Jeffries, Mike Lapointe, Kristi Miller, et al. “Conservation physiology in practice: how physiological knowledge has improved our ability to sustainably manage Pacific salmon during up-river migration”. In: *Philosophical Transactions of the Royal Society B: Biological Sciences* 367.1596 (2012), pp. 1757–1769.

[45] Steven J Cooke, Lawren Sack, Craig E Franklin, Anthony P Farrell, John Beardall, Martin Wikelski, and Steven L Chown. “What is conservation physiology? Perspectives on an increasingly integrated and essential science”. In: *Conservation Physiology* 1.1 (2013).

[46] William Cronon. “The trouble with wilderness: or, getting back to the wrong nature”. In: *Environmental history* 1.1 (1996), pp. 7–28.

[47] William Cronon. *Uncommon Ground: Rethinking the Human Place in Nature*. W. W. Norton & Company, 1997.

[48] Samuel A Cushman. “Effects of habitat loss and fragmentation on amphibians: a review and prospectus”. In: *Biological conservation* 128.2 (2006), pp. 231–240.

[49] Samuel A Cushman. “Animal movement data: GPS telemetry, autocorrelation and the need for path-level analysis”. In: *Spatial complexity, informatics, and wildlife conservation*. Springer, Berlin, Germany, 2010, pp. 131–149.

[50] Samuel A Cushman. "Space and time in ecology: noise or fundamental driver?" In: *Spatial complexity, informatics, and wildlife conservation*. Springer, Berlin, Germany, 2010, pp. 19–41.

[51] Samuel A Cushman, Michael Chase, and Curtice Griffin. "Elephants in space and time". In: *Oikos* 109.2 (2005), pp. 331–341.

[52] Samuel A Cushman and Falk Huettmann. *Spatial Complexity, Informatics, and Wildlife Conservation*. Springer, Tokyo, 2010.

[53] Samuel A Cushman and Erin L Landguth. "Scale dependent inference in landscape genetics". In: *Landscape ecology* 25.6 (2010), pp. 967–979.

[54] Samuel A Cushman and Jesse S Lewis. "Movement behavior explains genetic differentiation in American black bears". In: *Landscape ecology* 25.10 (2010), pp. 1613–1625.

[55] Samuel A Cushman, Jesse S Lewis, and Erin L Landguth. "Why did the bear cross the road? Comparing the performance of multiple resistance surfaces and connectivity modeling methods". In: *Diversity* 6.4 (2014), pp. 844–854.

[56] Samuel A Cushman and Kevin McGarigal. *Hierarchical, multi-scale decomposition of species-environment relationships*. 2002.

[57] Samuel A Cushman, Kevin S McKelvey, and Michael K Schwartz. "Use of empirically derived source-destination models to map regional conservation corridors". In: *Conservation Biology* 23.2 (2009), pp. 368–376.

[58] Samuel A Cushman, Brad H McRae, Frank Adriaensen, Paul Beier, Mark Shirley, and Kathy Zeller. "Biological corridors and connectivity [Chapter 21]". In: *In: Macdonald, DW; Willis, KJ, eds. Key Topics in Conservation Biology 2. Hoboken, NJ: Wiley-Blackwell. p. 384-404.* (2013), pp. 384–404.

[59] Samuel A Cushman, MG Raphael, LF Ruggiero, AS Shirk, TN Wasserman, and EC O'Doherty. "Limiting factors and landscape connectivity: the American marten in the Rocky Mountains". In: *Landscape ecology* 26.8 (2011), pp. 1137–1149.

[60] Samuel A Cushman, Andrew J Shirk, and Erin L Landguth. "Separating the effects of habitat area, fragmentation and matrix resistance on genetic differentiation in complex landscapes". In: *Landscape ecology* 27.3 (2012), pp. 369–380.

[61] Samuel A Cushman, Andrew J Shirk, and Erin L Landguth. "Landscape genetics and limiting factors". In: *Conservation Genetics* 14.2 (2013), pp. 263–274.

[62] D Richard Cutler, Thomas C Edwards Jr, Karen H Beard, Adele Cutler, Kyle T Hess, Jacob Gibson, and Joshua J Lawler. *Random forests for classification in ecology*. 2007.

[63] Ubiratan d'Ambrosio. "Ethnomathematics and its place in the history and pedagogy of mathematics". In: *For the learning of Mathematics* 5.1 (1985), pp. 44–48.

[64] Wade Davis. *The wayfinders: Why ancient wisdom matters in the modern world*. House of Anansi, 2009.

[65] Donald L DeAngelis and Wolf M Mooij. "Individual-based modeling of ecological and evolutionary processes". In: *Annu. Rev. Ecol. Evol. Syst.* 36 (2005), pp. 147–168.

[66] Philip Dixon. "VEGAN, a package of R functions for community ecology". In: *Journal of Vegetation Science* 14.6 (2003), pp. 927–930.

[67] Stephane Dray, Manuela Royer-Carenzi, and Clement Calenge. "The exploratory analysis of autocorrelation in animal-movement studies". In: *Ecological Research* 25.3 (2010), pp. 673–681.

[68] John B Dunning Jr, David J Stewart, Brent J Danielson, Barry R Noon, Terry L Root, Roland H Lamberson, and Ernest E Stevens. "Spatially explicit population models: current forms and future uses". In: *Ecological Applications* 5.1 (1995), pp. 3–11.

[69] Nicholas B Elliot, Samuel A Cushman, Andrew J Loveridge, Godfrey Mtare, and David W Macdonald. "Movements vary according to dispersal stage, group size, and rainfall: the case of the African lion". In: *Ecology* 95.10 (2014), pp. 2860–2869.

[70] Nicholas B Elliot, Samuel A Cushman, David W Macdonald, and Andrew J Loveridge. "The devil is in the dispersers: predictions of landscape connectivity change with demography". In: *Journal of Applied Ecology* 51.5 (2014), pp. 1169–1178.

[71] Rebecca D Ellis, Todd J McWhorter, and Martine Maron. "Integrating landscape ecology and conservation physiology". In: *Landscape Ecology* 27.1 (2012), pp. 1–12.

[72] Almo Farina. *Principles and methods in landscape ecology*. Vol. 21. Springer, 1998.

[73] George K Francis. *A topological picturebook*. Vol. 2. Springer, 1987.

[74] Beatrice Frank, Jenny A Glikman, and Silvio Marchini. *Human–wildlife interactions: turning conflict into coexistence*. Vol. 23. Cambridge University Press, 2019.

[75] Amitav Ghosh. *The Nutmeg's Curse: Parables for a Planet in Crisis*. University of Chicago Press, 2021.

[76] Robert Ghrist. *Elementary Applied Topology*. Createspace, 2014.

[77] James P Gibbs. "Amphibian movements in response to forest edges, roads, and streambeds in southern New England". In: *The Journal of Wildlife Management* (1998), pp. 584–589.

[78] S. Gillies, B. Ward, and A.S. Peterson. *Rasterio: Geospatial raster I/O for Python programmers*. 2013. URL: `https://github.%20com/mapbox/rasterio`.

[79] Lucrezia Gorini, John DC Linnell, Roel May, Manuela Panzacchi, Luigi Boitani, Morten Odden, and Erlend B Nilsen. "Habitat heterogeneity and mammalian predator–prey interactions". In: *Mammal review* 42.1 (2012), pp. 55–77.

[80] Beth Greenhough. "More-than-human Geographies". In: *The SAGE Handbook of Human Geography* (2014), pp. 94–119.

[81] His Holiness the XIV Dalai Lama Tenzin Gyatso. *Beyond religion: Ethics for a whole world*. Random House, 2012.

[82] Thich Nhat Hanh. *The heart of Buddha's teaching*. Random House, 2008.

[83] Thich Nhat Hanh. *The miracle of mindfulness, gift edition: An introduction to the practice of meditation*. Beacon Press, 2016.

[84] Matthew C Hansen, Peter V Potapov, Rebecca Moore, Matt Hancher, Svetlana A Turubanova, Alexandra Tyukavina, David Thau, SV Stehman, Scott J Goetz, Thomas R Loveland, et al. *High-resolution global maps of 21st-century forest cover change*. 2013.

[85] William W Hargrove, Forrest M Hoffman, and Rebecca A Efroymson. "A practical map-analysis tool for detecting potential dispersal corridors". In: *Landscape Ecology* 20.4 (2005), pp. 361–373.

[86] Andrew J Hearn, Samuel A Cushman, Joanna Ross, Benoit Goossens, Luke TB Hunter, and David W Macdonald. *Spatio-temporal ecology of sympatric felids on Borneo. Evidence for resource partitioning?* 2018.

[87] Troy M Hegel, Samuel A Cushman, Jeffrey Evans, and Falk Huettmann. *Current state of the art for statistical modelling of species distributions*. 2010.

[88] Julie A Heinrichs, Joshua J Lawler, and Nathan H Schumaker. "Intrinsic and extrinsic drivers of source–sink dynamics". In: *Ecology and evolution* 6.4 (2016), pp. 892–904.

[89] Jodi A Hilty, William Z Lidicker Jr, and Adina M Merenlender. *Corridor ecology: the science and practice of linking landscapes for biodiversity conservation*. 1st. Island Press, Washington D.C., USA, 2006, pp. 269–274.

[90] Timothy Hodgetts. "Connectivity as a multiple: In, with and as "nature"". In: *Area* 50.1 (2018), pp. 83–90.

[91] Timothy Hodgetts and Jamie Lorimer. "Methodologies for animals' geographies: Cultures, communication and genomics". In: *Cultural geographies* 22.2 (2015), pp. 285–295.

[92] Timothy Hodgetts and Jamie Lorimer. "Animals' mobilities". In: *Progress in Human Geography* 44.1 (2020), pp. 4–26.

[93] Robert D Holt. *Bringing the Hutchinsonian niche into the 21st century: ecological and evolutionary perspectives*. 2009.

[94] Robert D Holt. *Reflections on niches and numbers*. 2020.

[95] Marcel Holyoak, Renato Casagrandi, Ran Nathan, Eloy Revilla, and Orr Spiegel. "Trends and missing parts in the study of movement ecology". In: *Proceedings of the National Academy of Sciences* 105.49 (2008), pp. 19060–19065.

[96] Johan van den Hoogen et al. *Soil nematode abundance and functional group composition at a global scale*. 2019.

[97] Bell Hooks. *All about love: New visions*. Harper Perennial, 2001.

[98] G. Evelyn Hutchinson. *Concluding remarks*. 1957.

[99] Tim Ingold. "The temporality of the landscape". In: *World archaeology* 25.2 (1993), pp. 152–174.

[100] Tim Ingold. *The perception of the environment: essays on livelihood, dwelling and skill*. 1st. Routledge, Abingdon-on-Thames, UK, 2000, pp. 13–26.

[101] Tim Ingold. "A circumpolar night's dream". In: *The Perception of the Environment*. Routledge, 2002.

[102] Tim Ingold. "Culture, nature, environment: steps to an ecology of life". In: *The Perception of the Environment*. Routledge, 2002, pp. 27–29.

[103] Tim Ingold. "Rethinking the animate, re-animating thought". In: *Ethnos* 71.1 (2006), pp. 9–20.

[104] Tim Ingold. "Ways of mind-walking: reading, writing, painting". In: *Visual Studies* 25.1 (2010), pp. 15–23.

[105] Andy Jarvis, Hannes Isaak Reuter, Andy Nelson, and Edward Guevara. *[dataset] Hole-filled seamless SRTM data V4*. 2008. URL: `https://srtm.csi.cgiar.org/`.

[106] Florian Jeltsch, Dries Bonte, Guy Pe'er, Björn Reineking, Peter Leimgruber, Niko Balkenhol, Boris Schröder, Carsten M Buchmann, Thomas Mueller, Niels Blaum, et al. "Integrating movement ecology with biodiversity research-exploring new avenues to address spatiotemporal biodiversity dynamics". In: *Movement Ecology* 1.1 (2013), pp. 1–13.

[107] Megan K Jennings, Katherine A Zeller, and Rebecca L Lewison. "Supporting adaptive connectivity in dynamic landscapes". In: *Land* 9.9 (2020), p. 295.

[108] Jay T Johnson, Richard Howitt, Gregory Cajete, Fikret Berkes, Renee Pualani Louis, and Andrew Kliskey. "Weaving Indigenous and sustainability sciences to diversify our methods". In: *Sustainability Science* 11.1 (2016), pp. 1–11.

[109] Peter Kareiva and Michelle Marvier. "What is conservation science?" In: *BioScience* 62.11 (2012), pp. 962–969.

[110] Peter Kareiva and Nanako Shigesada. "Analyzing insect movement as a correlated random walk". In: *Oecologia* 56.2 (1983), pp. 234–238.

[111] Żaneta Kaszta, Samuel A Cushman, Andrew J Hearn, Dawn Burnham, Ewan A Macdonald, Benoit Goossens, Senthilvel KSS Nathan, and David W Macdonald. *Integrating Sunda clouded leopard (Neofelis diardi) conservation into development and restoration planning in Sabah (Borneo)*. 2019.

[112] Żaneta Kaszta, Samuel A Cushman, and Rob Slotow. "Temporal Non-stationarity of Path-Selection Movement Models and Connectivity: An Example of African Elephants in Kruger National Park". In: *Frontiers in Ecology and Evolution* 9 (2021), p. 207.

[113] Annika TH Keeley, Paul Beier, Brian W Keeley, and Matthew E Fagan. "Habitat suitability is a poor proxy for landscape connectivity during dispersal and mating movements". In: *Landscape and Urban Planning* 161 (2017), pp. 90–102.

[114] Robin Wall Kimmerer. *Braiding sweetgrass: Indigenous wisdom, scientific knowledge and the teachings of plants*. Milkweed editions, 2013.

[115] Jack Kornfield. *The wise heart: Buddhist psychology for the West*. Random House, 2008.

[116] Jérôme Laliberté and Martin-Hugues St-Laurent. "Validation of functional connectivity modeling: The Achilles' heel of landscape connectivity mapping". In: *Landscape and Urban Planning* 202 (2020), p. 103878.

[117] John Fire Lame Deer and Richard Erdoes. *Lame Deer, seeker of visions*. Simon and Schuster, 1994.

[118] Erin L Landguth and Samuel A Cushman. "CDPOP: a spatially explicit cost distance population genetics program". In: *Molecular ecology resources* 10.1 (2010), pp. 156–161.

[119] Erin L Landguth, Samuel A Cushman, Michael K Schwartz, Kevin S McKelvey, M Murphy, and G Luikart. "Quantifying the lag time to detect barriers in landscape genetics". In: *Molecular ecology* 19.19 (2010), pp. 4179–4191.

[120] Simon A Levin. "The problem of pattern and scale in ecology: the Robert H. MacArthur award lecture". In: *Ecology* 73.6 (1992), pp. 1943–1967.

[121] Mark A Lewis, Philip K Maini, and Sergei V Petrovskii. "Dispersal, individual movement and spatial ecology". In: *Lecture Notes in Mathematics (Mathematics Bioscience Series)* 2071 (2013).

[122] Jamie Lorimer. *Wildlife in the Anthropocene: conservation after nature*. University of Minnesota Press, 2015.

[123] David W Macdonald, Luca Chiaverini, Helen M Bothwell, Żaneta Kaszta, Eric Ash, Gilmoore Bolongon, Özgün Emre Can, Ahimsa Campos-Arceiz, Phan Channa, Gopalasamy Reuben Clements, et al. *Predicting biodiversity richness in rapidly changing landscapes: climate, low human pressure or protection as salvation?* 2020.

[124] Ewan A Macdonald, Samuel A Cushman, Erin L Landguth, Andrew J Hearn, Yadvinder Malhi, and David W Macdonald. "Simulating impacts of rapid forest loss on population size, connectivity and genetic diversity of Sunda clouded leopards (Neofelis diardi) in Borneo". In: *PLoS One* 13.9 (2018), e0196974.

[125] BFL Manly, Lyman McDonald, Dana L Thomas, Trent L McDonald, and Wallace P Erickson. *Resource selection by animals: statistical design and analysis for field studies*. Springer Science & Business Media, 2007.

[126] Nathan Mantel. "The detection of disease clustering and a generalized regression approach". In: *Cancer research* 27.2 Part 1 (1967), pp. 209–220.

[127] Lauren Martin and Anna J Secor. "Towards a post-mathematical topology". In: *Progress in Human Geography* 38.3 (2014), pp. 420–438.

[128] María C Mateo-Sánchez, Niko Balkenhol, Samuel A Cushman, Trinidad Pérez, Ana Domínguez, and Santiago Saura. "A comparative framework to infer landscape effects on population genetic structure: are habitat suitability models effective in explaining gene flow?" In: *Landscape Ecology* 30.8 (2015), pp. 1405–1420.

[129] María C Mateo-Sánchez, Niko Balkenhol, Samuel A Cushman, Trinidad Pérez, Ana Domínguez, and Santiago Saura. "Estimating effective landscape distances and movement corridors: comparison of habitat and genetic data". In: *Ecosphere* 6.4 (2015), pp. 1–16.

[130] Nayanika Mathur. *Crooked cats: beastly encounters in the Anthropocene*. University of Chicago Press, 2021.

[131] Derek McCormack. “Geography and abstraction: Towards an affirmative critique”. In: *Progress in Human Geography* 36.6 (2012), pp. 715–734.

[132] Kevin McGarigal and Samuel A Cushman. “The gradient concept of landscape structure [Chapter 12]”. In: *In: Wiens, John A.; Moss, Michael R., eds. Issues and Perspectives in Landscape Ecology. Cambridge University Press. p. 112-119.* (2005), pp. 112–119.

[133] Kevin McGarigal, Ho Yi Wan, Kathy A Zeller, Brad C Timm, and Samuel A Cushman. *Multi-scale habitat selection modeling: a review and outlook*. 2016.

[134] Brad H McRae, Brett G Dickson, Timothy H Keitt, and Viral B Shah. “Using circuit theory to model connectivity in ecology, evolution, and conservation”. In: *Ecology* 89.10 (2008), pp. 2712–2724.

[135] Maurice Merleau-Ponty. *Phenomenology of perception*. Routledge, 1965.

[136] Chunrong Mi, Falk Huettmann, Yumin Guo, Xuesong Han, and Lijia Wen. *Why choose Random Forest to predict rare species distribution with few samples in large undersampled areas? Three Asian crane species models provide supporting evidence*. 2017.

[137] EJ Milner-Gulland, Prue Addison, William NS Arlidge, Julia Baker, Hollie Booth, Thomas Brooks, Joseph W Bull, Michael J Burgass, Jon Ekstrom, Sophus OSE zu Ermgassen, et al. “Four steps for the Earth: mainstreaming the post-2020 global biodiversity framework”. In: *One Earth* 4.1 (2021), pp. 75–87.

[138] John Milnor. *Lectures on the h-cobordism theorem*. Vol. 2258. Princeton university press, 2015.

[139] Atte Moilanen. “On the limitations of graph-theoretic connectivity in spatial ecology and conservation”. In: *Journal of Applied Ecology* (2011), pp. 1543–1547.

[140] Henrik Moller, Fikret Berkes, Philip O’Brian Lyver, and Mina Kislalioglu. “Combining science and traditional ecological knowledge: monitoring populations for comanagement”. In: *Ecology and society* 9.3 (2004).

[141] Ran Nathan, Wayne M Getz, Eloy Revilla, Marcel Holyoak, Ronen Kadmon, David Saltz, and Peter E Smouse. “A movement ecology paradigm for unifying organis-

mal movement research". In: *Proceedings of the National Academy of Sciences* 105.49 (2008), pp. 19052–19059.

[142] John G Neihardt. *Black elk speaks*. Dramatic Publishing, 1996.

[143] John Ashworth Nelder and Robert WM Wedderburn. *Generalized linear models*. 1972.

[144] Herbert Ntuli, Sverker C Jagers, Amanda Linell, Martin Sjöstedt, and Edwin Muchapondwa. "Factors influencing local communities' perceptions towards conservation of transboundary wildlife resources: the case of the Great Limpopo Trans-frontier Conservation Area". In: *Biodiversity and Conservation* 28.11 (2019), pp. 2977–3003.

[145] L Osipova, MM Okello, SJ Njumbi, S Ngene, D Western, MW Hayward, and N Balkenhol. "Using step-selection functions to model landscape connectivity for African elephants: Accounting for variability across individuals and seasons". In: *Animal Conservation* 22.1 (2019), pp. 35–48.

[146] Mikhail Yu Paltsyn, James P Gibbs, and Giorgos Mountrakis. "Integrating traditional ecological knowledge and remote sensing for monitoring rangeland dynamics in the Altai Mountain region". In: *Environmental management* 64.1 (2019), pp. 40–51.

[147] Paul C Paquet, Chris T Darimont, et al. "Wildlife conservation and animal welfare: two sides of the same coin". In: *Animal Welfare* 19.2 (2010), pp. 177–190.

[148] Hannah E Parathian, Matthew R McLennan, Catherine M Hill, Amélia Frazão-Moreira, and Kimberley J Hockings. "Breaking through disciplinary barriers: human–wildlife interactions and multispecies ethnography". In: *International Journal of Primatology* 39.5 (2018), pp. 749–775.

[149] Juno Salazar Parreñas. *Decolonizing Extinction*. 1st. Duke University Press, Durham, North Carolina, USA, 2018, pp. 1–30.

[150] Raj Patel and Jason W Moore. "Cheap Nature". In: *A history of the world in seven cheap things: A guide to capitalism, nature, and the future of the planet*. University of California Press, 2017.

[151] Fabian Pedregosa, Gaël Varoquaux, Alexandre Gramfort, Vincent Michel, Bertrand Thirion, Olivier Grisel, Mathieu Blondel, Peter Prettenhofer, Ron Weiss, Vincent Dubourg, et al. *Scikit-learn: Machine learning in Python*. 2011. URL: `https://www.`

jmlr.org/papers/volume12/pedregosa11a/pedregosa11a.pdf?source=post_page----------.

[152] Ugyen Penjor, Christos Astaras, Samuel A Cushman, Żaneta Kaszta, and David W Macdonald. "Contrasting effects of human settlement on the interaction among sympatric apex carnivores". In: *Proceedings of the Royal Society B* 289.1973 (2022), p. 20212681.

[153] M Nils Peterson, Jessie L Birckhead, Kirsten Leong, Markus J Peterson, and Tarla Rai Peterson. "Rearticulating the myth of human–wildlife conflict". In: *Conservation Letters* 3.2 (2010), pp. 74–82.

[154] Chris Philo and Chris Wilbert. *Animal spaces, beastly places*. Routledge, 2004.

[155] Naiara Pinto and Timothy H Keitt. "Beyond the least-cost path: evaluating corridor redundancy using a graph-theoretic approach". In: *Landscape Ecology* 24.2 (2009), pp. 253–266.

[156] Simon Pooley, Maan Barua, William Beinart, Amy Dickman, G Holmes, Jamie Lorimer, Andrew J Loveridge, David W Macdonald, et al. "An interdisciplinary review of current and future approaches to improving human–predator relations". In: *Conservation Biology* 31.3 (2017), pp. 513–523.

[157] Simon Pooley, J Andrew Mendelsohn, and EJ Milner-Gulland. "Hunting down the chimera of multiple disciplinarity in conservation science". In: *Conservation Biology* 28.1 (2014), pp. 22–32.

[158] Steven D Prager and William A Reiners. "Historical and emerging practices in ecological topology". In: *ecological complexity* 6.2 (2009), pp. 160–171.

[159] Michael G Pullinger and Chris J Johnson. "Maintaining or restoring connectivity of modified landscapes: evaluating the least-cost path model with multiple sources of ecological information". In: *Landscape Ecology* 25.10 (2010), pp. 1547–1560.

[160] Bronwyn Rayfield, Marie-Josée Fortin, and Andrew Fall. "The sensitivity of least-cost habitat graphs to relative cost surface values". In: *Landscape Ecology* 25.4 (2010), pp. 519–532.

[161] PA Reddy, J-P Puyravaud, Samuel A Cushman, and H Segu. "Spatial variation in the response of tiger gene flow to landscape features and limiting factors". In: *Animal Conservation* 22.5 (2019), pp. 472–480.

[162] Dawn M Reding, Samuel A Cushman, Todd E Gosselink, and William R Clark. "Linking movement behavior and fine-scale genetic structure to model landscape connectivity for bobcats (Lynx rufus)". In: *Landscape Ecology* 28.3 (2013), pp. 471–486.

[163] Andrea Raya Rey and Falk Huettmann. *Telecoupling analysis of the Patagonian Shelf: A new approach to study global seabird-fisheries interactions to achieve sustainability.* 2020.

[164] Susana Rostro-García, Lhendup Tharchen, Leandro Abade, Christos Astaras, Samuel A Cushman, and David W Macdonald. "Scale dependence of felid predation risk: identifying predictors of livestock kills by tiger and leopard in Bhutan". In: *Landscape Ecology* 31.6 (2016), pp. 1277–1298.

[165] Doborah Rudnick, Sadie J Ryan, Paul Beier, Samuel A Cushman, Fred Dieffenbach, Clinton Epps, Leah R Gerber, Joel N Hartter, Jeff S Jenness, Julia Kintsch, et al. "The role of landscape connectivity in planning and implementing conservation and restoration priorities. Issues in Ecology". In: (2012).

[166] Enrique Salmón. "Kincentric ecology: Indigenous perceptions of the human–nature relationship". In: *Ecological applications* 10.5 (2000), pp. 1327–1332.

[167] Sarah C Sawyer, Clinton W Epps, and Justin S Brashares. "Placing linkages among fragmented habitats: do least-cost models reflect how animals use landscapes?" In: *Journal of Applied Ecology* 48.3 (2011), pp. 668–678.

[168] Nathan H Schumaker. "Using landscape indices to predict habitat connectivity". In: *Ecology* (1996), pp. 1210–1225.

[169] Nathan H Schumaker and Allen Brookes. "HexSim: a modeling environment for ecology and conservation". In: *Landscape Ecology* 33.2 (2018), pp. 197–211.

[170] Nathan H Schumaker, Allen Brookes, Jeffrey R Dunk, Brian Woodbridge, Julie A Heinrichs, Joshua J Lawler, Carlos Carroll, and David LaPlante. "Mapping sources, sinks, and connectivity using a simulation model of northern spotted owls". In: *Landscape Ecology* 29.4 (2014), pp. 579–592.

[171] Michael K Schwartz, Jeffrey P Copeland, Neil J Anderson, John R Squires, Robert M Inman, Kevin S McKelvey, Kristy L Pilgrim, Lisette P Waits, and Samuel A Cushman. "Wolverine gene flow across a narrow climatic niche". In: *Ecology* 90.11 (2009), pp. 3222–3232.

[172] Skipper Seabold and Josef Perktold. *Statsmodels: Econometric and statistical modeling with python*. 2010. URL: https://pdfs.semanticscholar.org/3a27/6417e5350e29cb6bf04ea5a47856(pdf.

[173] Nitin Sekar and Derek Shiller. "Engage with animal welfare in conservation". In: *Science* 369.6504 (2020), pp. 629–630.

[174] Sherub Sherub, Wolfgang Fiedler, Olivier Duriez, and Martin Wikelski. "Bio-logging, new technologies to study conservation physiology on the move: a case study on annual survival of Himalayan vultures". In: *Journal of Comparative Physiology A* 203.6 (2017), pp. 531–542.

[175] Andrew J Shirk, Erin L Landguth, and Samuel A Cushman. "A comparison of regression methods for model selection in individual-based landscape genetic analysis". In: *Molecular ecology resources* 18.1 (2018), pp. 55–67.

[176] Andrew J Shirk, Michael A Schroeder, Leslie A Robb, and Samuel A Cushman. "Empirical validation of landscape resistance models: insights from the Greater Sage-Grouse (Centrocercus urophasianus)". In: *Landscape Ecology* 30.10 (2015), pp. 1837–1850.

[177] Andrew J Shirk, DO Wallin, Samuel A Cushman, CG Rice, and KI Warheit. "Inferring landscape effects on gene flow: a new model selection framework". In: *Molecular ecology* 19.17 (2010), pp. 3603–3619.

[178] B. W. Silverman. *Density Estimation for Statistics and Data Analysis*. Chapman & Hall, 1986.

[179] Jorge Soberón. *Grinnellian and Eltonian niches and geographic distributions of species*. 2007.

[180] Astrid V Stronen, Nathan H Schumaker, Graham J Forbes, Paul C Paquet, and Ryan K Brook. "Landscape resistance to dispersal: simulating long-term effects of human disturbance on a small and isolated wolf population in southwestern Manitoba, Canada". In: *Environmental Monitoring and Assessment* 184.11 (2012), pp. 6923–6934.

[181] Heidi K Swanson, Martin Lysy, Michael Power, Ashley D Stasko, Jim D Johnson, and James D Reist. *A new probabilistic method for quantifying n-dimensional ecological niches and niche overlap*. 2015.

[182] Henrik Thurfjell, Simone Ciuti, and Mark S Boyce. "Applications of step-selection functions in ecology and conservation". In: *Movement ecology* 2.1 (2014), pp. 1–12.

[183] Lutz Tischendorf and Lenore Fahrig. "On the usage and measurement of landscape connectivity". In: *Oikos* 90.1 (2000), pp. 7–19.

[184] Isabella Tree. *Wilding: The return of nature to a British farm*. Pan Macmillan, 2018.

[185] Marlee A Tucker, Katrin Böhning-Gaese, William F Fagan, John M Fryxell, Bram Van Moorter, Susan C Alberts, Abdullahi H Ali, Andrew M Allen, Nina Attias, Tal Avgar, et al. "Moving in the Anthropocene: Global reductions in terrestrial mammalian movements". In: *Science* 359.6374 (2018), pp. 466–469.

[186] Siddharth Unnithan Kumar. "The Wasteland is Enchanted". In: *Personal blog* (2022). URL: `https://siddharthunnithankumar.wordpress.com/2022/04/30/the-wasteland-is-enchanted/`.

[187] Siddharth Unnithan Kumar and Samuel A Cushman. "Connectivity modelling in conservation science: a comparative evaluation". In: *Scientific reports* 12.1 (2022), pp. 1–12.

[188] Siddharth Unnithan Kumar, Żaneta Kaszta, and Samuel A Cushman. "Pathwalker: A New Individual-Based Movement Model for Conservation Science and Connectivity Modelling". In: *ISPRS International Journal of Geo-Information* 11.6 (2022), p. 329.

[189] Siddharth Unnithan Kumar, Philip K Maini, Luca Chiaverini, Andrew J Hearn, David W Macdonald, Żaneta Kaszta, and Samuel A Cushman. "Smoothing and the environmental manifold". In: *Ecological Informatics* 66 (2021), p. 101472.

[190] Siddharth Unnithan Kumar, Jonathon Turnbull, Oscar Hartman Davies, Timothy Hodgetts, and Samuel A Cushman. "Minimal Ecologies". In: *Digital Ecologies Blog* (2022). URL: http://www.digicologies.com/2022/02/23/siddharth-unnithan-kumar-et-al/.

[191] Siddharth Unnithan Kumar, Jonathon Turnbull, Oscar Hartman Davies, Timothy Hodgetts, and Samuel A Cushman. "Moving beyond landscape resistance: Considerations for the future of connectivity modelling and conservation science". In: *Landscape Ecology* 37.10 (2022), pp. 2465–2480.

[192] María Vergara, Samuel A Cushman, and Aritz Ruiz-González. "Ecological differences and limiting factors in different regional contexts: Landscape genetics of the stone marten in the Iberian Peninsula". In: *Landscape Ecology* 32.6 (2017), pp. 1269–1283.

[193] Pauli Virtanen, Ralf Gommers, Travis E Oliphant, et al. "SciPy 1.0: fundamental algorithms for scientific computing in Python". In: *Nature methods* 17.3 (2020), pp. 261–272.

[194] Arian D Wallach, Marc Bekoff, Chelsea Batavia, Michael Paul Nelson, and Daniel Ramp. "Summoning compassion to address the challenges of conservation". In: *Conservation Biology* 32.6 (2018), pp. 1255–1265.

[195] Tzeidle N Wasserman, Samuel A Cushman, Michael K Schwartz, and David O Wallin. "Spatial scaling and multi-model inference in landscape genetics: Martes americana in northern Idaho". In: *Landscape ecology* 25.10 (2010), pp. 1601–1612.

[196] WCS and CIESIN. *[dataset] Last of The Wild data version 2, (LTW-2): global human footprint dataset*. 2005. URL: https://sedac.ciesin.columbia.edu/data/collection/wildareas-v2.

[197] Michael S Webster, Peter P Marra, Susan M Haig, Staffan Bensch, and Richard T Holmes. "Links between worlds: unraveling migratory connectivity". In: *Trends in ecology & evolution* 17.2 (2002), pp. 76–83.

[198] Mark J Whittingham, Philip A Stephens, Richard B Bradbury, and Robert P Freckleton. *Why do we still use stepwise modelling in ecology and behaviour?* 2006.

[199] John A Wiens. *Spatial scaling in ecology*. 1989.

[200] Alexander DM Wilson, Martin Wikelski, Rory P Wilson, and Steven J Cooke. "Utility of biological sensor tags in animal conservation". In: *Conservation Biology* 29.4 (2015), pp. 1065–1075.

[201] Kristin Zambucka. *'Ano 'ano: the seed*. Mana publishing co., 1978.

[202] Katherine A Zeller, Megan K Jennings, T Winston Vickers, Holly B Ernest, Samuel A Cushman, and Walter M Boyce. "Are all data types and connectivity models created equal? Validating common connectivity approaches with dispersal data". In: *Diversity and Distributions* 24.7 (2018), pp. 868–879.

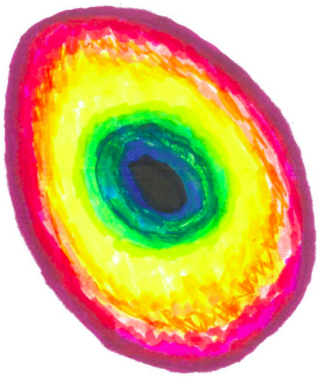
[203] Katherine A Zeller, Rebecca Lewsion, Robert J Fletcher, Mirela G Tulbure, and Megan K Jennings. "Understanding the importance of dynamic landscape connectivity". In: *Land* 9.9 (2020), p. 303.

[204] Katherine A Zeller, Kevin McGarigal, Paul Beier, Samuel A Cushman, T Winston Vickers, and Walter M Boyce. "Sensitivity of landscape resistance estimates based on point selection functions to scale and behavioral state: pumas as a case study". In: *Landscape Ecology* 29.3 (2014), pp. 541–557.

[205] Katherine A Zeller, Kevin McGarigal, and Andrew R Whiteley. "Estimating landscape resistance to movement: a review". In: *Landscape ecology* 27.6 (2012), pp. 777–797.

Truth Beauty Goodness

Unity



the Source of Infinite Possibility

Harmony

Balance Equilibrium